STUDY OF OOCYTE-TO-EMBRYO TRANSITION REGULATORS,
OMA-1 AND OMA-2 IN *C. elegans*

APPROVED BY SUPERVISORY COMMITTEE

Rueyling Lin, Ph.D.

Scott Cameron, M.D., Ph.D.

Dennis McKearin, Ph.D.

William Snell, Ph.D.

DEDICATION

I would like to thank my parents, Hiroyoshi Nishi and Kumiko Nishi

STUDY OF OOCYTE-TO-EMBRYO TRANSITION REGULATORS, OMA-1 AND OMA-2 IN *C. elegans*

by

YUICHI NISHI

DISSERTATION

Presented to the Faculty of the Graduate School of Biomedical Sciences

The University of Texas Southwestern Medical Center at Dallas

In Partial Fulfillment of the Requirements

For the Degree of

DOCTOR OF PHILOSOPHY

The University of Texas Southwestern Medical Center at Dallas

Dallas, Texas

April, 2007

ACKNOWLEDGEMENTS

I would like to thank my mentor, Rueyling Lin for her support and encouragement. Her patient guidance and the scientifically stimulating environment she created in the lab made my graduate study very fruitful. I also would like to thank my thesis committee, Scott Cameron, Dennis McKearin, and Bill Snell for their insights and advice.

I would like to thank the past and present members of the Lin lab for their help and discussions. Particularly, some of my thesis research stemmed from Manisha Patel and Angela Collins' discoveries. Specifically, Manisha's painstaking RNAi-based screen for OMA-1 degradation regulators seeded my analysis of *gsk-3* described in Chapter 3. Angela's yeast two-hybrid screens led to my protein-protein interaction study described in Chapter 5. I truly respect their dedications in research.

I would like to thank the following researchers for their generosity on reagent sharing. First of all, this work was greatly facilitated by worm strains and DNA clones from Dr. Geraldine Seydoux (Johns Hopkins University, MD) and antibodies from Dr. James Priess (Fred Hutchinson Cancer Center, WA). Edward Kipreos (University of Georgia, Athens), Yuji Kohara (National Institute of Genetics, Japan), and Caenorhabditis Genetics Center also provided various DNA clones and strains critical for this study.

STUDY OF OOCYTE-TO-EMBRYO TRANSITION REGULATORS, OMA-1 AND OMA-2 IN *C. elegans*

Publication No. _____

Yuichi Nishi, Ph.D.

The University of Texas Southwestern Medical Center at Dallas, 2007

Supervising Professor: Rueyling Lin, Ph.D.

A non-dividing, developmentally dormant oocyte is transformed into a rapidly dividing, differentiating embryo during a short period termed oocyte-to-embryo transition. Oocyte-to-embryo transition encompasses oocyte maturation and fertilization and is characterized by both cell cycle and developmental events. Understanding the mechanisms underlying oocyte-to-embryo transition is a fundamental goal for developmental biology and reproductive medicine. However, our current understanding of the transition is very limited. Two CCCH Tis-11 type zinc finger proteins of *C. elegans*, OMA-1 and OMA-2 are expressed exclusively in oocytes and 1-cell embryos, and are rapidly degraded at the first

mitosis. Previous studies suggested that *oma-1* and *oma-2* are redundantly required for oocyte maturation, and the degradation of OMA-1/2 proteins at the end of the 1-cell stage is essential for embryogenesis. However, their roles in the 1-cell embryo, and the mechanism of the OMA-1/2 degradation were elusive. In addition, the molecular functions of OMA-1/2 proteins were unknown. In this study, I investigated the mechanism controlling OMA-1/2 degradation as well as the molecular and genetic functions of OMA-1/2. I showed that two proline directed kinases, MBK-2/DYRK2 and GSK-3 directly and likely sequentially phosphorylate OMA-1/2 to mark them for degradation at the end of the 1-cell stage. My data further suggest that SCF and/or ECS E3 ubiquitin ligase and the proteasome are likely responsible for the execution of OMA-1/2 degradation. Secondly, I characterized the molecular and genetic functions of OMA-1/2 in oocytes and 1-cell stage embryos. My data suggest that OMA-1/2 regulate multiple processes. These processes include transcription and translation. At the 1-cell stage, transcription is inactive. My data suggest that OMA-1/2 render 1-cell embryos transcriptionally quiescence by preventing the nuclear localization of a general transcription factor, TAF-4. OMA-1/2 (*oma-1/2*) interact with translational regulators, MEX-3 and SPN-4 physically, and other translation factors, *puf-3/5/8*, and *cpb-3* genetically, suggesting that OMA-1/2 also regulate translation in oocytes and 1-cell embryos. In summary, my study revealed that phosphorylation and ubiquitination events regulate the degradation of OMA-1/2 proteins, and provided insights into functions of OMA-1/2 during oocyte-to-embryo transition.

TABLE OF CONTENTS

PUBLICATIONS

Nishi, Y. and Lin, R. (2005). DYRK2 and GSK-3 phosphorylate and promote the timely degradation of OMA-1, a key regulator of the oocyte-to-embryo transition in C. elegans. *Dev Biol* **288**, 139-49.

LIST OF FIGURES

LIST OF TABLES

LIST OF ABBREVIATIONS

aPKC- atypical protein kinase C

3AT- 3-amino-1,2,4-triazole

ATP – Adenosine 5’ Triphosphate

BSA – Bovine Serum Albumin

CPEB – Cytoplasmic polyadenylation element binding protein

DAPI - 4',6-Diamidino-2-phenylindole

DIC- Differential Interference Contrast

DMF- Dimethylformamide

dsRNA- double stranded RNA

DTT- Dithiothreitol

DYRK- Dual-specificity YAK1 Related Kinase

ER- Endoplasmic Reticulum

GTP - Guanosine 5’ Triphosphate

GAP – GTPase Activating Protein

GFP- Green Fluorescent Protein

GSK-3 – Glycogen Synthase Kinase 3

GST – Glutathione S-transferase

IPTG - Isopropyl β-D-1-thiogalactopyranoside

KD – Kinase dead

LB – Luria Broth

LG – Linkage Group

LPS- Lipopolysaccharide

MAPK – Mitogen Activated Protein Kinase

MBP – Maltose Binding Protein

MEK – MAPK/Erk Kinase

MSP – Major Sperm Protein

NGM – Nematode Growth Medium

WT – Wild Type

MTOC- Microtubule Organizing Center

ORF- Open Reading Frame

PFA- Paraformaldehyde

RNAi – RNA interference

SC- Synthetic Complete

SRS- SOS Recruitment System

TAF- TBP Associated Factor

TBP- TATA binding protein

UTR- Untranslated Region

CHAPTER ONE
Introduction

I. Oocyte-to-embyro transition

Late ocytes are cell cycle-arrested and developmentally dormant. During oocyte-to-embryo transition, which encompasses two evolutionarily conserved events --oocyte maturation and fertilization --, a dormant oocyte is transformed into a rapidly dividing, actively differentiating embryo. Understanding the mechanisms of the transition is a fundamental goal for developmental biology and reproductive medicine. Although regulations of the meiotic cell cycle of the transition have been intensively studied and well-understood, the regulation of developmental processes during the transition is poorly understood.

1. Meiotic cell cycle progression

In the ovary, germline stem cells mitotically divide to constitute a reservoir population of germ cells. Germ cells that leave the mitotic division cycle enter meiosis and begin the oogenesis program, which is characterized by two important aspects: meiotic progression and accumulation of maternal factors. Meiosis is a gonad-specific cell cycle that produces haploid male and female gametes via a single round of DNA replication followed by two cell divisions (Figure 1.1). Following DNA replication, a proteinous attachment termed synaptonemal complex forms between homologs (Kleckner 1996). The formation of synaptonemal complex is completed before cells entering the pachytene phase. During pachytene,

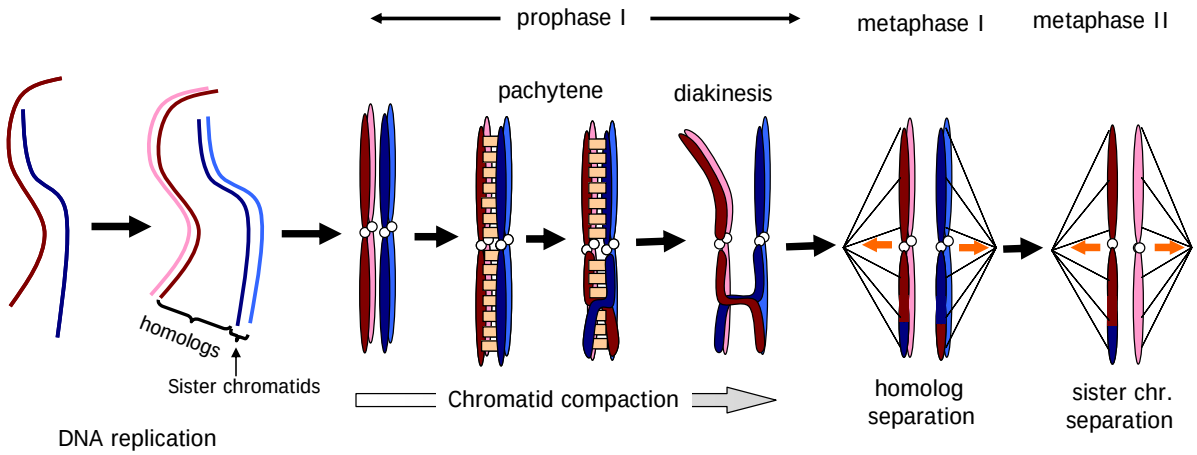

Figure1.1 Meiotic cell cycle progression
Blue and red indicate paternal and maternal homologs and light blue and magenta their sister chromatids. Sister chromatids are held together DNA replication. As the cell cycle enters prophase I, chromatids begin to condense and homolgs align throughout their entire lengths. Symaptonemal complex (indicated as yellow boxes) that hold homologs tight together form before pachytene phase. After the completion of homologous recombination during pachytene, most of chrosomomal attachments between homologs are released (diakinesis). Homologs are separated via metaphase I, followed by sister chromatid separation via metaphase II.

homologs recombine to exchange paternal and maternal genetic material (Kleckner 1996). Recombined chromosomes eventually loose synaptonemal complex while homologs remain attached by a distinct complex to enter diakinesis of prophase I (Figure 1.1) (Kleckner 1996). The nucleus undergoes two rounds of divisions that first separate homologs then sister chromosomes, producing a haploid gamete (Figure 1.1). Meiosis during male spermatogenesis proceeds without interruption. On the other hand, the final steps of female meiosis are tightly controlled through two evolutionarily conserved cellular events: oocyte maturation and fertilization (Figure 1.2).

Oocyte nuclei at diakinesis of prophase I do not progress further through the cell cycle, until they receive a specific extracellular signal. The reception of the signal lifts the arrest

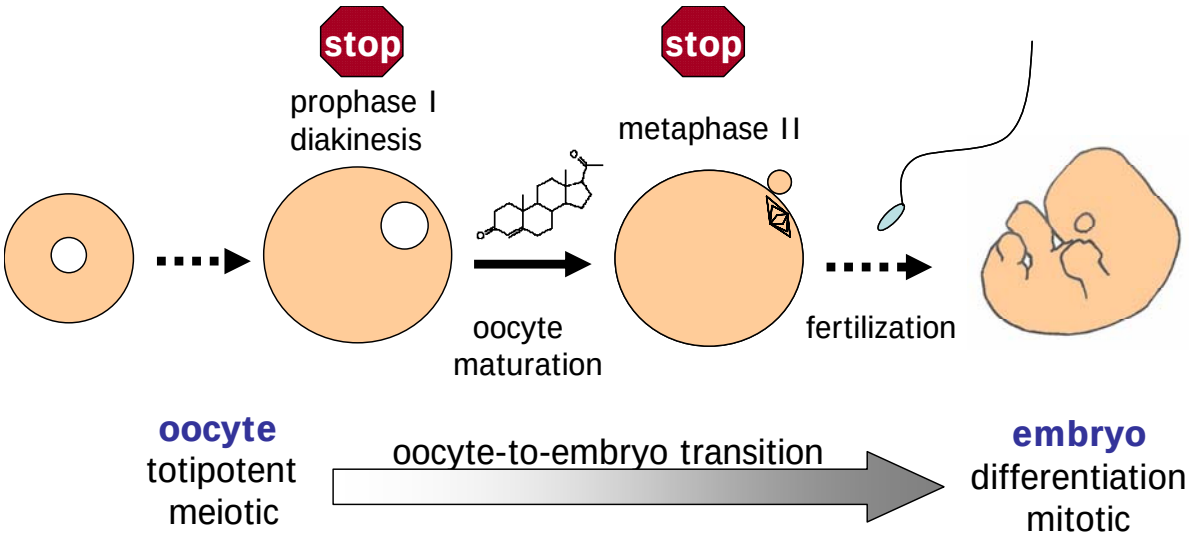

Figure 1.2 Oocyte-to-embryo transition in human
Meiotic cell cycle progression during female meiosis is regulated via cellular events. In human, oocytes arrest at diakinesis of prophase I. This arrest is relieved via signaling event triggered by the hormone, progesterone (oocyte maturation), however, the oocyte soon reaches the second arrest point at metaphase II. The second arrest is lifted by fertilization to complete meiosis and enter mitotic division. Through a transition period encompassing oocyte maturation and fertilization, a totipotent, meiotic oocyte is transformed into a differentiating, mitotic embryo.

and allows for the completion of meiosis I. The meiotic cell cycle, however, soon reaches the second arrest point, metaphase of meiosis II (Mehlmann 2005). This release of oocyte prophase I arrest is termed oocyte maturation, and is a prerequisite for fertilization. Oocyte maturation also is characterized by several other events important for cell cycle progression, cell division, fertilization, and embryogenesis (Jamnongjit and Hammes 2005). For example, nuclear envelope breakdown, MAPK activation, and the rearrangement of cortex properties occur in response to a maturation signal (Ferrell 1999; Schmitt and Nebreda 2002; Brunet and Maro 2005). Oocyte maturation, in addition, appears to potentiate the differentiation capabilities of the oocyte (Carroll et al. 1996).

Fertilization releases the second meiotic arrest at metaphase II and allow for the completion of meiosis II to generate a haploid maternal pronucleus. Maternal and paternal pronuclei fuse to enter mitosis and begin embryogenesis. An important aspect of fertilization is a rise in cytoplasmic Ca^{2+} (Runft et al. 2002). Sperm contact induces a G protein-induced release of Ca^{2+} from the ER lumen, which triggers cyclin destruction and cell cycle progression (Runft et al. 2002). Elevated cytoplasmic Ca^{2+} level also is thought to initiate developmental programs, however, the precise mechanism is unknown (Runft et al. 2002).

Unlike prophase I-arrested oocytes, which can stay arrested for several decades in human, mature oocytes at metaphase II need to be fertilized in a span of hours to days to initiate successful embryogenesis. Thus, ocyte maturation and fertilization are temporally coupled. For example, oocyte maturation and mating behavior are triggered by a common hormonal action in the mouse (Moss and McCann 1973; Pfaff 1973; McNatty et al. 2004). Hence oocyte maturation and fertilization constitute a temporally continuous functional unit, oocyte-to-embryo transition, which concludes oogenesis and initiates embryogenesis.

Critical aspects of oocyte-to-embryo transition are well conserved between vertebrates and the nematode *C. elegans* (Ward and Carrel 1979; McCarter et al. 1999). *C. elegans* has two sexes: the self-fertilizing hermaphrodite, which constitutes 99.9% of the natural population, and the rare male. An adult hermaphrodite bears a pair of tube-shaped female gonads connected to the sperm storage compartment, spermatheca (one of a female gonad pair is shown in Figure 1.3). A young hermaphrodite operates oogenesis constitutively like an assembly-line, with an oocyte sent to the spermatheca every 23 minutes to fertilize with

own sperm. The fertilized egg is expelled into the uterus where it undergoes early stages of embryogenesis.

Oogenesis of *C. elegans* begins when germ cells leave the distal tip of the female gonad, where germ cells mitotically divide (Figure 1.3). Germ cells that have left the distal tip enter and progress through meiosis as they migrate away from the distal tip on the inner surface of the gonad as a syncytium layer (Figure 1.3). Around the loop region, where the gonad makes a near 180-degree turn, germ cells exit the pachytene stage to enter diakinesis of prophase I (Figure 1.1) and become fully enclosed (cellularized) by the plasma membrane (Figure 1.3). Cellularized germ cells (oocytes) grow in size as they line up in a single row toward the spermatheca (Figure 1.3). These oocytes remain at diakinesis until they are induced to undergo oocyte maturation (McCarter et al. 1999).

Oocyte maturation in *C. elegans* is regulated directly by the availability of sperm via a sperm-derived factor, MSP (major sperm protein) (Miller et al. 2001). MSP is released from sperm and thought to signal oocytes to initiate maturation by a cell surface receptor-mediated process (Miller et al. 2003b; Kosinski et al. 2005). In a young hermaphrodite, the spermatheca is filled with own sperm, thus oocyte maturation is constitutive. However, in the absence of sperm, and therefore in the absence of MSP, oocyte maturation and ovulation cease and oocytes become arrested at diakinesis of prophase I (McCarter et al. 1999). Oocyte maturation can be resumed by the introduction of sperm or purified MSP (McCarter et al. 1999; Miller et al. 2001). Although there are evident differences between oocyte maturation in vertebrate and *C. elegans*, many hallmark events of oocyte maturation are surprisingly well conserved. For example, nuclear envelope breakdown, cortical

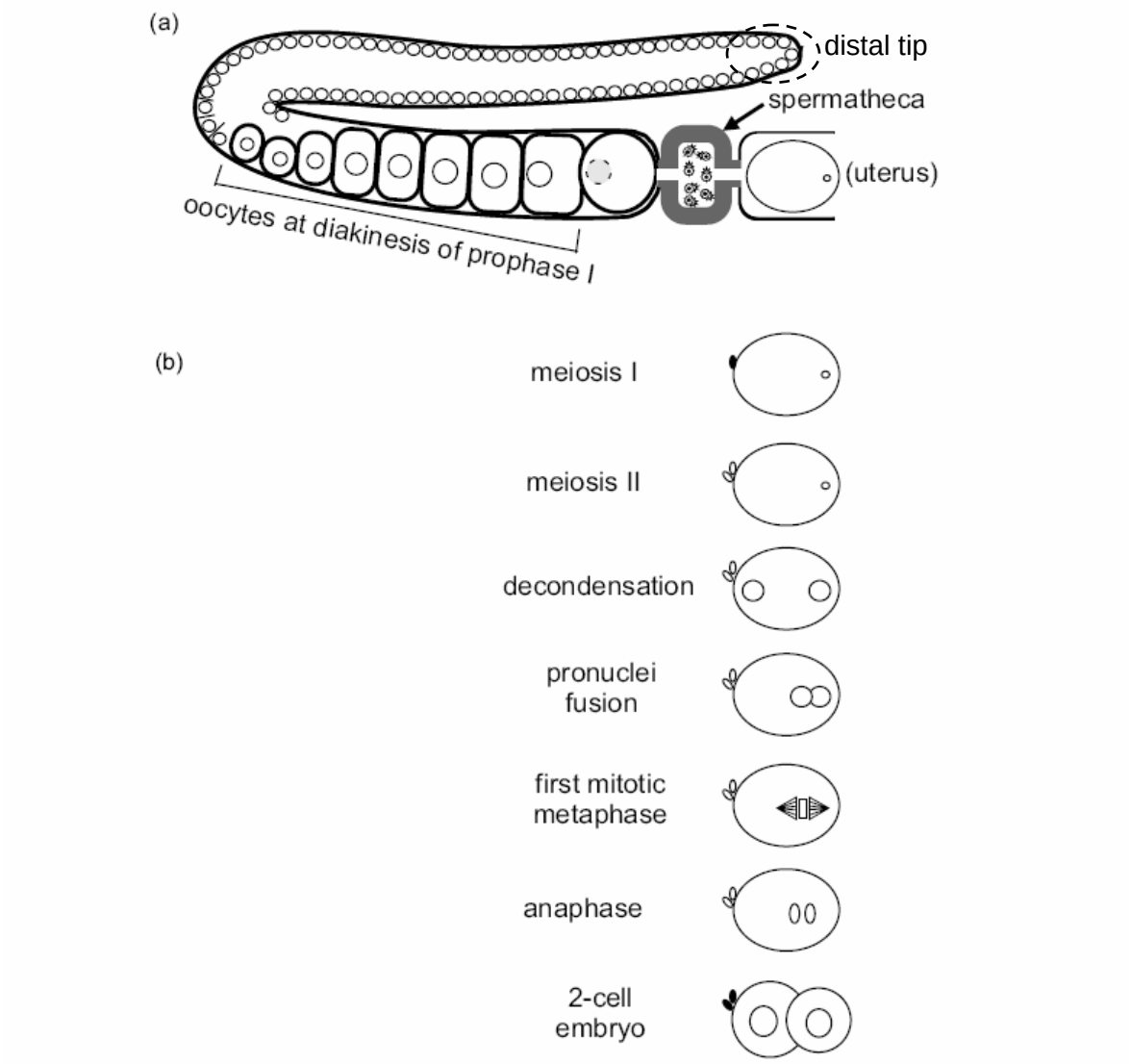

Figure 1.3 Reproductive system and 1-cell embryonic stages of *C. elegans*

(a) U-shaped hermaphrodite gonad arm is connected to the spermatheca, which then is connected to the uterus. Germline nuclei (circles) migrate on the inner surface of the gonad towards the spermatheca as they undergo oogenic development. Around the loop region, they become cellularized and reach diakinesis of prophase I. The oocyte immediately next to the spermatheca undergoes oocyte maturation and ovulate into the spermatheca, where fertilization takes place immediately. The fertilized egg promptly moves to the uterus, where early embryogenesis goes on.

(b) Stages of *C. elegans* 1-cell embryo. Fertilization occurs before the completion of meiosis I in *C. elegans*. Meiosis II follows immediately after meiosis I. After maternal and paternal pronuclei decondense, they fuse to form a zygote. The resulting zygote immediately enters mitotic cell cycle and embryogenesis.

rearrangement, and MAP kinase activation all occur upon maturation in *C. elegans* (McCarter et al. 1999). Both in vertebrates and *C. elegans*, oocytes undergo maturation at diakinesis of prophase I (McCarter et al. 1999). As in vertebrate, oocyte maturation is prerequisite for fertilization in *C. elegans*.

A maturing oocyte is ovulated into the spermatheca and become fertilized by own sperm immediately (Ward and Carrel 1979; McCarter et al. 1999) (Figure 1.3). Unlike vertebrates, both meiosis I and II are completed after fertilization and the second meiotic arrest at metaphase II does not exist in *C. elegans* (Ward and Carrel 1979)(Figure 1.3). However, as in vertebrates, the successful completion of meiosis II requires fertilization in *C. elegans* (McNally and McNally 2005). After the completion of meiosis II, the maternal and paternal pronuclei decondense and fuse together, and the resulting zygote enters rapid mitotic cell cycle (Figure 1.3). Oocyte-to-embryo transition occurs very rapidly in *C. elegans*. It takes approximately 20 minutes to complete meioses after oocyte maturation, and only additional 40 minutes are required to initiate and complete the first mitotic division (Ward and Carrel 1979; Albertson 1984).

2. Maternal factors and control of their activity

Although sperm and oocytes each provide a haploid genome to the embryo, their cytosolic contributions are asymmetrical. Oocyte cytoplasm is filled with a plethora of factors that will function in early embryogenesis, whereas cytosolic contributions by sperm appear to be very limited (Gosden et al. 1997).

As oogenesis progresses, various factors including yolk, ribosomes, and embryonic cell

fate determinants are synthesized in the oocyte as well as transported from neighboring cells into the oocyte (Gosden et al. 1997). These factors will later support high energy consumption, rapid cell division, and active differentiation events in early embryogenesis. A central question of developmental biology is how the activities and consumption of these maternal factors are differentially regulated in the oocyte and in the embryo. Particularly, developmental regulators must undergo tight temporal regulation. They need to remain dormant in the oocyte so as not to reprogram the totipotent oocyte nucleus, however, they need to become activated in a timely and organized manner during and after oocyte-to-embryo transition to participate in differentiation events of early embryogenesis. Although a number of maternally deposited factors have been cataloged, the mechanisms of their regulation are unclear in most cases. However, translational regulation emerged as a key mechanism in controlling maternally deposited developmental programs, as exemplified by the following two cases.

The first example is the polarization of the *Drosophila* embryo by maternal mRNAs. The anterior-posterior polarity of the *Drosophila* embryo is determined before fertilization by the asymmetrical depositions of mRNAs encoding cell fate determinants (Nusslein-Volhard et al. 1987). The mRNAs encoding Bicoid and Nanos are transported from surrounding cells and placed at opposite poles in the oocyte (Frigerio et al. 1986; Berleth et al. 1988; Sander and Lehmann 1988; Lehmann and Nusslein-Volhard 1991). These mRNAs are translationally inactive in the oocyte, whereas after fertilization, they become activated to form opposing gradients of their protein products that specify the anterior-posterior polarity and segment identities in the embryo (Driever and Nusslein-Volhard 1988; Tautz 1988; Hulskamp et al.

1989; Irish et al. 1989; Salles et al. 1994; Smibert et al. 1996). Thus the embryonic distributions of Nanos and Bicoid are predicted by their mRNA localization in the oocyte, however, their cell fate-determining activity is absent in the oocyte due to the lack of translation.

The second example is the repression of somatic fates in meiotic germ cells by the translational regulators, GLD-1 and MEX-3 in *C. elegans*. GLD-1 and MEX-3 are known to be translational regulators expressed in the germline gonad and early embryos (Draper et al. 1996; Jones et al. 1996). GLD-1 has been shown to repress translation of a number of factors in germ cells, whereas MEX-3 is known to regulate translation during early embryogenesis (Evans et al. 1994; Hunter and Kenyon 1996; Lee and Schedl 2001b; Huang et al. 2002; Lee and Schedl 2004). GLD-1 and MEX-3 are expressed in meiotic germ cells in a reciprocal pattern (Draper et al. 1996; Jones et al. 1996). This pattern is thought to be achieved partly via translational repression of MEX-3 by GLD-1 because in *gld-1(-)* gonad, MEX-3 is ectopically expressed in the distal gonad where GLD-1 is normally expressed (Ciosk et al. 2004; Mootz et al. 2004). Strikingly, the simultaneous depletion of GLD-1 and MEX-3 resulted in the transdifferentiation of germ cells into somatic cell types (Ciosk et al. 2006). The somatic markers observed in the mutant gonad were of intestine, pharyngeal muscle, body wall muscle, and neuron, covering most tissue types of *C. elegans* (Ciosk et al. 2006). On the other hand, a germline specific marker, P-granule was lost in some germ cells in the mutant gonad (Ciosk et al. 2006). These results suggest that GLD-1 and MEX-3 prevent meiotic germ cells from taking somatic fates (Ciosk et al. 2006). As GLD-1 and MEX-3 are translational regulators, it is likely that they repress developmental regulators in meiotic germ

cells. However, their targets responsible for the germline-to-soma transformations have not been identified. In addition, the regulations of GLD-1 and MEX-3 activity are unclear. Despite its apparent differentiation repressing activity, MEX-3 and GLD-1 are present in some differentiating somatic blastomeres in the early embryo (Draper et al. 1996; Jones et al. 1996). Thus their somatic fate-repressing activity needs to be turned off in these blastomeres. Furthermore, not all meiotic germ cells expressed somatic markers in *gld-1(-) mex-3(-)* mutant gonad, suggesting that (an) additional unidentified factor(s) might contribute to the somatic fates repression in the gonad (Ciosk et al. 2006).

3. Transcriptional quiescence during oocyte-to-embryo transition

The earliest stages of embryonic development lack polII-mediated transcription due to maternal-to-zygotic transcriptional transition (Seydoux et al. 1996; Schultz 2002). Transcription is extremely active in early stages of oogenesis to synthesize various factors for early embryogenesis (Roller et al. 1989). Transcription ceases in late oogenesis and remains dormant in the earliest stages of embryogenesis. The start of zygotic transcription, namely, zygotic genome activation (ZGA), breaks the transcriptional quiescence at the 1-cell stage in the mouse, and 4-cell stage in *C. elegans* (Latham et al. 1992; Vernet et al. 1992; Seydoux and Fire 1994). In mammals in which ZGA is better-characterized, not only maternal and zygotic *de novo* transcription has a clear boundary, but also existing maternal transcripts are replaced with newly synthesized zygotic transcripts (Thompson et al. 1998). Even transcripts found both in the oocyte and in the embryo are turned over by the destruction of maternal transcripts and the replenishment with new zygotic transcripts (Thompson et al. 1998). The

significance of the transcriptional quiescence during oocyte-to-embryo transition is not fully understood. It is likely to be critical, however, for animal development because this phenomenon is widely conserved throughout metazoan.

4. Developmental events during and shortly after oocyte-to-embryo transition

Without active transcription, differentiation events at the earliest stages of embryogenesis must rely on maternally supplied factors. Players of embryogenesis that were rendered inactive in the oocyte now need to become activated in a temporally and spatially controlled manner to drive early embryogenesis. The following paragraphs will describe the current understanding of the beginning of embryogenesis. Both in vertebrate and *C. elegans* systems, events during oocyte-to-embryo transition appear to have a direct impact on the polarity determination of early embryos. Although the maternal programs regulating early *C. elegans* embryogenesis are well studied, that of mammalian embryogenesis are very enigmatic.

4-1. Early developmental events in vertebrate systems

In mammals, analyses of the beginning of embryogenesis have been limited to lineage tracing of live embryos, because virtually no molecular marker is available to monitor developmental potentials at such early stages of embryogenesis (Zernicka-Goetz 2006). Recent studies collectively showed that oocyte-to-embryo transition is likely to have a direct impact on the polarity determinaiton of the non-prepatterned mouse oocyte (Zernicka-Goetz 2006). These studies suggest that the first cleavage plane is influenced both by the location

of polar body extrusion and the site of sperm entry, thus multiple steps during oocyte-to-embryo transition are important for the initial patterning of the embryo (Plusa et al. 2002; Plusa et al. 2005). An additional study suggested a differential cell fate decision at the 2-cell stage, thus the first cleavage axis decision might have a direct impact on the outcome of mammalian embryogenesis (Deb et al. 2006).

In the frog *Xenopus larvaes*, oocytes are asymmetrical along the animal-vegetal axis. The animal pole contains dark pigments and is known to have the potential to form ectoderm (De Robertis et al. 2000). The other end of the embryo, the vegetal pole, is enriched with yolk and is thought to be pre-determined to take endoderm fates (De Robertis et al. 2000). The oocyte has no other axis before fertilization. This radial symmetry is broken by sperm entry. Sperm entry induces microtubule-driven rotation of the cortex by approximately 30° relative to the cytoplasm (Vincent et al. 1986; Elinson and Rowning 1988). The cortical rotation results in a series of molecular interactions that determines the dorsal-ventral axis of the embryo (De Robertis et al. 2000). Thus, fertilization plays a critical and direct role in determining an embryonic axis in the frog embryo.

4-2. Early developmental events in *C. elegans*

4-2 a. Generation of A-P/soma-germline asymmetry in 1-cell embryo

C. elegans eggs are not prepatterned. All the polarity regulators mentioned below are maternally deposited and are distributed uniformly in the oocyte. Sperm entry breaks the uniformity of those proteins and determines the A-P axis, thus like in mammals and frog, oocyte-to-embryo transition has a direct role in the patterning of the embryo (Goldstein and

Hird 1996; O'Connell et al. 2000; Wallenfang and Seydoux 2000). A sperm-derived microtubule organizing center (MTOC) and similarly sperm-contributed GTPase activating protein (GAP), CYK-4, initiate a cascade of events that results in an asymmetrical distribution of cell fate determinants in the 1-cell zygote, generating two blastomeres with strikingly distinct developmental potentials after the first mitotic division (Lyczak et al. 2002; Jenkins et al. 2006). Specifically, the sperm-contributed MTOC and CYK-4/GAP induce organized contractions of the cortical actiomyosin meshwork that drive a cortically localized kinase-complex, PAR-3/PAR-6/aPKC, away from the site of sperm entry (Cheeks et al. 2004; Munro et al. 2004) (Figure 1.4). Now anteriorly localized cortical PAR-3/PAR-6/aPKC releases a RING ringer protein, PAR-2, from the anterior cortex via direct phosphorylation, restricting the cortical PAR-2 to the posterior (Hao et al. 2006)(Figure 1.4). PAR-2 stabilizes the distribution of the PAR proteins along the A-P axis by counteracting the PAR-3/PAR-6/aPKC complex in the posterior, likely by its suggested ubiquitin ligase activity (Cuenca et al. 2003; Hao et al. 2006). The anterior PAR-3/PAR-6/aPKC also posteriorly limits the localization of another cortical kinase, PAR-1, likely via PAR-2 (Guo and Kemphues 1995) (Figure 1.4). PAR-1 is responsible for anteriorly localizing the cytoplasmic Tis-11 like CCCH zinc finger proteins, MEX-5 and MEX-6 (Schubert et al. 2000)(Figure 1.4). MEX-5/6 are required to limit several other developmental regulators to the posterior (Schubert et al. 2000)(Figure 1.4). These posterior factors include the Tis-11 like CCCH zinc finger protein, PIE-1, and the germ-granule, P-granule, both of which are thought to be essential for the germline identity (Strome and Wood 1983; Mello et al. 1992; Mello et al. 1996) (Figure 1.4). Upon the first mitotic division along the A-P axis, the

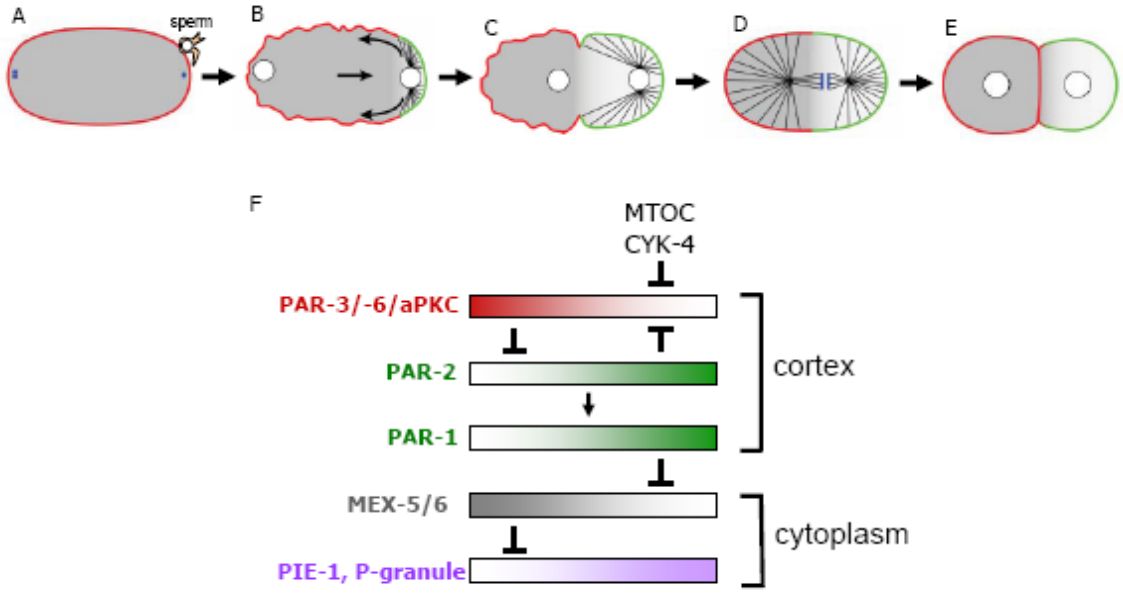

Figure 1.4. Mechanisms underlying the polarization of *C. elegans* 1-cell embryo (Reproduced from Nance 2005 and Pellettieri and Seydoux 2002)
(A-E) Schematic description of polarity formation in 1-cell embryo. Red: PAR-3/-6/aPKC complex, green: PAR-2 and PAR-1, grey: MEX-5/6, blue: chromosomes. (A,B) sperm-contributed microtubule organizing center and CYK-4 induces cortical contractions, driving PAR-3/-6/aPKC to the anterior, permitting PAR-2 and PAR-1 to localize to the posterior cortex (C). This cortical polarity result in cytoplasmic polarity in 1-cell stage with MEX-5/6 in the anterior and PIE-1 and P-granule in the posterior (C and D). The cortical and cytoplasmic polarity persist through the first mitotic division (D), and the cell division happening along A-P axis divides the anterior and posterior factors into different blastomeres (E).
(F) Hierarchy of the localization of polarity determining factors. Sperm contributed microtubule organizing center (MTOC) and CYK-4 drives cortical PAR-3/-6/aPKC complex towards to the anterior. PAR-3/-6/aPKC then limits PAR-2 to the posterior. PAR-2 localizes PAR-1 to the posterior, while antagonizing PAR-3/-6/aPKC in the posterior, stabilizing the PAR-polarity along the A-P axis. PAR-1 localizes the cytoplasmic MEX-5/6 to the anterior, which then limits PIE-1 and P-granule to the posterior.

anterior factors are inherited to the anterior somatic blastomere, AB, and the posterior factors, including germline fate-determining PIE-1 and P-granule, are segregated to the posterior germline precursor P1, resulting in two blastomeres bearing distinct developmental potentials (Figure 1.4).

4-2 b. Soma-germline asymmetry is shaped by ZIF-1 E3 ligase

The first asymmetric division segregates the germline potential only to the posterior blastomere of 2-cell stage, P1, likely by the segregation of germline-fate determinants (such as PIE-1 and P-granule) to P1. Similar asymmetric divisions reiterate in the germline lineage 3 more times with each division segregating the germline potential only to one of the two daughters (Kemphues 2000). Like the first mitotic division, the PARs, MEX-5/6, PIE-1, and P-granule polarize along the division axis and asymmetrically segregate into respective daughters (Kemphues 2000).

In addition to the PAR-mediated polarization, recent studies showed that ubiquitin/proteasome-mediated protein degradation plays a important role in the soma-germline asymmetry (DeRenzo et al. 2003). A germline-fate determinant, PIE-1, is polarized before each germline precursor division, and is segregated mostly to the germline daughter (Mello et al. 1996; Reese et al. 2000). However, immediately after each division, a small fraction of PIE-1 protein is found in the somatic daughter (Reese et al. 2000). PIE-1 expression in somatic blastomeres could be hazardous to the embryo because PIE-1 is a germline-fate determinant (Mello et al. 1992; Seydoux et al. 1996). Such somatic PIE-1 is scavenged via specific proteasomal degradation mediated by the E3 ligase, ZIF-1 (DeRenzo et al. 2003). ZIF-1 is required for the somatic PIE-1 degradation *in vivo*, and physically interacts with the domain of PIE-1 responsible for the degradation in soma (first CCCH zinc finger domain) (Reese et al. 2000; DeRenzo et al. 2003)(Figure 1.5). Thus ZIF-1 is thought to directly drive the degradation of PIE-1 specifically in somatic blastomeres. ZIF-1 also regulates the localizations of germline-enriched factors, POS-1, MEX-1, and MEX-5/6 via

their CCCH zinc finger domain (Reese et al. 2000; DeRenzo et al. 2003). ZIF-1 similarly interacts with zinc fingers of POS-1, MEX-1, and MEX-5/6, and is required for their degradation in somatic blastomeres (DeRenzo et al. 2003). Thus, ZIF-1 is thought to be an key factor generating the germline-soma asymmetry. Consistent with the importance of ZIF-1-mediated degradation in embryogenesis, the depletion of *zif-1* results in embryonic lethality (DeRenzo et al. 2003). On the other hand, ectopic expression of ZIF-1 activity, thus precocious degradation of its targets, would be undesirable for embryogenesis because all the known ZIF-1 targets are essential for embryogenesis (Mello et al. 1992; Tabara et al. 1999; Schubert et al. 2000; DeRenzo et al. 2003). Hence, ZIF-1 expression and/or activity must be temporally and spatially controlled. Temporally, it has been suggested that ZIF-1 activity is not present before 4-cell stage (Reese et al. 2000; DeRenzo et al. 2003). Spatially, ZIF-1 activity needs to be asymmetrically localized at and after 4-cell stage because ZIF-1-mediated degradation must happen only in somatic blastomeres (Reese et al. 2000; DeRenzo et al. 2003). However, neither temporal nor spatial control of ZIF-1 expression and/or activity has been revealed.

4-2 c. Translational regulations pattern early embryos

Expression of certain cell-cell signaling molecules and cell-fate determining transcription factors is regulated at the translation level during oogenesis and early embryogenesis. Often, their transcripts are deposited in the oocyte and localized uniformly in the embryo, however, their protein products are expressed in specific blastoemeres in the

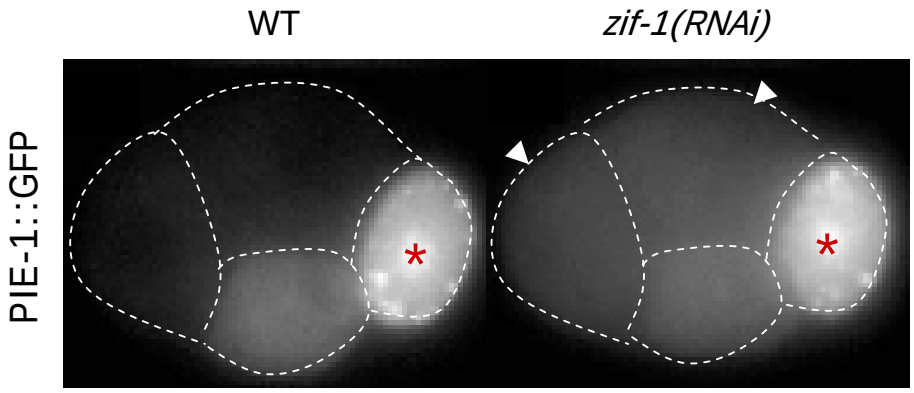

Figure 1.5 ZIF-1 E3 ligase is required to properly localize germline proteins (Reproduced from DeRenzo and Seydoux 2004)
4-cell embryos expressing PIE-1::GFP, with and without *zif-1* RNAi treatment. The blastomeres marked with asterisk are the germline precursor, P2. All others are somatic blastomeres. PIE-1 is ectopically expressed in the two somatic blastomeres indicated by arrowheads in *zif-1* RNAi embryo.

embryo, but not in the oocyte. Recent studies revealed that such temporal and special translational regulations are achieved by RNA-binding proteins during early *C. elegans* embryogenesis. As discussed in an earlier section, translational regulation might be a commonly used mechanism to maternally deposit cell-fate determinants without reprogramming the totipotent oocyte nucleus.

PAL-1 is a caudal-like transcription factor essential for the C-blastomere cell fate (Hunter and Kenyon 1996). Although *pal-1* mRNA is uniformly present in the oocyte and early embryos, PAL-1 protein is expressed only at and after the 4-cell stage in a specific spatial pattern (Hunter and Kenyon 1996). A series of studies identified *cis*-regulatory elements (a region of 3'UTR of *pal-1* mRNA) and *trans*-factors (RNA-binding proteins) that translationally control PAL-1 expression (Hunter and Kenyon 1996; Huang et al. 2002;

Mootz et al. 2004). In the gonad, KH proteins GLD-1 and MEX-3 repress PAL-1 translation in the distal and proximal region, respectively (Hunter and Kenyon 1996; Mootz et al. 2004). In early embryos, MEX-3 and its binding partners, an RRM-domain protein, SPN-4, and a CCCH zinc finger protein, MEX-6, positively regulate PAL-1 translation to achieve the specific temporal and spatial pattern of PAL-1 protein expression (Huang et al. 2002). MEX-3, SPN-4, and MEX-6 are all asymmetrically localized in the embryo, and their localization patterns are likely to contribute to the spatial expression pattern of PAL-1 (Draper et al. 1996; Ogura et al. 2003; Tenlen et al. 2006).

Another example is GLP-1/Notch. Similarly, temporal and spatial translational regulation governs GLP-1 expression in the gonad and early embryo (Evans et al. 1994). It has been shown that GLD-1, pumilio-FBF related proteins PUF-5/6/7, SPN-4, and a CCCH zinc finger protein, POS-1, participate in the regulation of GLP-1 translation. Specifically, GLD-1, POS-1 and SPN-4 interact with *glp-1* 3'UTR, to spatially regulate GLP-1 translation (Marin and Evans 2003; Ogura et al. 2003). GLD-1 and POS-1 appear to regulate GLP-1 negatively, whereas SPN-4 acts positively (Marin and Evans 2003; Ogura et al. 2003). In addition, GLD-1 and PUF-5/6/7 temporally repress GLP-1 translation in the gonad (Marin and Evans 2003; Lublin and Evans 2007). In *gld-1* null mutant and *puf-5/6/7* triple RNAi animals, GLP-1 is precociously expressed in the distal and proximal gonad respectively, suggesting that GLD-1 and PUFs repress GLP-1 expression in different regions in the gonad (Marin and Evans 2003; Lublin and Evans 2007). Consistent with the temporally differential roles of GLD-1 and PUFs in GLP-1 translation, GLD-1 is expressed in the distal gonad and early

embryos whereas PUF-5 is expressed in the proximal gonad (Jones et al. 1996; Lublin and Evans 2007).

II. MBK-2 as a key regulator of oocyte-to-embryo transition

1. Proline directed serine/threonine kinases, DYRK

A serine/threonine kinase, MBK-2 has emerged as a key regulator of oocyte-to-embryo transition lately, because maternal *mbk-2* is critical for several steps during and shortly after the transition, including meiosis-to-mitosis transition and early embryonic development (Pellettieri et al. 2003; Quintin et al. 2003; Pang et al. 2004). MBK-2 is the *C. elegans* homolog of the proline directed serine/threonine kinase, DYRK2 (Raich et al. 2003). DYRK kinases are implicated in several important pathologies and physiological processes such as Down syndrome (Smith and Rubin 1997; Smith et al. 1997; Altafaj et al. 2001), neural function (Tejedor et al. 1995; Fotaki et al. 2002; Raich et al. 2003), and cancer (Lee et al. 2000; Miller et al. 2003a). However, our knowledge on the regulation and targets of DYRK kinases has been very limited. To date, no regulatory activation step for DYRK kinases has been elucidated. Several substrates have been suggested through *in vitro* studies, however, *in vivo* validations of these phosphorylation events, and *in vivo* analysis of the consequences of the phosphorylation has been largely lacking. Particularly, the genetic dissection of DYRK2 has just begun with the recent studies of the *C. elegans* homolog, *mbk-2* (Pellettieri et al. 2003; Quintin et al. 2003; Raich et al. 2003; Pang et al. 2004).

2. The *C. elegans* DYRK2 homolog, MBK-2

Recent isolations of *C. elegans mbk-2* mutants opened the door to the genetic analysis of DYRK2 kinases (Pellettieri et al. 2003; Quintin et al. 2003; Raich et al. 2003; Pang et al. 2004). Although there appears to be a zygotic function for *mbk-2,* becasue *mbk-2* null homozygotes are sick and slow-growing (Raich et al. 2003), the analysis of *mbk-2* mutants has been focused on severe and penetrant maternal-effect embryonic phenotypes (Pellettieri et al. 2003; Quintin et al. 2003; Pang et al. 2004). Embryos from homozygous *mbk-2* mutants exhibit penetrant embryonic lethality with apparently pleiotropic defects (Pellettieri et al. 2003; Quintin et al. 2003; Pang et al. 2004). Although certain steps of the initial A-P polarity formation in the 1-cell embryo appear to happen, multiple key cellular and developmental processes at the 1-cell stage and later fail to occur properly in the mutant embryo (Pellettieri et al. 2003; Quintin et al. 2003; Pang et al. 2004). Prominent known embryonic defects are delays in the degradeation of multiple maternally supplied proteins as described below. The degradation of a) MEI-1, b) a class of CCCH zinc finger proteins, and c) OMA-1 was shown to be delayed in the mutant embryo (Pellettieri et al. 2003; Quintin et al. 2003; Pang et al. 2004). These 3 degradation processes appear to be regulated by distinct ubiquitin E3 ligases (DeRenzo et al. 2003; Furukawa et al. 2003; Pintard et al. 2003; Xu et al. 2003). All 3 degradation processes are thought to be essential for embryogenesis (Clandinin and Mains 1993; Clark-Maguire and Mains 1994; DeRenzo et al. 2003; Lin 2003). Importantly, degradation delays are specific because the degradation of cyclinB at the 1-cell stage is independent of *mbk-2* (Pellettieri et al. 2003). Thus *mbk-2* is required for specific degradation events during and/or shortly after oocyte-to-embryo transition.

2-1. Protein degradation defects of *mbk-2* mutant

2-1 a. MEI-1/katanin degradation

Embryos from *mbk-2* homozygous mutants protrude two polar bodies, suggesting the successful completion of both meioses, however, these embryos fail to form and position mitotic spindles properly, leading to abnormal cleavages (Pellettieri et al. 2003; Quintin et al. 2003; Pang et al. 2004). This cleavage defect was convincingly explained by a mis-regulation of the meiosis-specific microtubule regulator, MEI-1. MEI-1 is a microtubule severing protein required for the formation of small meiotic spindles (Srayko et al. 2000). Previous molecular and genetic analyses suggested that MEI-1 protein must be degraded before the first mitosis or mitotic spindles fail to form properly (Clandinin and Mains 1993; Clark-Maguire and Mains 1994). The cleavage defect of the *mbk-2* mutants is strikingly reminiscent of the mutants defective in MEI-1 degradation (Clandinin and Mains 1993; Clark-Maguire and Mains 1994; Pellettieri et al. 2003; Quintin et al. 2003; Pang et al. 2004). Indeed, *mbk-2* mutants exhibit a delay in MEI-1 protein degradation, with MEI-1 ectopically localized to the mitotic spindle (Pellettieri et al. 2003; Quintin et al. 2003; Pang et al. 2004). Furthermore, the mitotic spindle formation defect of *mbk-2* mutants was suppressed by the depletion of *mei-1* (Quintin et al. 2003; Pang et al. 2004). Thus the cleavage defect of *mbk-2* mutants is likely due to the failure to degrade MEI-1 protein in a timely manner.

2-1 b. ZIF-1 mediated protein degradation

Another prominent defect is delays in the degradation of maternally provided developmental regulators (Pellettieri et al. 2003). Tis-11-like CCCH zinc finger proteins,

PIE-1, MEX-5/6, and POS-1 are cell fate determinants essential for early embryogenesis (Mello et al. 1996; Tabara et al. 1999; Schubert et al. 2000). They exhibit intricately patterned expressions that are thought to be important for differential cell fate determination in the early embryo (Mello et al. 1996; Tabara et al. 1999; Schubert et al. 2000). Their proper expressions at and after the 4-cell stage rely on ZIF-1 E3 ligase-mediated proteasomal degradation (Reese et al. 2000; DeRenzo et al. 2003). Whereas the degradation of MEI-1 is thought to be mediated by MEL-26 E3 ligase, the degradations of these zinc finger proteins require the E3 ligase, ZIF-1 (DeRenzo et al. 2003; Furukawa et al. 2003; Pintard et al. 2003; Xu et al. 2003). ZIF-1-mediated degradation is thought to be essential for embryogenesis as the depletion of *zif-1* results in embryonic lethality (DeRenzo et al. 2003). *mbk-2* depleted embryos showed delays in the degradation of PIE-1, MEX-5, and POS-1, suggesting that MBK-2 directly or indirectly regulate ZIF-1-mediated proteasomal degradation (Pellettieri et al. 2003).

2-1 c. OMA-1 degradation

As described in detail below, OMA-1 is another CCCH zinc finger protein previously suggested in oocyte maturation (Detwiler et al. 2001). OMA-1 protein is maternally provided and becomes rapidly degraded at the first mitotic division (Lin 2003). Although the mechanism mediating the OMA-1 degradation at the first mitosis was not previously characterized, this degradation event has been thought to be critical for embryogenesis, because a gain-of-function mutation, *oma-1(zu405)* delays the degradation timing of OMA-1 and causes embryonic lethality (Lin 2003). Unlike MEI-1 and PIE-1/MEX-5/POS-1, OMA-

1 degradation does not rely on MEL-26 or ZIF-1 (DeRenzo et al. 2003)(Yuichi Nishi and Rueyling Lin, unpublished results). *mbk-2* RNAi resulted in a severe delay in OMA-1 degradation (Pellettieri et al. 2003). Interestingly, a previous study showed that *oma-1(zu405)* mutant exhibits a degradation delay of PIE-1, MEX-5, and POS-1 (Lin 2003). Thus it is possible that the degradation delay of PIE-1, MEX-5, and POS-1 in the *mbk-2* mutants is secondary to the mis-regulation of OMA-1.

2-2. Proposed activation of MBK-2 after meiosis I

Consistent with its roles during and shortly after oocyte-to-embryo transition, MBK-2 is thought to be activated during the transition, shortly after meiosis I, based on the following two observations. First, the completion of meiosis I is a prerequisite for *mbk-2* dependent processes (Pellettieri et al. 2003). In meiosis I-arresting *mat-1* mutant embryos, *mbk-2* dependent processes at the 1-cell stage, the polarization of POS-1 and the degradation of OMA-1 and MEI-1 did not occur (Pellettieri et al. 2003). On the other hand, an *mbk-2* independent process, the polarization of PIE-1 at the early 1-cell stage, was observed in the *mat-1* mutant (Pellettieri et al. 2003). Secondly, GFP::MBK-2 localization dramatically changes shortly after meiosis I. GFP::MBK-2 was uniformly localized on the cortex in the oocyte and early 1-cell stage until the completion of meiosis I (Pellettieri et al. 2003). The cortical GFP::MBK-2 localization changes abruptly and dramatically to exhibit punctuating pattern after meiosis I (Pellettieri et al. 2003). This change in localization has been proposed to coincide with the activation of MBK-2 (Pellettieri et al. 2003; Stitzel et al. 2006). Indeed, the change in GFP::MBK-2 localization and the execution of *mbk-2*-dependent process

coincide. In a *mat-1* mutant, in which *mbk-2*-dependent processes fail to occur (see above), the change in GFP::MBK-2 localization did not happen (Pellettieri et al. 2003). On the other hand, the depletion of *wee-1* resulted in a precocious change in GFP::MBK-2 localization and a coinciding precocious excecution of a *mbk-2*-dependent process in the oocyte (Stitzel et al. 2006).

The requirement of the completion of meiosis I indicates that oocyte maturation is required for MBK-2 activation, because the completion of meiosis I requires the completion of oocyte maturation (Detwiler et al. 2001). Furthermore, a recent study showed that the change in GFP::MBK-2 localization at the normal kinetics requires fertilization (McNally and McNally 2005), suggesting that multiple layers of temporal control exist for MBK-2 activation during oocyte-to-embryo transition.

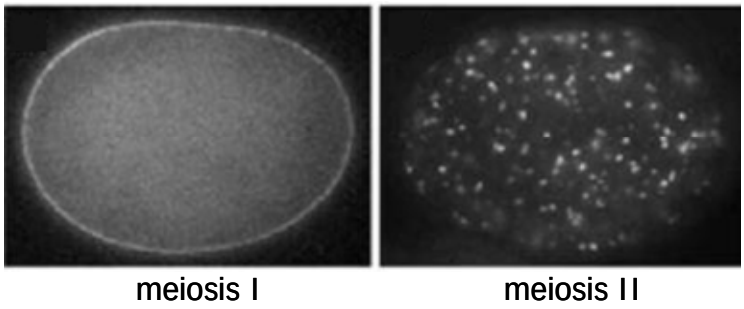

Figure 1.6 GFP::MBK-2 localization dynamically changes after meiosis I (Reproduced from Pelletieri *et al.* 2003)
1-cell stage embryos at meiosis I and meiosis II expressing GFP::MBK-2 transgene.

GSK-3 in Early Embryogenesis

1. Biochemistry of GSK-3 – +4 priming rule -

Another proline directed serine/threonine kinase, GSK-3 has been implicated in a number of cellular processes including early embryogenesis (Woodgett 2001). GSK-3 kinase is unique among serine/threonine kinases in that it requires pre-phosphorylation, or priming phosphorylation, on most of its substrates (Frame et al. 2001). Importantly, GSK-3 kinase is active in most cell types, thus the priming phosphorylation determines when and where GSK-3-mediated phosphorylation should happen. Hence, the priming is a key aspect in understanding GSK-3 function. By far the best known mode of GSK-3 priming is +4 site phosphorylation (Frame et al. 2001). For many GSK-3 substrates, 4 residues C-terminal to the serine/threionine phosphorylated by GSK-3 is serine or threonine (+4 site), and phosphorylation by another kinase on +4 residue (priming phosphorylation) enhances GSK-3 phosphorylation greatly (400-1000-fold) (Frame et al. 2001)(Figure 1.7).

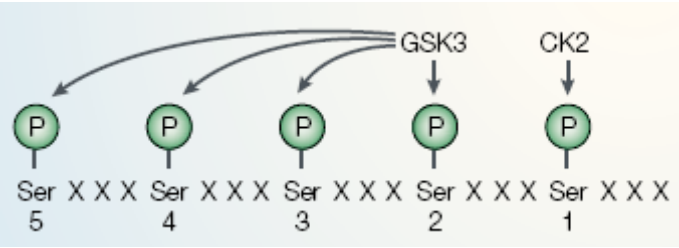

Figure 1.7 +4 site priming allows phosphorylation by GSK-3 (Reproduced from Cohen, P and Frame, S, 2001)
Schematic representation of GSK-3 phosphorylation site on glycogen synthase. CK2 phosphorylation on +4 site (marked as Ser1) allows GSK-3 phosphorylation at Ser2 through Ser 5 residues (Fiol et al. 1987). Note that all 5 serines are separated by 3 residues, allowing for sequential phosphorylation by GSK-3 at Ser3-5.

2. Genetic roles of GSK-3 in early embryos

GSK-3 plays multiple critical roles during embryogenesis including its well-known function in canonical Wnt pathway (Logan and Nusse 2004). In both frog and fly

development, GSK-3 controls patterning and cell fate decisions via negatively regulating a Wnt signaling effecter, β-catenin (Woodgett 2001). In the absence of the Wnt signal, GSK-3 phosphorylates β-catenin to induce its proteasomal degradation (Peifer et al. 1994; Aberle et al. 1997). Upon a stimulation of the Wnt signaling, the GSK-3 phosphorylation is interrupted, resulting in the stabilization of β-catenin and β-catenin-dependent transcriptional events (Peifer et al. 1994; Aberle et al. 1997). The GSK-3-mediated canonical Wnt pathway is employed in various developmental processes including the dorsal-ventral axis formation in *Xenopus* and segment polarity determination in *Drosophila* (DiNardo et al. 1985; Dickinson and McMahon 1992). GSK-3 is also involved in many other developmental events including hedgehog signaling- and insulin/IGF signaling-mediated cell fate determination processes (Logan and Nusse 2004).

During *C. elegans* early embryogenesis, the EMS blastomere of the 4-cell stage rotates its mitotic spindles and produces daughters with different developmental potentials (Goldstein 1992; Goldstein 1995). Both spindle rotation and differential cell fate decision require an inductive Wnt signaling from a neighboring blastomere (Goldstein 1992; Rocheleau et al. 1997; Thorpe et al. 1997). *gsk-3* depletion phenocopies mutants of Wnt signaling components with respect to the spindle rotation and the EMS cell fate decision defects, suggesting that GSK-3 positively regulate the Wnt pathway in the early *C. elegans* embryo (Schlesinger et al. 1999). In addition, GSK-3 appears to have a Wnt-independent function at the 4-cell stage. The transcription factor SKN-1 has an essential role in determining the cell fate of the EMS blastomere (Bowerman et al. 1992; Bowerman et al. 1993). GSK-3 has been shown to regulate SKN-1 via direct phosphorylation in an adult *C. elegans* tissue and is

implied to regulate SKN-1 in a similar manner at the 4-cell stage (Maduro et al. 2001; An et al. 2005). Thus GSK-3 might regulate the EMS fate in Wnt-dependent and independent manners in the early *C. elegans* embryo.

IV. OMA-1/2 and oocyte-to-embryo transition

1. Redundant genetic role of *oma-1* and *oma-2* in oocyte maturation

Two closely related *C. elegans* paralogs, *oma-1* and *oma-2* are redundantly required for oocyte maturation during oocyte-to-embryo transition (Detwiler et al. 2001). Although single loss-of-function mutant of *oma-1* or *oma-2* does not exhibit sterility, the simultaneous inactivation of both genes results in fully penetrant sterility, which cannot be rescued by the introduction of wild-type sperm (Detwiler et al. 2001). Conversely, *oma-1(-); oma-2(-)* homozygous males can fertilize wild-type hermaphrodites as efficiently as wild-type males, indicating female specific sterility (Detwiler et al. 2001). Further characterizations revealed specific defects during oocyte maturation. In the *oma-1(-); oma-2(-)* mutant oocyte exposed to an oocyte maturation signal, chromosomes do not form a metaphase plate, and AIR-2/*Eg2*, which normally localizes to the chromosome upon maturation, does not become associated with the chromosome (Detwiler et al. 2001). On the other hand, MAPK activation occurred at least initially, and the nuclear envelope, although not breaking down completely, showed a disrupted appearance (Detwiler et al. 2001). Furthermore, overall oocyte appearance in the *oma-1(-); oma-2(-)* mutant is maturation signal dependent. In the absence of a maturation signal, wild-type and mutant oocytes exhibit similar apparences, however, in the presence of sperm, mutant oocytes show an appearance distinct from the wild-type (Detwiler et al. 2001).

These results suggest that *oma-1* and *oma-2* are redundantly required for the completion, but not initiation, of oocyte maturation (Detwiler et al. 2001).

2. OMA-1/2 are Tis-11-like CCCH zinc finger proteins

oma-1 and *oma-2* encode highly related proteins sharing 64% identity throughout their 407 and 393 amino acid coding sequences. The biochemical function of OMA-1/2 proteins is unknown, however, as discussed below, they are suspected to be RNA-binding translational regulators.

OMA-1/2 belong to Tis11-like CCCH zinc finger protein family. This protein family is characterized by the presence of 2 copies of CCCH zinc finger domain. Family members share high sequence similarities within the zinc finger domain, however, similarities outside the domain are typically very poor. Tis-11-like CCCH zinc finger protein family include mammalian Tis11, and *C. elegans* OMA-1/2, PIE-1, POS-1, MEX-1 and MEX-5/6. For most family members, biochemical functions have not been experimentally determined, however, recent studies began to establish this protein family as RNA-binding translational regulators (Carballo et al. 1998; Huang et al. 2002; Ogura et al. 2003; Brown 2005). A well studied example is mammalian Tis-11. Tis-11 is a cytoplasmic protein shown to control inflammatory response via translational regulation (Carballo et al. 1998). Tis-11 achieves this task by repressing the translation of TNFα via direct binding to the 3'UTR of TNFα transcript in a signal dependent manner (Carballo et al. 1998). Consistent with its biochemical function, a mouse Tis-11 mutant shows TNFα misregulation and impaired inflammatory response (Carballo et al. 1998). In *C. elegans,* PIE-1, POS-1, MEX-1, and

MEX-5/6 are critical for early embryogenesis (Mello et al. 1992; Tabara et al. 1999; Schubert et al. 2000). Like mammalian Tis-11, POS-1 and MEX-5/6 have been shown to regulate translation via direct binding to the 3'UTR of their target transcripts, and PIE-1 has been speculated to regulate its target in a similar manner (Tenenhaus et al. 2001; Huang et al. 2002; Ogura et al. 2003; Tenlen et al. 2006).

3. Exclusive expression in oocytes and 1-cell embryo

OMA-1/2 are cytoplasmic proteins expressed in an essentially identical pattern starting in developing oocytes and peaking in the maturing oocyte, consistent with their cell autonomous role in oocyte maturation (Detwiler et al. 2001) (Figure 1.8). Interestingly, OMA-1/2 expression remains high for approximately 1 hour after oocyte maturation until the first mitotic division, when the expression level abruptly declines (Lin 2003)(Figure 1.8).

The expression of OMA-1/2 proteins in the germline gonad/oocyte is regulated partly via translational repression mediated by the KH-domain protein, GLD-1. Although *oma-1/2* transcripts are present in both pachytene region and developing oocytes, OMA-1/2 proteins are absent in the pachytene region where GLD-1 is expressed (Jones et al. 1996; Detwiler et al. 2001). GLD-1 physically interacts with the 3'UTR of *oma-1/2* transcripts, and OMA-1/2 proteins are precociously expressed in the *gld-1(-)* mutant gonad, consistent with GLD-1 directly repressing OMA-1/2 translation (Lee and Schedl 2001b; Lee and Schedl 2004). As GLD-1 protein diminishes via an unknown mechanism in late oocytes, OMA-1/2 proteins begin to accumulate and eventually peak in the maturing oocyte (Detwiler et al. 2001).

Unlike the initiation of OMA-1/2 expression mediated by GLD-1, the molecular mechanism dictating the termination of OMA-1/2 expression has been enigmatic. OMA-1/2 proteins remain expressed throughout the 1-cell stage, followed by an abrupt and rapid decline at the first mitotic division (Lin 2003)(Figure 1.8). GLD-1 is absent in the 1-cell stage embryo, thus this decline of OMA-1/2 expression is not due to increased GLD-1-dependent translational repression (Jones et al. 1996). The rapid kinetics of the decline implies tightly regulated protein degradation, however, the exact mechanism(s) controlling this precisely timed protein destruction was unknown (Lin 2003).

4. *oma-1(zu405)* causes a delay in OMA-1 protein degradation and lethality

Genetic evidence has suggested, however, that the timing of OMA-1/2 protein degradation is critical for embryogenesis. *oma-1(zu405)* is a temperature sensitive, maternal effect mutation in the *oma-1* coding sequence (Lin 2003). The mutation causes a severe delay in OMA-1 degradation (Lin 2003). Consistent with the importance of the degradation timing, *oma-1(zu405)* shows a fully penetrant embryonic lethality at a restrictive temperature (Lin 2003). *oma-1(zu405)* mutation changes proline 240 to leucine (Lin 2003). In an agreement with its importance in OMA-1 protein degradation, P_{240} is part of a potential PEST sequence (Lin 2003). PEST motifs are generally associated with protein degradation, although the mechanism by which the PEST motif promotes OMA-1 protein degradation was unknown (Rogers et al. 1986; Lin 2003).

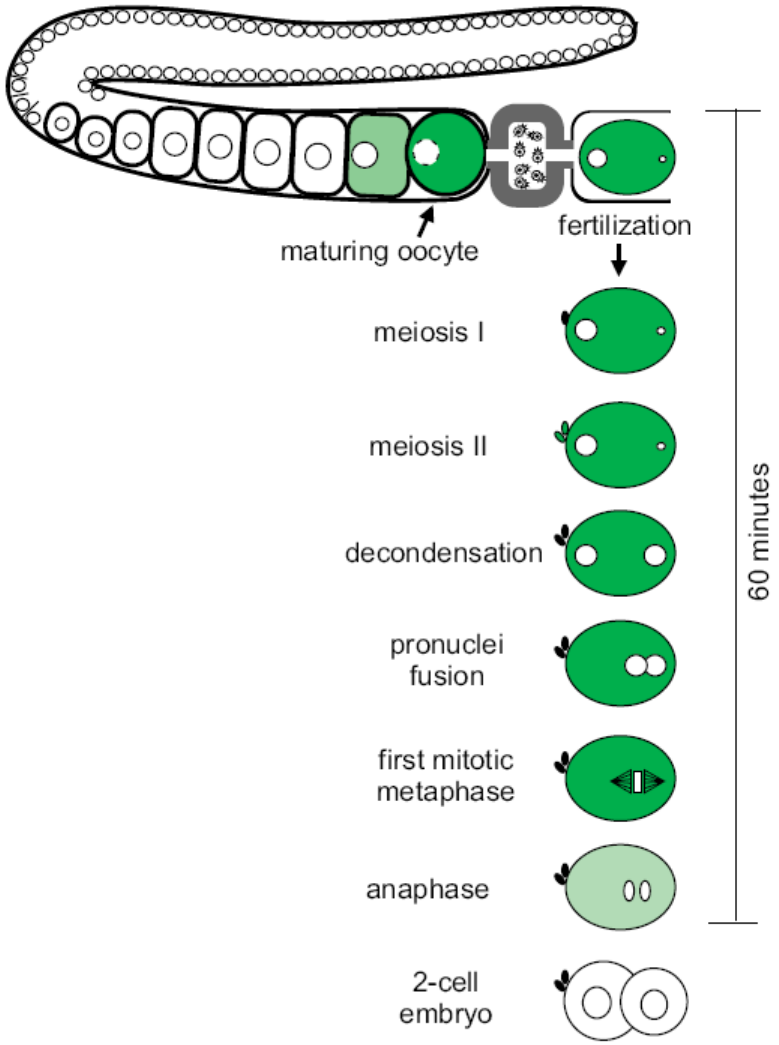

Figure 1.8 Expression of OMA-1 and OMA-2 proteins
OMA-1 and OMA-2 proteins are expressed essentially in an identical pattern (indicated by green filling). OMA proteins accumulate in late oocytes and peak in maturing oocyte and 1-cell embryo. OMA-1/2 proteins are excluded from the nucleus. Their expressions decline abruptly at the end of 1-cell stage.

oma-1(zu405) mutation results in a cell fate transformation that leads to abnormally large pharynx and intestine (Lin 2003). A mis-expression of transcription factor, SKN-1 has been attributed to the cell fate transformation leading to the gross terminal phenotype (Lin 2003).

However, careful examinations revealed that several other cell fate determinants are also mis-localized at early embryonic stages (Lin 2003). These mis-regulated factors include the KH domain protein, MEX-3, and the CCCH zinc finger proteins that are targeted to ZIF-1-mediated proteasomal degradation, PIE-1, MEX-1, MEX-5, and POS-1 (Lin 2003). All of these factors are essential cell fate determinants localized in specific patterns in the early embryo, thus their mis-regulations in *oma-1(zu405)* mutant are likely to contribute to the lethality and phenotype of the mutant (Mello et al. 1992; Draper et al. 1996; Mello et al. 1996; Tabara et al. 1999; Schubert et al. 2000).

Unlike *oma-1(-); oma-2(-)* mutant, *oma-1(zu405)* or *oma-1(zu405); oma-2(RNAi)* mutant does not show an oocyte maturation defect, indicating that OMA-1 *zu405*/P_{240}L is functional in oocyte maturation (Lin 2003). As discussed below, previous data implicate (a) function(s) of OMA-1/2 in embryogenesis. Although clearly functional for oocyte maturation, the functionality of OMA-1 P_{240}L protein for embryogenesis has not been examined. Thus potentially, an alteration of OMA-1 protein property and OMA-1 degradation delay could both contribute to the phenotypes of *oma-1(zu405)*.

5. Potential embryonic function of OMA-1/2

Developmental defects of *oma-1(zu405)* mutant imply that OMA-1/2 have developmental function(s) (Lin 2003). Additionally, my previous genetic analysis also implied that *oma-1/2* are important for embryogenesis because a double reduction-of-function mutant of *oma-1/2* shows impenetrant oocyte maturation defect and produces dead embryos (Nishi and Lin 2005). Intriguingly, OMA-1/2 expression persist throughout the 1-cell stage, for

approximately 60minutes after oocyte maturation (Figure 1.8)(Lin 2003). This persistence is not due to the absence of general protein degradation activity, because protein degradation can be detected as early as meiosis II (Srayko et al. 2000; Liu et al. 2004; Sonneville and Gonczy 2004). Thus the persistence of OMA-1/2 expression through the 1-cell stage implies their role in the 1-cell embryo. Together, OMA-1/2 might have a developmental function at the 1-cell stage. However, direct assessments of such a role have been hampered by the fully penetrant oocyte maturation defect of *oma-1(-); oma-2(-)* mutant (Detwiler et al. 2001). The 1-cell embryo has a critical task to initiate embryogenesis. A number of processes rendered dormant in the oocyte need to be activated in coordinated manners at or shortly after the 1-cell stage. An interesting possibility is that OMA-1/2 control developmental processes in the oocyte and 1-cell stage embryo to regulate the initiation of embryogenesis.

In this study, I investigated mechanisms regulating the OMA protein degradation at the end of the 1-cell stage and the developmental functions of OMA-1/2 at the 1-cell stage. First, I showed that likely sequential phosphorylation by MBK-2/DYRK2 and GSK-3 marks OMA proteins for degradation at the end of the 1-cell stage, likely via SCF and/or ECS E3 ligase-mediated ubiquitination and proteasomal degradation. Second, I performed genetic and protein-protein interaction analyses to investigate OMA-1/2 function, particularly in the 1-cell stage embryo. These analyses suggest multiple functions for OMA-1/2. I showed that a general transcription factor, TAF-4 physically interacts with OMA-1 and that the intracellular localization of TAF-4 correlates with polII-dependent transcriptional activity during early embryogenesis. On the other hand, translational regulators, MEX-3, GLD-1, and SPN-4

physically interact with OMA-1 and translation factors, *puf-3/5* and *cpb-3*/CPEB genetically interact with *oma* mutations, suggesting OMA-1/2 in translational regulation. Additionally, thes analyses identified two candidate OMA target processes, GLD-1 expression and ZIF-1-mediated protein degradation. GLD-1 protein expression and ZIF-1-dependet proteasomal degradation are repressed in *oma-1(zu405)* mutant, whereas *oma-1/2* depleted animals show precocious GLD-1 expression and ZIF-1-mediated degradation activity. Lastly, my analyses suggest that phosphorylation of OMAs at the 1-cell stage is important for their proper embryonic function. Specifically, phosphorylation of OMA-1/2 is likely to negatively control ZIF-1-mediated proteasomal degradation. These results suggest that MBK-2/DYRK2 and GSK-3 phosphorylation at the 1-cell stage regulates embryonic development by controlling the function and degradation of OMA proteins, and implicate developmental functions of OMAs in the 1-cell embryo.

CHAPTER TWO

REGULATION OF OMA-1/2 PROTEIN DEGRADATION IN 1-CELL EMBRYO

MBK-2/DYRK2 and GSK-3 Phosphorylation Marks OMA-1/2 for Ubiquitin-Proteasome Mediated Degradation

Summary

Previous studies showed that OMA proteins are specifically expressed in the developing oocyte and 1-cell embryo. OMA protein expression declines abruptly and rapidly at the first mitotic division likely due to protein degradation. The properly timed OMA degradation at the first mitosis is thought to be critical for embryogenesis because *oma-1(zu405)* mutation results in a delay in OMA-1 degradation and fully penetrant embryonic lethality. In this chapter, I show that likely sequential phosphorylation of OMA proteins by MBK-2 at T_{239} and GSK-3 at T_{339} marks OMAs for proteasomal degradation. *In vivo*, MBK-2 phosphorylation occurs shortly before OMA protein degradation at the 1-cell stage. *oma-1(zu405)*/$P_{240}L$ mutation interferes with MBK-2 phosphorylation at $T_{239,}$ providing a molecular explanation for the OMA-1 degradation delay in *oma-1(zu405)* mutant. Furthermore, my RNAi analysis suggests that SCF and/or ECS ubiquitin E3 ligase execute OMA protein degradation via the proteasome pathway, likely in response to the MBK-2 and GSK-3 phosphorylation. In summary, my data suggest that a critical step of oocyte-to-embryo transition, temporally regulated OMA protein degradation, is regulated by a cascade of phosphorylation and ubiquitination events in the 1-cell embryo.

INTRODUCTION

OMA protein expression declines abruptly and rapidly likely via protein degradation at the first mitotic division (Lin 2003). The rapid kinetics implies a tight temporal regulation and the importance of the degradation timing. Consistently, *oma-1(zu405)* that causes a delay in OMA-1 protein degradation, exhibits embryonic lethality, suggesting that the degradation timing is critical for embryogenesis (Lin 2003). Although it was shown that the amino-acid residue changed in *zu405* allele, P_{240}, is a part of a potential PEST motif, which is generally associated with protein degradation, genetic and molecular mechanisms underlying the temporal regulation of OMA protein degradation was unclear (Rogers et al. 1986; Lin 2003).

Mutants of the *C. elegans* DYRK2 homolog, *mbk-2* show defects in early embryogenesis, including abnormal cell divisions and delays in the degradation of maternal proteins: MEI-1, PIE-1, MEX-5, POS-1 and OMA-1 (Pellettieri et al. 2003; Quintin et al. 2003; Raich et al. 2003; Pang et al. 2004). MBK-2 is proposed to be activated after meiosis I based on molecular and genetic evidence (Pellettieri et al. 2003). The lack of MBK-2-mediated phosphorylation events is likely to be responsible for the embryonic *mbk-2* phenotypes because its kinase activity is essential for genetic rescue of the embryonic phenotypes (Stitzel et al. 2006). However, no substrate of MBK-2 was identified previously.

GSK-3 is another kinase implicated in *C. elegans* embryogenesis. GSK-3 has been suggested in developmental events at the 4-cell stage (Schlesinger et al. 1999; Maduro et al. 2001). GSK-3 is unique among kinases in that it is constitutively active in many tissues and

developmental stages (Woodgett 2001). The phosphorylation by GSK-3 is typically regulated by pre-phosphorylation, or priming phosphorylation, on its substrates (Frame et al. 2001). The best known priming is +4 site phosphorylation (4 residues C-terminal to a GSK-3 target S/T residue). GSK-3 exhibits 400- to 1,000-fold higher activity toward substrates phosphorylated at +4 site, thus such pre-phosphorylation functions as an on/off switch for GSK-3 phosphorylation (Fiol et al. 1987; Frame et al. 2001). Although this +4 site-priming is widely observed for many different substrates, existence of other types of priming is an open question.

Like phosphorylation, ubiquitin-proteasome mediated protein degradation is a tightly controlled process shown to be critical for many biological functions. The proteasomal protein degradation is initiated by the conjugation of a small protein, ubiquitin, to lysine residues of degradation targets by a set of enzymes, ubiquitin-activating enzyme (E1), ubiquitin-conjugating enzyme (E2), and E3 ubiquitin ligase (Coux et al. 1996; Hershko and Ciechanover 1998). In most cases, the E3 ligase makes a direct contact with its ubiquitination substrate and determines the substrate specificity of the conjugation reaction (Coux et al. 1996; Hershko and Ciechanover 1998). SCF and ECS E3 ligases have drawn attention recently due to their unique multi-subunit, modular structures and involvements in many important biological processes (Deshaies 1999). The SCF complex comprises a small RING finger protein Rbx1, Skp1, Cullin1, and a substrate binding subunit, F-box protein (Deshaies 1999). ECS uses Rbx1, ElonginB, ElonginC, Cullin2, and a SOCS box-containing substrate binding subunit (Kile et al. 2002). Although Rbx1 is the only common peptide between SCF and ECS, SCF and ECS show striking resemblance at the structure level

(Deshaies 1999; Kile et al. 2002). The substrate recognition by SCF is well known for being phosphorylation dependent (Skowyra et al. 1997). For example, a CDK inhibitor, Sic1 is ubiquitinated by SCF only when Sic1 is phosphorylated by the Cdc28 kinase at late G1 (Krek 1998; Nash et al. 2001). On the other hand, the contribution of substrate phosphorylation for ECS-mediated ubiquitination is less clear. Instead, proline hydroxylation is known to regulate ECS-mediated ubiquitination of HIF-1 (Ivan et al. 2001; Jaakkola et al. 2001). Whether or not proline hydroxylation is a general regulation of ECS ubiquitination is unclear at this point.

In this chapter, I present my data suggesting that specific phosphorylation and ubiquitination reactions of OMA-1/2 promote their proteasomal degradation at the end of the 1-cell stage. I show that MBK-2/DYRK2 phosphorylates OMA-1 at T_{239}, and this phosphorylation occurs shortly before the OMA-1 degradation at the 1-cell stage. The *zu405* mutation, $P_{240}L$, greatly diminishes the MBK-2 phosphorylation on T_{239}, suggesting that the degradation delay seen in *oma-1(zu405)* mutant is likely due to a decrease in MBK-2-mediated T_{239} phosphorylation. Furthermore, I show that GSK-3 phosphorylates OMA-1 on T_{339} and this phosphorylation is critical for OMA-1 degradation. Imporantly, my biochemical analysis suggests that the GSK-3 phosphorylation at T_{339} is facilitated by the MBK-2 phosphorylation at T_{239}, thus MBK-2 and GSK-3 phosphorylation are likely to be sequential. My attempts to reveal the molecular pathway linking the phosphorylation and proteasomal degradation of OMA proteins identified components of E3 ligases potentially responsible for the ubiquitination of OMA proteins in the 1-cell embryo. They are SCF and ECS components that I show are required for the OMA-1 degradation *in vivo*, suggesting that

either or both SCF and ECS E3 ligases ubiquitinate OMA proteins to target them for proteasomal degradation, likely in response to the MBK-2 and GSK-3 phosphorylation.

EXPERIMENTAL PROCEDURES

Strains

N2 was used as the wild-type strain (Brenner 1974). Genetic markers used are: LGII, *rrf-3(pk1426);* LGIII, *unc-119(ed3)*; LGIV, *oma-1(te33), oma-1(zu405), mbk-2(pk1427), teIs1*{pRL475 (*$P_{oma\text{-}1}$oma-1::gfp), pDPmm016[unc-119 (+)]*}; LGV, *oma-2(te51), nT1(IV;V)*, LG unknown: *teIs75*{pRL475 (*$P_{oma\text{-}1}$oma-1::gfp), pDPmm016[unc-119 (+)]*}. Transgenic strains were generated by microparticle bombardment (Praitis et al. 2001) and consistency of expression patterns was confirmed in at least three independent lines. The following representative integrations were selected for detailed analyses: *teIs20[pRL1284 ($P_{oma\text{-}1}$oma-1ΔN::gfp)]*; *teIs21[pRL1285 ($P_{oma\text{-}1}$oma-1ΔN $_{T239A}$::gfp)]*; *teIs23[pRL1287($P_{oma\text{-}1}$oma-1ΔN $_{T239A\ S302A}$::gfp)]*; *teIs22[pRL1286 ($P_{oma\text{-}1}$oma-1ΔN $_{S302A}$::gfp)]*; *teIs61[pRL1337($P_{oma\text{-}1}$oma-1ΔN $_{T339A}$::gfp)]*; *teIs27[pRL1343 ($P_{oma\text{-}11}$oma-1ΔN $_{T239D}$::gfp)]*; *teIs69[pRL1600($P_{oma\text{-}11}$oma-1ΔN $_{T239E}$::gfp)]*; *teIs68[pRL1599($P_{oma\text{-}11}$oma-1ΔN $_{S331D\ S335D\ T339A}$::gfp)]*, *teIs81[pRL1951($P_{oma\text{-}1}$oma-1_{S302A}::gfp)]*.

Plasmid Construction

All expression clones except OMA-1(S_{302}A)::GFP clone were generated using the Gateway technology (Invitrogen). All site-directed mutagenesis was performed using the Quick Change kit (Stratagene).

For Transgenesis

To construct the full-length OMA-1::GFP clone harboring $S_{302}A$ mutation (pRL1951), site-directed mutagenesis was performed on pRL475, which contains a genomic *oma-1* loci with 2.1 kb upstream, and 2.7 kb downstream of the OMA-1 coding sequence (Lin 2003). To generate ΔN OMA-1::GFP translational reporter, cDNA-derived OMA-1 coding sequence (amino acids 111-407) was shuttled from a Gateway donor vector to the $P_{oma\text{-}1}gfp$ destination vector, pRL781 via the Gateway LR recombination reaction (Invitrogen). To construct the $P_{oma\text{-}1}gfp$ destination vector pRL781, the Nae I fragment downstream of the *oma-1* locus was deleted from pRL475 (Lin 2003), then most of the *oma-1* coding sequence was replaced with the Gateway cassette frame A (Invitrogen) using the HpaI and NotI sites in the coding sequence. A rescuing *unc-119* PvuII fragment from pDP#mm016B (a gift from Morris Maduro, UC Riverside) was inserted at the EcoRV site in the vector backbone, resulting in pRL781. pRL781 contains 2.1 kb upstream, and 1 kb downstream of the OMA-1 coding sequence and a rescuing *unc-119* genomic fragment, which was used to select for transformants following microparticle bombardment (Praitis et al. 2001).

For Biochemistry

pMALp2X(NEB)-derived destination vector, pDEST MAL was LR-recombined with cDNA-derived full-length OMA-1, CYB-1, or MBK-2 coding sequence to express N-terminal MBP-fusions in *E.coli.* Similarly, pcDNA3.1(Invitrogen)-derived FLAG-tag destination vector, pRL1312 was recombined with cDNA-derived *C. e*GSK-3 full-length coding sequence to

express N-terminally FLAG-tagged *C. e* GSK-3 in mammalian cultured cells. The following list is the expression clones used for the biochemical works in this chapter:

MBP::OMA-1: pRL1220 (WT), pRL1254 ($T_{239}A$), pRL1255($S_{302}A$), pRL1228($T_{239}A$ $S_{302}A$), pRL1256($P_{240}L$), pRL1257($P_{240}L$ $S_{302}A$), pRL1336($T_{339}A$), pRL1557($T_{239}A$ $T_{339}A$), pRL1496($T_{239}D$), pRL1499($T_{239}D$ $T_{339}A$), pRL1537($T_{239}E$), pRL1538($S_{331}A$ $S_{334}A$ $S_{335}A$ $S_{338}A$ $T_{339}A$ $S_{341}A$ $S_{346}A$ $S_{347}A$), pRL1597($S_{331}D$ $S_{335}D$ $T_{339}E$)

MBP::OMA-2: pRL1260(WT), pRL1572($T_{327}A$)

MBP::CYB-1: pRL1219 (WT)

MBP::MBK-2: pRL1221 (WT), pRL1229 ($Y_{237}A$ kinase dead)

FLAG::*C. e*GSK-3: pRL1510 (WT), pRL1513 ($Y_{196}F$ kinase dead)

For RNAi

The *gsk-3* and *elc-1* feeding RNAi clones, pRL1516 and pRL1822 contain respective spliced full-length coding sequence in pDONRdT7, which produces double-stranded RNA in *E.coli* using T7 promoter and T7 terminator on each side of the insert (Reddien et al. 2005).

Following pPD129.36 (L4440)-based clones were isolated from the Ahringer library (Fraser et al. 2000; Kamath et al. 2003). The identities of the clones were verified by sequencing with M13-21 primer followed by an NCBI BLAST search. pRL-names are aliases given for convenience: pRL1843 (*rbx-1*), pRL2147 (*skr-1*), pRL2148 (*skr-2*), pRL1841 (*zyg-11*), pRL1805 (*elb-1*). pRL451 contains the entire spliced *oma-2* coding sequence in pPD129.36. RNAi clones for other *skr* genes were directly used from the Ahringer library without DNA purification or sequencing. Following feeding RNAi clones

are generous gifts from Dr. Edward Kipreos (University of Georgia, Athens) and contain full-length coding sequences in pPD129.36 (L4440): pRL1328 (*cul-1*), pRL1184 (*cul-2*), pRL1329 (*cul-3*), pRL1330 (*cul-4*). (pRL-names are aliases).

Kinase Assays

Protein purification

All substrates and kinases except for GSK-3 were MBP-tagged and produced in *E.coli*.

MBP fusions were produced in Rosetta (DE3) pLysS (Novagen) cells transformed with pMALp2X (New England Biolabs)-derived expression clones (see *Plasmid Construction*). For substrates, cells were sonicated in MBP binding buffer (20 mM Tris pH7.5, 200 mM NaCl, 1 mM EDTA, 1 mM DTT, Complete protease inhibitor [Roche]), then treated with 0.1U/µl DNase and 0.01µg/µl RNaseA. After centrifuge cleared, MBP-fusion protein was absorbed to amylose resin (New England Biolabs). Protein bound resin was washed three times with MBP binding buffer, then eluted with 10 mM maltose in MBP binding buffer. For MBK-2 kinase, cells were sonicated in MBP buffer and treated with 1% TritonX-100, DNase and RNaseA. Lysates were centrifuge cleared then diluted 5 times with MBP buffer and MBP::MBK-2 was absorbed to amylase resin. Because MBP::MBK-2 failed to elute from the resin efficiently, kinase-bound resin was used directly for kinase assay.

Because GST- and MBP-fused *C. e* GSK-3 purified from *E.coli* were inactive, *C. e* GSK-3 was produced and isolated from cultured human cells. Sixty hours after transfection with a pcDNA3.1-derived FLAG::*C. e*GSK-3 clone (see *Plasmid Construction*), HEK293T cells

were lysed in RIPA buffer (10 mM NaPO4 pH 7.2, 150 mM NaCl, 1% NP40, 1 mM EDTA) supplemented with Complete protease inhibitor [Roche], phosphatase inhibitor cocktail I [Calbiochem], and 1 mM $NaVO_4$. The lysate was centrifuge cleared and FLAG::GSK-3 was immunoprecipitated using protein G beads (Pierce) and anti-FLAG M2 antibody (Sigma). After washing beads 3 times with RIPA buffer and once with GSK-3 kinase reaction buffer (see *Kinase reaction*), FLAG::GSK-3 was eluted with kinase reaction buffer containing 1 mM FLAG peptide (Sigma). Recombinant Rabbit GSK-3β was purchased from New England Biolabs.

Kinase reaction

MBK-2 (25 mM HEPES pH7.6, 5 mM $MgCl_2$, 5 mM $MnCl_2$, 0.5 mM DTT, 30 nM cold ATP and 0.5 μCi [γ-^{32}P] ATP) and GSK-3 (20 mM Tris-Cl pH 7.2, 10 mM $MgCl_2$, 5 mM DTT, 30 nM cold ATP and 0.5 μCi [γ-^{32}P] ATP) kinase assays were performed at 25ºC for 15 and 10 minutes, respectively. Products were separated by SDS-PAGE and incorporation of ^{32}P was visualized by autoradiography.

RNA Interference (RNAi)

All RNAi experiments were performed using the feeding RNAi technique (Timmons and Fire 1998). Briefly, cultures of HT115 transformants were induced with 0.4mM IPTG for 3 hr at room-temperature before spin-concentrated 10 times and put onto NGM plates containing 1mM IPTG. Overnight saturated cultures were induced, except for *gsk-3*, which showed markedly stronger OMA-1 degradation delay phenotype by inducing during log-

phase. Bacteria-seeded RNAi plates were air-dried briefly at room-temperature then inoculated with worms at L1 stage. Plates were incubated at 25ºC, or 20ºC for *rrf-3* mutation-carrying strains, until the inoculated worms were scored at the young adult stage. *rrf-3* (*pk1426)* mutation was used for the tests for *skr* genes and *gsk-3* to enhance RNAi effect (Simmer et al. 2002). The test for *skr* genes were performed by directly inoculating *E.coli* transformants from the Ahringer library without DNA purification. For all other experiments, sequence verified plasmids (described above under *Plasmid Construction*) were freshly transformed into HT115.

OMA-1$_{S302A}$ rescue assay

Standard feeding RNAi (as described above) for *oma-2* was performed by putting L1 larvae of *oma-1(te33)*; $P_{oma\text{-}1}$*oma-1::gfp,* or *oma-1(te33)*; $P_{oma\text{-}1}$*oma-1(*S_{302}*A)::gfp* onto *oma-2* RNAi plates and incubating at 20ºC. At the same RNAi condition, *oma-1(te33)* animals show fully penetrant sterility. Fertility of the inoculated worms was scored for within a day after they reached adulthood. To score for embryonic lethality, embryos from 20 dissected adult worms were collected onto an agar pad prepared on a slide glass. A coverslip was overlaid and the slide was incubated in a humidifying chamber for 24hr at 20ºC. The number of embryos put on the slide and number of embryo stayed unhatched after the 24hr incubation were recorded to determine %hatch.

Antibody production and immunofluorescence

Anti-T_{239}-P antibody was generated by immunizing rabbits with the peptide [HPLEMFARPS**T**(PO_4)PDEPAAK] in which T_{239} (in bold) is phosphorylated. The antibodies were precleared with the non-phosphorylated peptide counterpart before being affinity-purified using the phosphorylated peptide (Bethyl Laboratory, Inc). The specificity of this antibody was demonstrated in two ways. First, in ELISA assays, the affinity-purified anti-T_{239}-P antibody reacts with the phosphorylated peptide (compared to the unphosphorylated counterpart or an unrelated peptide) with at least 100-fold higher affinity. Second, in the immunofluorescence assay, the cytoplasmic staining observed in 1-cell wild-type embryos was abolished in 1-cell *oma-1(zu405);oma-2(RNAi)* embryos (see text). However, this affinity-purified antibody fails to detect any protein in worm extracts or recombinant OMA-1 phosphorylated by MBK-2 as assayed by western blots.

Immunofluorescence of embryos using anti-T_{239}-P was performed as described (Lin et al. 1998) except with mild squashing for 5 minutes in 4% paraformaldehyde. In all staining, the anti-PIE-1 or anti-MEX-5 monoclonal antibody (Mello et al. 1996; Schubert et al. 2000) was used to co-stain the embryos to ensure proper fixation. Antibody dilutions: anti-T_{239}-P, 1/300, anti-PIE-1, 1/10, anti-MEX-5, 1/2, Alexa488 goat-anti-rabbit IgG, 1/250, Alexa568 goat-anti-mouse IgG, 1/250.

Analysis of embryos and imaging

Imaging live embryos was performed as described previously (Rogers et al. 2002). The filter wheels (Ludl Electronic Product) and shutter controller were driven by a custom software package (*os4d 1.0*, freely available upon request to jwaddle@mail.smu.edu).

RESULTS

I. MBK-2 phosphorylates OMA-1 *in vitro* primarily at T_{239}

1. *In vitro* phosphorylation of OMA-1/2 by MBK-2

To determine whether or not MBK-2 regulates OMA protein degradation directly, I tested whether MBK-2 phosphorylates OMA-1 and OMA-2 *in vitro*. Using bacterially purified MBK-2 and substrates, I showed that MBK-2 specifically phosphorylates MBP:OMA-1 and MBP:OMA-2, but not MBP:*C. e*cyclinB (CYB-1) (Figure 2.1B). Previously, the phosphorylation consensus for DYRK1 and DYRK2 was determined to be RXXS/TP (Himpel et al. 2000; Campbell and Proud 2002). OMA-1 and OMA-2 contain two such sites: T_{239} and S_{302} for OMA-1 and T_{227} and S_{291} for OMA-2 (Figure 2.1A). In the kinase assay, mutating T_{239} to alanine in OMA-1 greatly diminished phosphorylation, whereas the S_{302} to alanine mutation resulted in a mild, yet significant decrease, suggesting that T_{239} is the major MBK-2 phosphorylation site, whereas S_{302} is a secondary site (Figure 2.1B). T_{239}A S_{302}A simultaneous mutant showed a phosphorylation level very close to the background, suggesting that most of *in vitro* MBK-2 phosphorylation of OMA-1 happens via these two sites (Figure 2.1B).

The gain-of-function mutation, *oma-1(zu405)* exhibits a severe delay in OMA-1 degradation timing (Lin 2003). This mutation changes the residue adjacent to T_{239}, P_{240}, to leucine (Lin 2003). Previous studies on mammalian DYRK kinases showed that +1 proline (like P_{240}) is critical for DYRK phosphorylation (Himpel et al. 2000; Campbell and Proud 2002). These studies showed that the substitution of +1 proline to alanine severely diminishes DYRK phosphorylation, whereas the substitution to a more hydrophobic residue, valine results in a moderate reduction in kinase reaction efficiency (Himpel et al. 2000; Campbell and Proud 2002). Thus these results predict that P_{240}L mutation will interfere with MBK-2 phosphorylation at T_{239}. I tested this prediction using the kinase assay system. Indeed, P_{240}L substitution resulted in a decrease in MBK-2 phosphorylation to a similar degree as T_{239}A mutant (Figure 2.1C). Likewise, P_{240}L S_{302}A mutant exhibited a severe reduction similar to T_{239}A S_{302}A mutant (Figure 2.1C). These results demonstrate that the *oma-1(zu405)* mutation, P_{240}L, indeed interferes with MBK-2 phosphorylation at T_{239} *in vitro*. These results further suggest that OMA-1 degradation delay observed in *oma-1(zu405)* mutant is likely to be a result of reduced MBK-2 phosphorylation at T_{239}.

2. *In vivo* localization of OMA-1/T_{239} phosphorylation

Since *in vitro* kinase assay and *oma-1(zu405)* mutant together suggest that T_{239} phosphorylation by MBK-2 is important for OMA-1 degradation timing, *in vivo* distribution of T_{239} phosphorylation was analyzed. To this purpose, immunofluorescence analysis was performed using antibodies that specifically recognize OMA-1 phosphorylated at T_{239} (anti-T_{239}-P, see Experimental Procedure). This assay revealed exclusive cytoplasmic signal in the

1-cell embryo, consistent with the signal being OMA-1 (Figure 2.2A, conduced by Rueyling Lin). Strikingly, the signal was limited only to a narrow time window of the 1-cell stage embryo, starting after meiosis II until the first mitotic anaphase (0/9 at meiosis I, 0/4 at meiosis II, 25/25 after meiosis II to the first mitotic metaphase, 0/2 at the first mitotic anaphase, 0/11 at the 2-cell stage, Figure 2.2A). No signal was detected in later stage embryos (data not shown). Although OMA-1 is highly expressed in lates oocytes, no signal was detected in the oocyte with anti- T_{239}-P antibody (data not shown). Importantly, the onset and the end of the phosphorylation signal are in close proximities to the proposed MBK-2 activation after meiosis I, and OMA-1 degradation at the first mitosis, respectively (Pellettieri et al. 2003)(Figure 2.2A). This is consistent with the notion that T_{239} phosphorylation is carried out by MBK-2 *in vivo*, and the phosphorylation signal is of OMA-1. Indeed, embryos derived from *mbk-2(pk1427)* homozygous mutant failed to exhibit anti-T_{239}-P immunofluorescence signal (n>500), although OMA-1 protein is expressed in the mutant at the stages examined, indicating that T_{239} phosphorylation is MBK-2 dependent *in vivo* (Figure 2.2B) (Pellettieri et al. 2003). *oma-1(zu405)* mutation, $P_{240}L$, interfered with the MBK-2 phosphorylation in my kinase assay (Figure 2.1B). In this anti-T_{239}-P immunofluorescence assay, *oma-1(zu405); oma-2(RNAi)* embryo failed to show any signal (n>70), demonstrating the specificity of the antibody (Figure 2.2B, *oma-2* was depleted to avoid potential cross-reactivity to OMA-2. *oma-2* RNAi does not affect OMA-1 expression (Detwiler et al. 2001)). Although I cannot exclude the possibility that $P_{240}L$ substitution itself, not the absence of T_{239} phosphorylation, abolishes T_{239}-P signal, this immunofluorescence result and the *in vitro* kinase assay data (Figure 2.2B) collectively

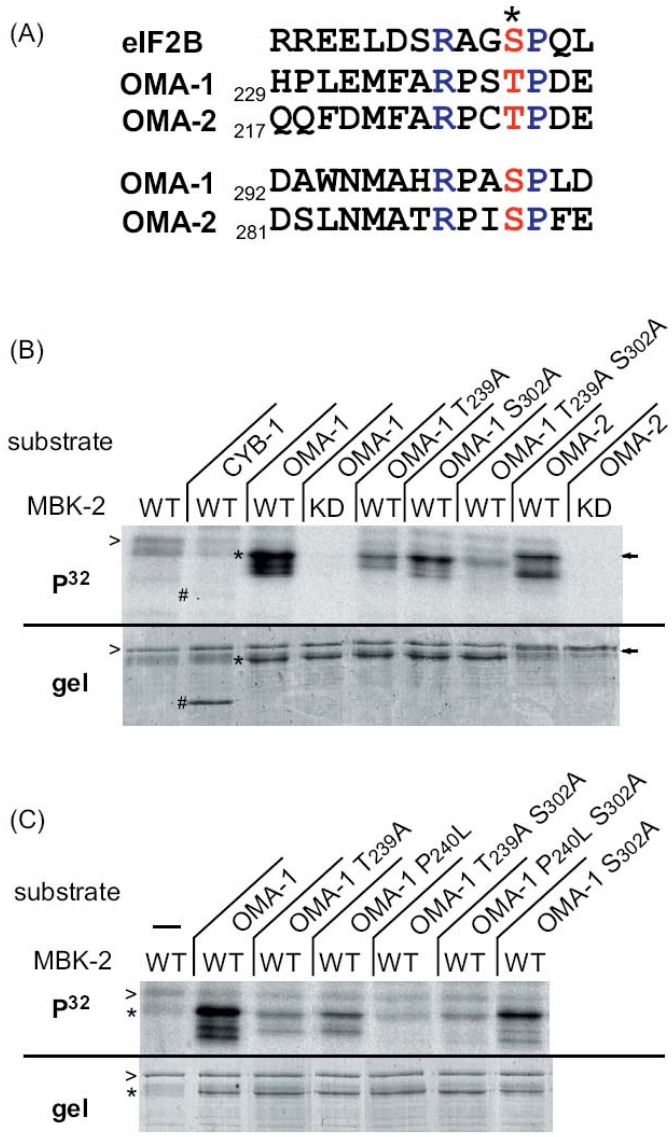

Figure 2.1 MBK-2 phosphorylates OMA-1 and OMA-2 *in vitro*

(a) Alignment of two regions of OMA-1 and OMA-2 with a known DYRK2 kinase substrate site in human eIF2B. Critical residues for DYRK phosphorylation are shown in blue. The residues phosphorylated are in red.

(b, c) *In vitro* kinase assay with MBK-2. Upper panel is autoradiography of coomassie stained gel shown in lower panel. Positions of each protein is marked as follows; MBK-2: >, CYB-1: #, OMA-1: *, and OMA-2: ←. Abbreviations: WT: wild-type, and KD: kinase dead mutant.

suggest that *in vivo*, *oma-1(zu405)* mutation impairs phosphorylation at T_{239}. *In vitro* phosphorylation of OMA-1 by MBK-2 at T_{239}, correlation between *in vivo* T_{239} phosphorylation and the proposed MBK-2 activation timing, and the dependence of *in vivo* T_{239} phosphorylation on *mbk-2* together strongly suggest that MBK-2 phosphorylates OMA-1 at T_{239} shortly before OMA-1 degradation at the first mitosis. The *in vitro* kinase assay and anti-T_{239}-P immunofluorescence assay suggest that *oma-1(zu405)* interferes with T_{239} phosphorylation *in vivo*. *oma-1(zu405)* mutation was previously shown to delay OMA-1 degradation (Lin 2003). Thus these data suggest that T_{239} phosphorylation by MBK-2 promotes OMA-1 degradation at the first mitosis.

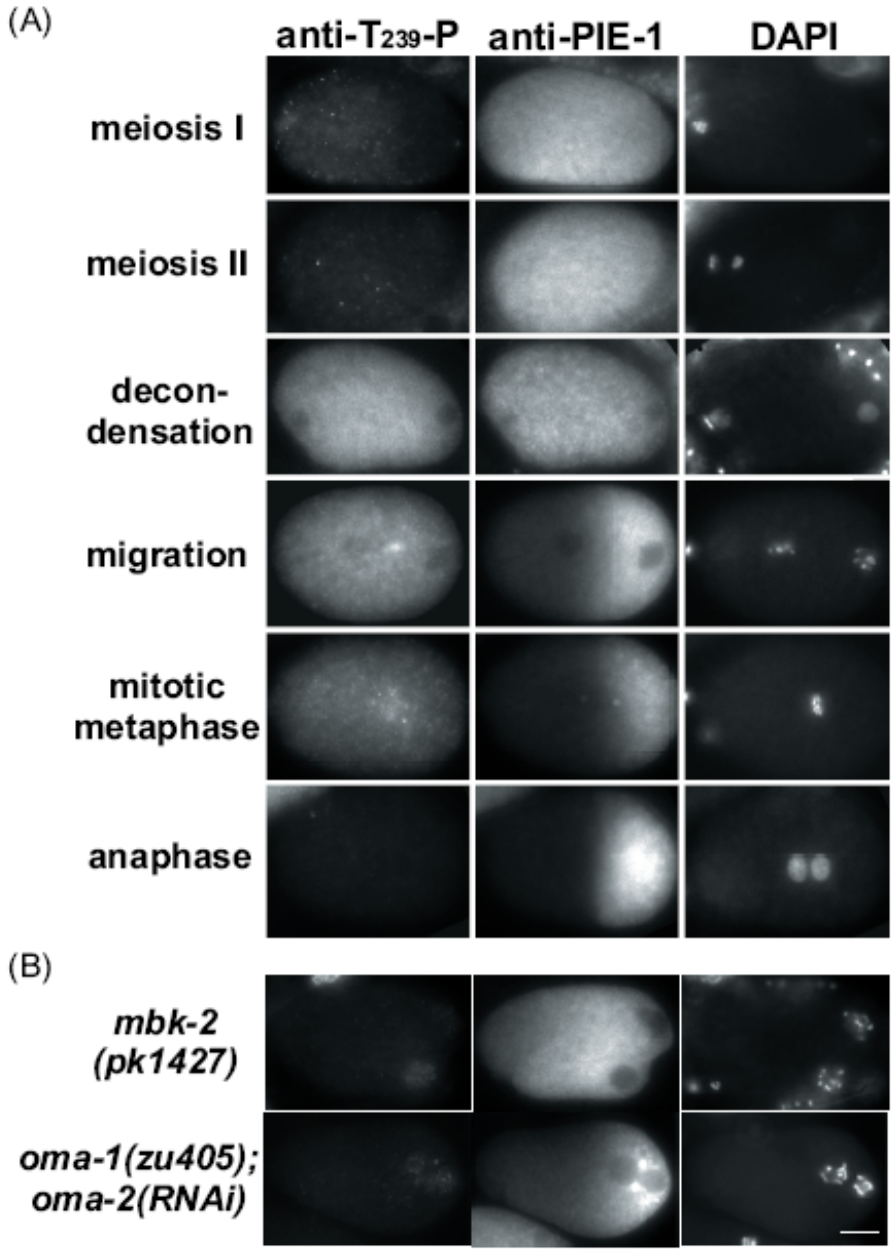

Figure 2.2 OMA-1 is phosphorylated at T_{239} *in vivo*
(Analysis performed by Rueyling Lin)

A. 1-cell stage embryos co-stained with anti-T239P (left column), anti-PIE-1 (middle column), and DAPI (right column).
B. Embryos at indicated genotypes at the pronuclear migration stage co-stained with anti-T239P, anti-PIE-1, and DAPI.

II. GSK-3 phosphorylates OMA-1/2 at T_{339}

1. *In vitro* phosphorylation of OMA-1/2 by GSK-3

GSK-3 kinase was previously identified as a factor required for the proper OMA-1 degradation timing (Manisha Patel and Rueyling Lin). The depletion of *gsk-3* severely delays the degradation timing of OMA-1 (Figure 2.3A). To ask whether GSK-3, in addition to MBK-2, has a direct role in regulating OMA-1 degradation, I tested whether GSK-3 phosphorylates OMA-1/2 *in vitro*. Indeed, *C. e*GSK-3 as well as rabbit GSK-3β phosphorylated OMA-1 and OMA-2 *in vitro* (Figure 2.3C and data not shown). OMA-1 and OMA-2 contain a typical GSK-3 consensus site that is highly conserved between the two proteins (Figure 2.3B). GSK-3 is known to be a priming-dependent kinase. For most of the GSK-3 substrates, +4 site (4 residues C-terminal to GSK-3 target serine/threonine) is serine or threonine. GSK-3 phosphorylates these substrates only when +4 site is pre-phosphorylated (Fiol et al. 1987; Frame et al. 2001). In case +4 site is aspartate or glutamate, GSK-3 phosphorylation becomes priming-independent because aspartate and glutamate mimic phosphorylated serine and threonine (Wang et al. 2001). GSK-3 phosphorylation sites often form a cluster of serines and threonines that are 4 residues apart. At such a cluster, GSK-3 phosphorylation of the most C-terminal serine/threonine leads to sequential phosphorylation of more N-terminal sites via priming by own phosphorylation (Fiol et al. 1987). The GSK-3 site in OMA-1 and OMA-2 are a cluster of three serine/threonines that are 4 residues apart from each other (Figure 2.3B). +4 site for the most C-terminal threonine (T_{339}) is aspartate (D_{343}), thus based on our current knowledge, this site should not require priming phosphorylation. In addition, the three residues would phosphorylate sequentially

toward the N-terminus, thus preventing phosphorylation at the most C-terminal residue, T_{339} would block phosphorylation at all three residues.

Although S_{331} S_{335} T_{339} are an excellent, priming-independent phosphorylation cluster for GSK-3, mutating T_{339} to alanine, which would block the phosphorylation at all three residues, only slightly decreased phosphorylation of OMA-1 (Figure 2.3C). Mutating T_{327} in OMA-2, which corresponds to T_{339} of OMA-1, to alanine also decreased, but did not abolish phosphorylation (Figure 2.3C). Further mutating all 8 serines and threonines around T_{339} in OMA-1 (from S_{331} to S_{347}) did not further decrease phosphorylation signal, suggesting that these surrounding sites are not phosphorylated by GSK-3 (data not shown). However, mutating T_{239} to alanine greatly decreased phosphorylation, suggesting that *in vitro*, this site could be phosphorylated by GSK-3. Depletion of *gsk-3* by RNAi caused a severe delay in OMA-1 degradation (Figure 2.3A). At the same RNAi condition, *in vivo* T_{239} phosphorylation detected by anti-T_{239}-P antibody was unaltered, suggesting that despite the *in vitro* phosphorylation, GSK-3 does not contribute to T_{239} phosphorylation significantly *in vivo* (Figure 2.3D). Rather, my previous data suggest that MBK-2 is responsible for T_{239} phosphorylation (Figure 2.2).

2. Pre-phosphorylation at T_{239} enhances GSK-3 phosphorylation at T_{339}

Intriguingly, mutating T_{239} to aspartate or glutamate, which can mimic phosphorylated serine and threonine, increased phosphorylation signal compared to T_{239}A mutant in the kinase assay (Figure 2.3C). Mutating T_{339} to alanine in addition to T_{239} to aspartate diminished phosphorylation (Figure 2.3C). These results suggest that MBK-2

phosphorylation at T_{239} facilitates GSK-3 phosphorylation at T_{339}. Conversely, mutating the GSK-3 cluster, $S_{333}S_{335}T_{339}$ to aspartate and glutamate ($S_{333}D$ $S_{335}D$ $T_{339}E$) did not enhance MBK-2 phosphorylation at T_{239} (data not shown), suggesting MBK-2-to-GSK-3 sequential phosphorylation, not mutual enhancements.

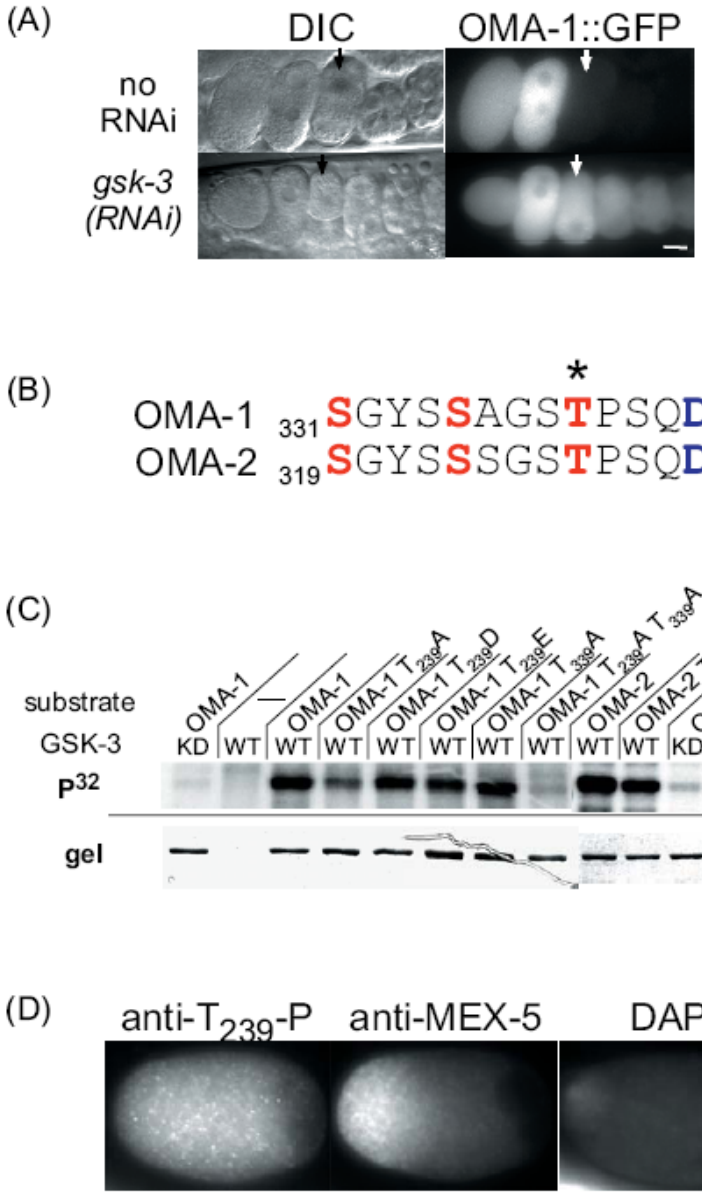

Figure 2.3 GSK-3 phosphorylates OMA-1 and is required for OMA-1 degradation

(a) *gsk-3* was depleted by RNAi in an OMA-1::GFP reporter strain. Arrows mark the 2-cell stage.
(b) Alignment of OMA-1 and OMA-2. Residues in blue indicate critical in GSK-3 phosphorylation. Residues marked in red are ones predicted to be phosphorylated by GSK-3.
(c) *In vitro* kinase assay with WT (wild-type) or KD (kinase dead) *C. e* GSK-3 kinase.
(d) *gsk-3* (RNAi) embryo at the pronuclear migration stage co-stained with anti-T239-P (left), anti-PIE-1(middle), and DAPI (right).

III. *In vivo* reporter analysis of the MBK-2 and GSK-3 sites on OMA-1 degradation

In order to assess *in vivo* significance of MBK-2 phosphorylation at T_{239} and GSK-3 phosphorylation at T_{339} in OMA protein degradation, the phosphorylation sites were mutated individually or in combination in a translational OMA-1::GFP reporter (Experimental Procedure). A previous study suggests that a delay in OMA-1 degradation timing is harmful for embryogenesis because *oma-1(zu405)* mutant shows embryonic lethality (Lin 2003). Thus it is likely that a functional OMA-1::GFP transgene harboring a degradation delaying mutation would cause lethality, therefore it would be impossible to obtain transgenic animals. To circumvent this problem, the first 110 amino acids of OMA-1 immediately before the first zinc finger domain was deleted (OMA-1ΔN::GFP, see Experimental Procedure). OMA-1ΔN::GFP was degraded shortly after the 1-cell stage, similar to full-length OMA-1::GFP and endogenous OMA-1, although the degradation kinetics was slightly slower (Lin 2003)(Figure 2.4). Consistent with MBK-2 phosphorylation at T_{239} being critical for OMA-1 degradation, T_{239}A mutation dramatically delayed the degradation of OMA-1ΔN::GFP (Figure 2.4). Additionally, T_{339}A mutation at the GSK-3 site delayed OMA-1ΔN::GFP

degradation to a similar extent, suggesting that GSK-3 phosphorylation at T_{339} is important for the OMA-1 degradation timing. I further tested whether phosphorylation of either site is sufficient for the degradation of OMA-1 by mutating the MBK-2 and GSK-3 sites to aspartate and glutamate. Aspartate and glutamate mimic phosphorylated serine and threonine in some cases. OMA-1 degradation at the first mitotic division relies on the proteasome (see below). If phosphorylation mimicking mutations target OMA-1ΔN::GFP for degradation in a constitutive manner, then I should be able to visualize GFP signal only when the proteasomal activity is compromised. However, in contrary to this prediction, T_{239}D, T_{239}E, and S_{331}D S_{335}D T_{339}E mutants all resulted in a severe delay in OMA-1ΔN::GFP degradation without proteasome depletion (data not shown). The degrees of the degradation delays were similar to T_{239}A and T_{339}A mutants. It is most likely that these mutations did not mimic phosphorylated serine and threonine *in vivo* to an extent sufficient for the normal response. It is known that often aspartate and glutamate substitutions fail to sufficiently mimic phosphorylated serine and threonine. For example, S_{218}E S_{222}E mutant form of MEK1 has only 1% of the activity of MEK1 phoshporylated both at S_{218} and S_{222} (Alessi et al. 1994).

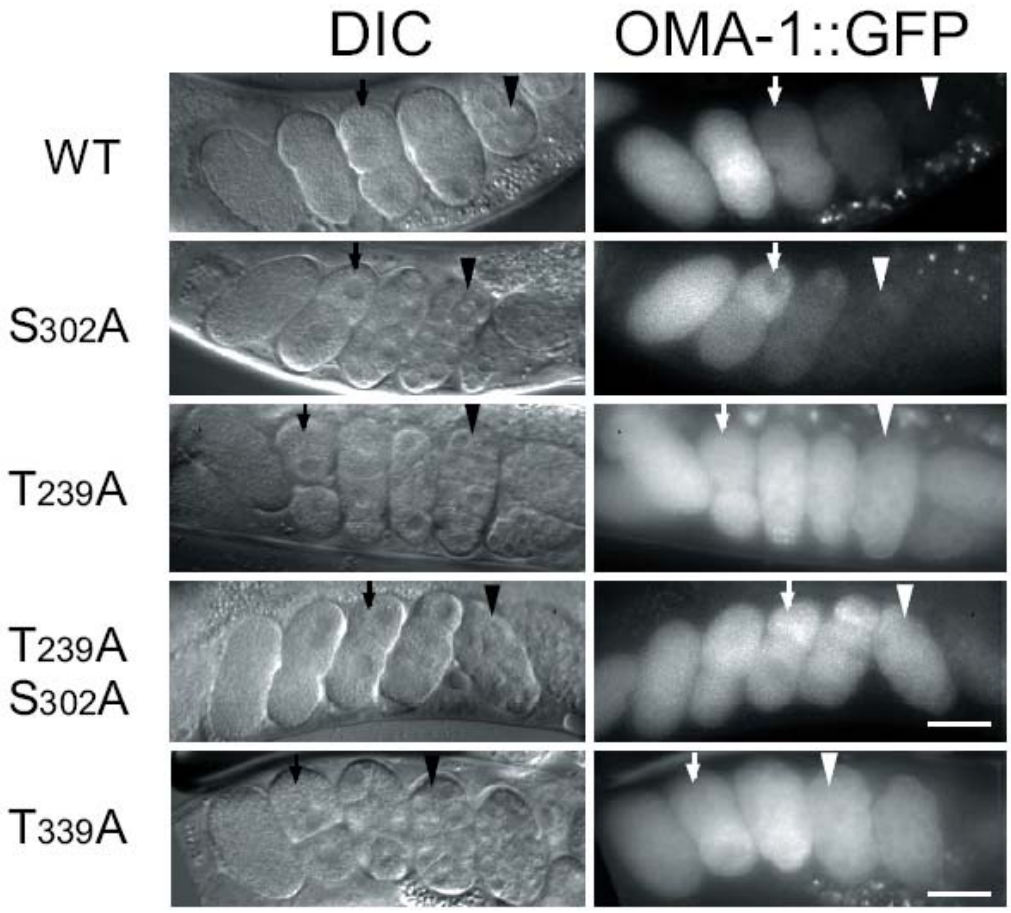

Figure 2.4 MBK-2 and GSK-3 phosphorylation sites are required for OMA-1 degradation
Early embryos *in utero* expressing N-ternimally truncated OMA-1::GFP reporter harboring indicated mutations. Arrows and arrowheads mark the 2- and 16-cell stage respectively.

IV. S_{302} is dispensable for OMA-1 degradation and function

In vitro, MBK-2 phosphorylates OMA-1 at S_{302} (Figure 2.1B). To examine *in vivo* significance of S_{302} phosphorylation in the context of OMA-1 degradation, S_{302}A mutation was introduced to the OMA-1ΔN::GFP reporter. OMA-1ΔN (S_{302}A)::GFP was degraded at

a similar kinetics as OMA-1ΔN::GFP, suggesting that S_{302} is dispensable for OMA-1 degradation (Figure 2.4). However, an alternative possibility is that MBK-2 phosphorylation at S_{302} is important for OMA-1 function, not degradation. I tested this possibility using a functional, full-length OMA-1::GFP transgene (see Experimental Procedure). Consistent with my assay with the OMA-1ΔN::GFP reporter, S_{302}A mutation did not change the expression pattern of the full-length OMA-1::GFP in a significant way, further suggesting that S_{302} is dispensable for OMA-1 degradation (data not shown). In order to test the functionality of OMA-1(S_{302}A) mutant, both OMA-1::GFP and OMA-1(S_{302}A)::GFP transgenics were generated in *oma-1(te33)* background, and *oma-2* was subsequently depleted by RNAi. Due to genetic redundancy, *oma-1(te33)* does not show any discernable phenotype, whereas *oma-1(te33); oma-2(RNAi)* animals show a fully penetrant oocyte maturation defect (Oma) (Detwiler et al. 2001). Upon *oma-2* RNAi, neither *oma-1(te33);* OMA-1::GFP nor *oma-1(te33);* OMA-1(S_{302}A)::GFP showed Oma phenotype or any other types of sterility (n>200). In addition, 95% of embryos from *oma-1(te33); oma-2(RNAi);* OMA-1(S_{302}A)::GFP were viable (n=50). On the other hand, 30% of the embryos from the control *oma-1(te33); oma-2(RNAi);* OMA-1::GFP were viable (n=50). The higher viability of the mutant transgenic strain likely reflects higher expression of the S_{302}A mutant transgene. Regardless, the high percentage of genetic rescue (95%) suggests that S_{302} is dispensable for the function of OMA-1. Thus either S_{302} phosphorylation does not happen or the phosphorylation does not have a significant consequence *in vivo*.

V. Toward the identification of the machinery executing OMA protein degradation

1. OMA protein degradation is proteasome-dependent

Although my data suggest that the phosphorylation by MBK-2 and GSK-3 promotes OMA protein degradation at the first mitosis, the downstream events executing the degradation in response to the phosphorylation was unknown. In order to identify such degradation execution events, I undertook a candidate approach to deplete factors involved in protein degradation using an OMA-1::GFP reporter (see Experimental Procedures). Through this analysis, I first demonstrated that OMA-1 degradation at the first mitosis is proteasome dependent. RNAi depletion of all 4 proteasome components tested, *rpn-6* and *rpn-8* (proteasome regulatory particle Non-ATPase), *pas-5* (proteasome alpha subunit), and *pbs-2* (proteasome beta subunit) resulted in a severe delay in the degradation of OMA-1::GFP, suggesting that OMA-1/2 are degraded through the proteasome (Figure 2.6 and data not shown).

2. Identification of potential ubiquitin E3 ligases for OMAs

2-1. ECS ubiquitin E3 ligase

Proteins targeted for proteasomal degradation are known to be ubiquitinated by a group of enzymes termed ubiquitin E3 ligases (Hershko and Ciechanover 1998). Ubiquitin E3 ligases confer specificity to a ubiquitination reaction via direct binding to ubiquitination targets (Hershko and Ciechanover 1998). In order to identify the link between the MBK-2 and GSK-3 phosphorylation and proteasomal degradation, I sought the E3 ligase for OMA proteins. A previous report showed that OMA-1 degradation depends on an ECS E3 ligase component, CUL-2 (Pellettieri et al. 2003). ECS is a class of multi-subunit E3 ligases

consisting of a small RING finger protein: Rbx1, cullin adaptor protein: Cullin2/CUL-2, Elongin B and C, and a substrate specificity subunit containing SOCS box motif (Figure 2.5)(Kile et al. 2002). Interestingly, the previous study reported that *elc-1/*ElonginC was dispensable for OMA-1 degradation (DeRenzo et al. 2003). This is unexpected because ElonginC is thought to be essential for the ECS E3 ligase function (Kile et al. 2002). As reported previously, the depletion of *cul-2* resulted in a severe delay in the degradation timing of OMA-1::GFP (Figure 2.6) (DeRenzo et al. 2003). Additionally, I showed that the depletion of *rbx-1* results in a similar delay (Figure 2.6). In agreement with the previous report, OMA-1 degradation was only slightly delayed in *elc-1* depleted embryos (Figure 2.6)(DeRenzo et al. 2003). I further showed that the depletion of the other Elongin of ECS E3 ligase, *elb-1*/ElonginB causes a marginal OMA-1 degradation delay similar to *elc-1* (Figure 2.6). In a parallel experiment, *elc-1* and *elb-1* depletions both caused a severe delay in the degradation of their known target, PIE-1, to a comparable extent as *rbx-1* and *cul-2* RNAi, arguing against an unsuccessful depletion (DeRenzo et al. 2003) (data not shown). These results raise a possibility that RBX-1 and CUL-2 form a novel E3 ligase that does not contain canonical components, ELC-1/ElonginC and ELB-1/ElonginB. Alternatively, *rbx-1* and *cul-2* might be directly or indirectly involved in OMA protein degradation through a non-E3 ligase function.

ZYG-11 is an evolutionarily conserved protein that contains a leucine-rich region. Studies in *C. elegans* suggested that ZYG-11 function with CUL-2 because *zyg-11* depletion phenocopied some of the *cul-2* RNAi phenotypes (Liu et al. 2004; Sonneville and Gonczy 2004). Specifically both *cul-2* and *zyg-11* depletions result in a delay in CyclinB degradation

at the 1-cell stage (Liu et al. 2004; Sonneville and Gonczy 2004). However, the biochemical role of ZYG-11 remains unclear. In order to test whether *zyg-11* is involved in OMA-1 degradation, I depleted *zyg-11* in the OMA-1::GFP strain. *zyg-11* depletion indeed resulted in a severe delay in OMA-1 degradation, suggesting that *zyg-11* directly or indirectly regulate OMA degradation (Figure 2.6).

2-2. SCF ubiquitin E3 ligase

In order to perform a more comprehensive analysis, I tested 3 other Cullins that have known embryonic functions in *C. elegans*: CUL-1, -3, and -4 (Kipreos et al. 1996; Pintard et al. 2003; Xu et al. 2003; Zhong et al. 2003). These cullins are sequence-related proteins thought to form multi-peptide E3 ligases of similar structures and properties (Deshaies 1999). In my analysis, individual RNAi depletion of *cul-3*, and *-4* did not affect OMA-1 degradation, whereas OMA-1 degradation was markedly delayed in *cul-1* RNAi embryos (Figure 2.6 and data not shown). Cul1 forms a complex with Rbx1, Skp1 and an F-box protein to function as a multi-subunit E3 ligase termed SCF E3 ligase (Figure 2.5)(Deshaies 1999). Although Rbx1 is the only shared component between ECS and SCF E3 ligases, ECS and SCF are known to be structurally analogous (Deshaies 1999). In order to ask whether CUL-1 affects OMA-1 degradation as an SCF E3 ligase complex, I tested Skp1 proteins. Whereas the human and yeast genomes encode only 1 Skp1 homolog, the *C. elegans* genome encode at least 21 Skp1-like proteins (SKR, Skp1-related) (Kipreos and Pagano 2000; Nayak et al. 2002; Yamanaka et al. 2002). Of the 21 candidate *skr* genes, ESTs for 18 (*-1, -2, -3, -4, -5, -7, -8, -9, -10, -12, -13, -14, -15, -16, -17, -19, -20,* and *-21*) have been reported,

suggesting that these genes are expressed (Nayak et al. 2002; Yamanaka et al. 2002). Physical interaction with CUL-1 is a hallmark of Skp1 proteins (Schulman et al. 2000). 7 of them (-1, -2, -3, -7, -8, -9, and -10) showed physical interaction with CUL-1, suggesting that they are likely to function as an SCF E3 ligase with CUL-1 (Nayak et al. 2002; Yamanaka et al. 2002). In addition, RNAi depletion of 6 of them (*-1, -2, -7, -8, -9, -10*) resulted in detectable phenotypes in these studies (Nayak et al. 2002; Yamanaka et al. 2002). In order to assess their potential function in OMA protein degradation, I depleted *skr-1, -2, -3, -5, -8, -9, -11, -12, -13, -15, -17, -18, -19,* and *-20* singly, and *–8/9, –12/13, –17/18,* and *-19/20* simultaneously using the feeding RNAi technique in a OMA-1::GFP reporter strain harboring a mutation that enhances RNAi response [*rrf-3(pk1427)* mutation, see Experimental Procedures, (Simmer et al. 2002)]. I showed that, at least in my assay condition, only *skr-1* and *skr-2* RNAi results in a detectable OMA-1 degradation delay (Figure 2.6 and data not shown). *skr-1* and *skr-2* show very extensive sequence similarity with 83% identity at nucleotide level and 81% at amino acid level throughout their coding sequences (Nayak et al. 2002; Yamanaka et al. 2002). Indeed, the RNAi clones used for my analysis contain multiple identical stretches that are long enough to cause cross-depletion, thus single RNAi to target either gene might deplete both gene products. These results suggest that CUL-1, RBX-1, and SKR-1 and/or -2 together regulate OMA degradation as a SCF E3 ligase, directly or indirectly.

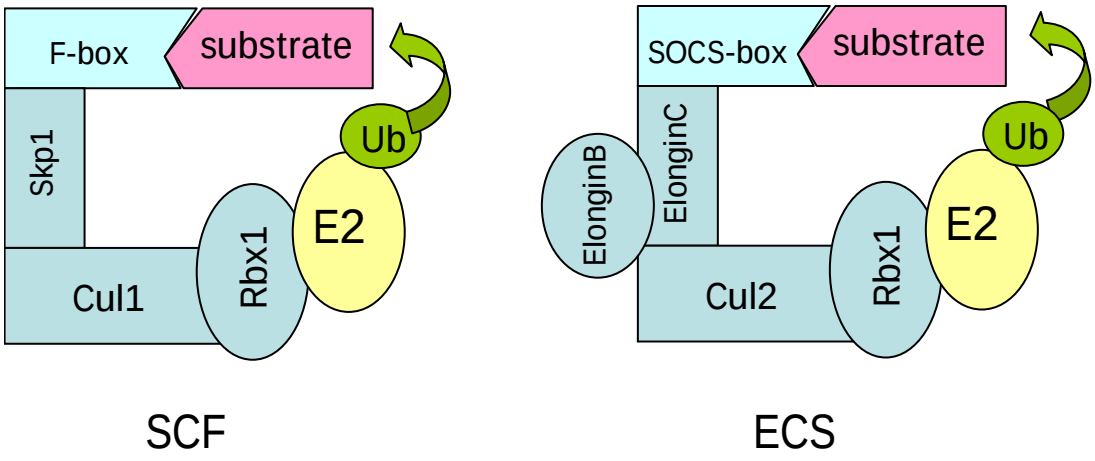

Figure 2.5 Schematic diagrams of SCF and ECS E3 ubiquitin ligases
Ubiquitin, E2 conjugating enzyme, E3 ligase components, and ubiquitination substrates are described in green, yellow, blue, and magenta respectively. In SCF, small RING finger protein Rbx1 interacts with E2 whereas an F-box containing protein interacts with substrate. Cul1 and Skp1 together bridge Rbx1 and F-box protein to form an E3 ligase. Similarly, Cul2 and ElonginB/C connect Rbx1 and the substrate-binding subunit, SOCS box protein to form an ECS E3 ligase.

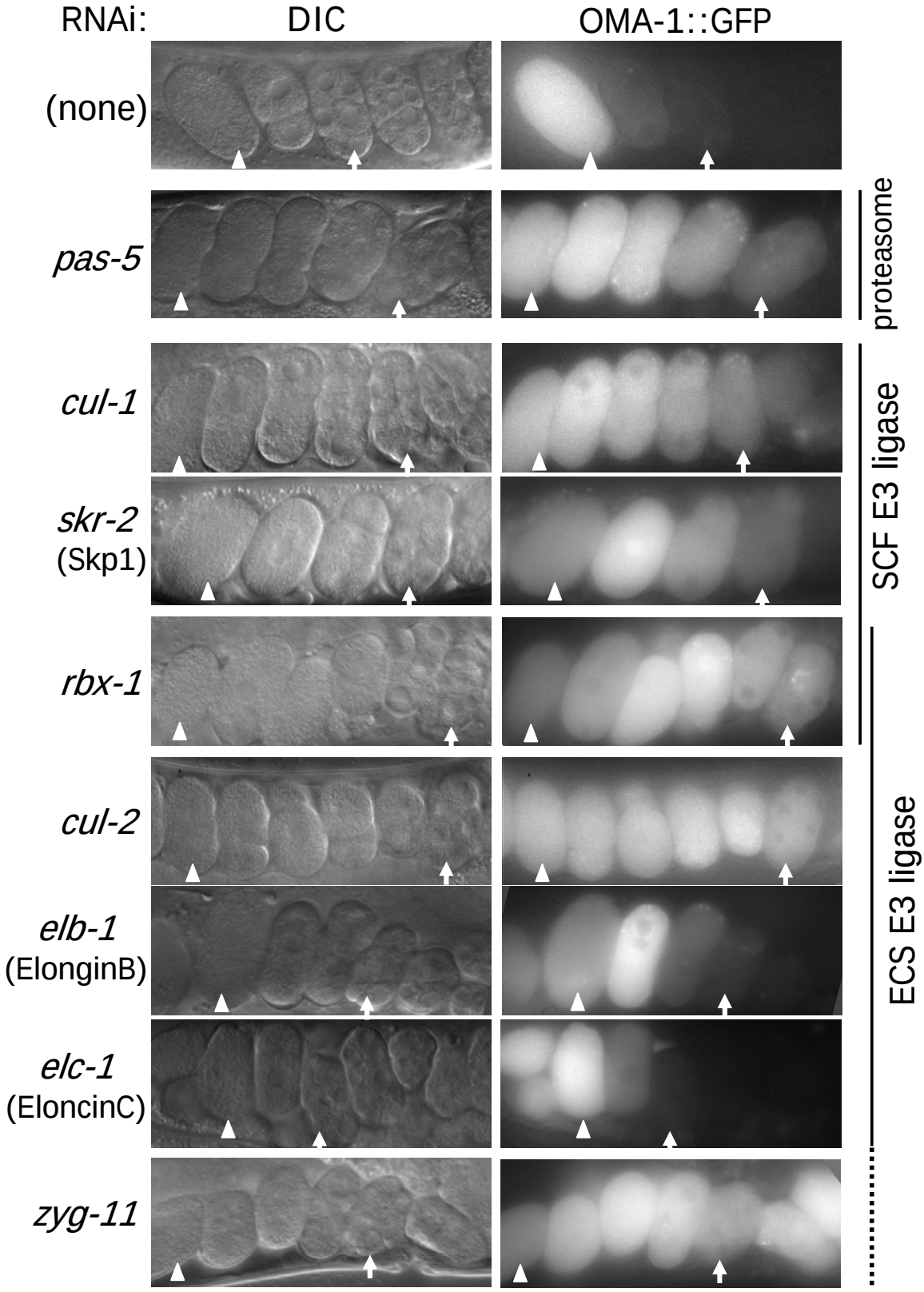
RNAi:
DIC
OMA-1::GFP
(none)
pas-5
cul-1
skr-2
(Skp1)
rbx-1
cul-2
elb-1
(ElonginB)
elc-1
(EloncinC)
zyg-11
proteasome
SCF E3 ligase
ECS E3 ligase

Figure 2.6 Proteasome and SCF and ECS E3 ligases are required for OMA-1 degradation
A strain carrying a full-length OMA-1::GFP reporter was treated with various RNAi. Arrowheads and arrows indicate the 1-cell and 8-16 cell stages, respectively.

DISCUSSION

mbk-2 and *gsk-3* kinases are required for the properly timed OMA-1 degradation at the first mitosis, as shown in a previous study and this study respectively (Pellettieri et al. 2003)(Figure 2.3A). Molecularly, I showed that likely sequential phosphorylation by MBK-2 at T_{239} and GSK-3 at T_{339} promotes the degradation of OMA proteins at the first mitosis. MBK-2 phosphorylates OMA-1 at T_{239} *in vitro*. T_{239}D substitution, which is predicted to mimic T_{239} phosphorylation, enhances GSK-3 phosphorylation at T_{339}. Both T_{239}A and T_{339}A mutations delay the degradation of an OMA-1::GFP reporter in early embryos, suggesting that T_{239} phosphorylation by MBK-2 and T_{339} phosphorylation by GSK-3 are important for the degradation of OMA-1. Using a phospho-specific antibody, T_{239} phosphorylation was detected *in vivo* shortly after meiosis II, in an *mbk-2* dependent manner. Thus the cascade of MBK-2 and GSK-3 phosphorylation events is likely to happen shortly before OMA protein degradation at the 1-cell stage. RNAi analysis using an OMA-1::GFP reporter suggest that ECS and/or SCF ubiquitin E3 ligases and the proteasome are responsible for the execution of OMA protein degradation, likely downstream of the MBK-2 and GSK-3 phosphorylation.

DYRK2/MBK-2 phosphorylation

OMA-1 is the first substrate for MBK-2 to be demonstrated. Moreover, it is the first DYRK2 phosphorylation to be demonstrated *in vivo*. *mbk-2* mutants exhibit pleiotropic phenotype including a cytokinesis defect and delays in the degradation of maternally provided proteins: MEI-1, OMA-1, PIE-1, MEX-5, and POS-1 (Pellettieri et al. 2003; Quintin et al. 2003; Pang et al. 2004). Interestingly, *oma-1(zu405)* mutant, which is defective in MBK-2 phosphorylation at T_{239}, exhibits degradation delays for several maternal proteins including PIE-1, MEX-5 and POS-1 along with OMA-1 degradation delay (Lin 2003). Thus the degradation delays of PIE-1, MEX-5, and POS-1 in *mbk-2* mutants might be secondary to the compromised phosphorylation of OMA-1. This speculation is indeed supported by my data presented in Chapter 3. Surprisingly, a change(s) in OMA-1 protein property as a result of compromised T_{239} phosphorylation, not the OMA-1 degradation delay *per se*, appears to be responsible for the degradation delay of PIE-1, MEX-5, and POS-1 (see Chapter 3). The degradation delay of MEI-1 has been considered to be causal to the cytokinesis defect of *mbk-2* mutants. Mutants showing MEI-1 degradation delay exhibit a cytokinesis defect similar to *mbk-2* mutant and the depletion of *mei-1* suppresses the cytokinesis defect in *mbk-2* mutant .(Pellettieri et al. 2003; Quintin et al. 2003; Pang et al. 2004). Indeed, *mbk-2* mutants show a delay in the degradation of MEI-1, which normally happens shortly after the completion of meioses at the 1-cell stage (Pellettieri et al. 2003; Quintin et al. 2003; Pang et al. 2004). *oma-1(zu405)* mutant does not show a cytokinesis defect, thus it is unlikely that MEI-1 degradation delay in *mbk-2* mutant is secondary to the OMA-1 phosphorylation defect. Indeed, a recent report suggests that MEI-1 is a direct target of MBK-2 (Stitzel et al. 2006). The authors demonstrated that MBK-2 directly

phosphorylates MEI-1 *in vitro*, that MBK-2 dependent MEI-1 phosphorylation occurs *in vivo* shortly before MEI-1 degradation, and that a mutation in MEI-1 that blocks the MBK-2 phosphorylation *in vitro,* prevents MEI-1 degradation *in vivo* (Stitzel et al. 2006). Thus MBK-2 phosphorylates at least two proteins: OMA-1 and MEI-1 in the 1-cell embryo, likely to regulate embryonic development and cell division, respectively.

An unanswered question is the mechanism underlying MBK-2 activation after meiosis I. GFP::MBK-2 undergoes a dramatic re-localization after meiosis I, and this change has been linked to the activation of MBK-2 (Pellettieri et al. 2003)(Figure 1.6). Consistent with this notion, cell cycle progression past meiosis I is necessary and sufficient for MBK-2-dependent processes (Pellettieri et al. 2003; Stitzel et al. 2006). Meiosis I-arresting *mat*-1 mutant fails to show an MBK-2-dependent process in the 1-cell embryo (Pellettieri et al. 2003). On the other hand, a premature release of meiosis I arrest via *wee-1* depletion results in a precocious MEI-1 degradation in the oocyte (Stitzel et al. 2006). A fertilization defective mutant, *spe-9* degrades MEI-1 in the embryo, suggesting that meiotic progression, not fertilization, is required for MBK-2 activation (Stitzel et al. 2006). In all cases, the expressions of MBK-2 dependent processes are accompanied by the change in the cortical GFP::MBK-2 localization, supporting the notion that the localization change of GFP::MBK-2 correlates with MBK-2 activation (Pellettieri et al. 2003; Stitzel et al. 2006). *oma-1* and *oma-2* are required for oocyte maturation (Detwiler et al. 2001). Oocyte maturation allows the completion of meiosis I. Thus the activation of MBK-2 and resulting OMA protein phosphorylation and degradation do not occur until OMA proteins perform their task for oocyte maturation. Thus, this requirement prevents premature OMA protein degradation

(and potential activation of OMA function for the 1-cell embryo) prior to oocyte maturation. Currently, it is unclear what signals to activate MBK-2 during oocyte-to-embryo transition. In addition, the biochemical understanding of the regulation of MBK-2/DYRK2 activity is lacking. Such knowledge would help us understand the regulation and coordination of oocyte-to-embryo transition as well as this poorly characterized DYRK2 kinase.

Facilitation of GSK-3 phosphorylation by MBK-2/DRYK2 from a distant site

The sequential phosphorylation by MBK-2 and GSK-3 is very intriguing. It has been known that GSK-3 is primed by phosphorylation at +4 site in many cases (Fiol et al. 1987; Frame et al. 2001). Indeed, an MBK-2 homolog, human DYRK2 has been shown to prime GSK-3 in this fashion (Skurat and Dietrich 2004). My biochemical analysis suggests that MBK-2 phosphoryaltion at T_{239} facilitate distant GSK-3 phosphoryaltion at T_{339}. To my knowledge, enhancement of GSK-3 phosphorylation from such a distance was not known prior to this study. However, such regulation might be prevalent in various biological processes in different organisms. A recent study suggests that the nuclear export of the transcription factor, NFAT is regulated by sequential phosphorylation by DYRK2 and GSK3 in human. Strikingly reminiscent of OMA-1, DYRK2 and GSK3 sites on NFAT are distant and DYRK2 phosphorylation enhances GSK3 phosphorylation *in vitro* (Gwack et al. 2006). Consistent with DYRK2-to-GSK3 sequential phosphorylation occurring *in vivo*, depletion of either gene resulted in the nucealr export of NFAT in cultured cells (Gwack et al. 2006). At this point, precise biochemical mechanism of the enhancement of GSK-3 phosphorylation by MBK-2 is unknown. MBK-2 phosphorylation at T_{239} might alter OMA-1 protein

conformation, making initially inaccessible T_{339} accessible for GSK-3. Alternatively, T_{239} and T_{339} might be in close proximity on OMA-1 protein surface, and GSK-3 directly recognizes the phosphorylation status of T_{239}.

An interesting discovery reported recently is the involvement of two additional kinases, KIN-19/casein kinase I (CKI) and CDK-1 in OMA degradation (Shirayama et al. 2006). In mutants of these genes, OMA-1 degradation is delayed, like in *mbk-2* and *gsk-3* depleted embryos (Shirayama et al. 2006). It will be interesting to determine if these kinases directly phosphorylate OMA proteins and if so, how their phosphorylation relate to MBK-2 and GSK-3 phosphorylation. Strikingly, in the context of NFAT, DYRK2 phosphorylation enhances CKI phosphorylation to promote NFAT nuclear export, suggesting that the sesquential phosphorylation by DYRK2, CKI, and GSK-3 is a battery of phosphorylation events (Gwack et al. 2006).

Why does OMA degradation require so many kinases? As discussed in Chapter 3, OMA proteins might have phosphorylation-dependent functions in the 1-cell embryo. Phosphorylation by different kinases might turn-on or turn-off different functions of OMAs in a temporally regulated manner. Alternatively or in parallel, having more phosphorylated residues provided by multiple kinases might ensure a change in OMA-1 properties, for example, an enhanced binding affinity for an E3 ligase.

Degradation execution machinery for OMAs

In this study, I showed that OMA-1 degradation is proteasome dependent. Additionally, I showed that the SCF E3 ligase is required for OMA-1 degradation. As reported before,

CUL-2 is required for OMA-1 degradation, however two other components of ECS, ELB-1/ElonginB and ELC-1/ElonginC do not appear to participate in this process, suggesting that CUL-2 might function in an ECS-independent process to influence OMA protein degradation (DeRenzo et al. 2003). ZYG-11 was proposed to be a substrate binding subunit of CUL-2-containing ECS E3 ligase (Liu et al. 2004; Sonneville and Gonczy 2004). My analysis showed that ZYG-11 is required for OMA-1 degradation, however, it is unclear how ZYG-11 regulates OMA-1 degradation, particularly given that Elongins are not required for OMA-1 degradation. A hallmark of a substrate binding subunit of ECS is physical association with both ElonginC and ubiquitination target (Deshaies 1999; DeRenzo et al. 2003). Using yeast two-hybrid system, I failed to detect interaction between ZYG-11 and ELC-1 or OMA-1, arguing against a direct involvement (data not shown).

Ubiquitination by SCF E3 ligase has been well known to be phosphorylation primed, thus is an attractive candidate for the E3 ligase for OMA-1/2. In many cases, phosphorylation on SCF ubiquitination substrate determines whether or not the protein should be ubiquitinated. Intriguingly, the sequences surrounding GSK-3 sites are highly conserved among *C. e*OMA-1, *C. e*OMA-2 and *C. b*OMA-1 (*C. briggsae*: related nematode species) beyond their requirement to be a GSK-3 site. Thus, this region is likely to have a functional significance more than being a GSK-3 site. One attractive possibility is that this is a binding site for an SCF E3 ligase. Although I showed that 3 out of the 4 components of SCF: RBX-1, CUL-1, and SKR-1/2, are required for OMA-1 degradation, the last component, substrate binding subunit must be identified to directly test this possibility. As substrate binding subunit is the determinant of the substrate specificity of the SCF E3 ligase, there exists a large repertoire of

them. For example, *C. elegans* genome encodes over 300 genes that are suspected to be substrate binding subunits of SCF (Kipreos and Pagano 2000). Identification of a substrate specificity subunit for OMA-1/2 will likely to greatly help understand the regulation of OMA protein degradation and the mechanism of oocyte-to-embryo transition.

CHAPTER THREE

TO PROBE FUNCTIONS OF OMA-1/2 THROUGH CHARACTERIZATION OF *oma-1(zu405)* MUTANT EMBRYOS

SUMMARY

OMA-1/2 are expressed specifically in the late oocyte and 1-cell embryo. A previous study established that *oma-1/2* are required for oocyte maturation. On the other hand, their developmental roles are less clear due to the fully penetrant sterility of *oma-1(-); oma-2(-)* animals. Based on previous results, I hypothesize that OMA proteins regulate developmental events. Such OMA function might involve the regulation of developmental events in the 1-cell embryo as well as the repression of embryonic processes before fertilization.

In this chapter, I describe my genetic analyses to probe developmental functions of OMA-1/2, mainly through the characterizations of *oma-1(zu405)* and *oma-1(zu405); oma-2(RNAi)* mutant embryos. *oma-1(zu405)*/P_{240}L mutation delays OMA-1 protein degradation. As the functionality of OMA-1 P_{240}L in the embryo was not previously analyzed, either or both alteration of OMA-1 property by P_{240}L substitution and OMA-1 degradation delay can be responsible for defects of *oma-1(zu405)* embryos. My analysis suggests that alteration of OMA-1 property and OMA-1 degradation delay both contribute to defects of *oma-1(zu405)* embryos. Alteration of OMA-1 property is likely to include the inability of OMA-1 to be efficiently phosphorylated by MBK-2, and likely by GSK-3.

oma-1(zu405) and *oma-1(zu405); oma-2(RNAi)* embryos show various defects including 1) abnormal PAR polarity at early embryonic stages, 2) downregulation of a translational regulator, GLD-1, 3) downregulation of ZIF-1-mediated protein degradation

activity, and 4) additional divisions of germline precursors. In the wild-type, OMAs might regulate these various processes to initiate embryogenesis in a coordinated manner. Indeed, I showed that GLD-1 expression and ZIF-1-mediated proteasomal degradation precociously occur in *oma-1/2* hypomorphic mutants. In addition, a previous study reported additional divisions of germline precursors in weak *oma-1/2* RNAi embryos. These results support the notion that at least some of the processes misregulated in *oma-1(zu405)* mutant are physiological targets of OMA proteins. In summary, my analyses identified likely candidates of OMA target processes. Because these processes are not thought to be related to each other, OMA protein might regulate multiple processes to orchestrate the initiation of embryogenesis.

INTRODUCTION

Oocytes and 1-cell embryos possess totipotency in *C. elegans*, whereas later blastomeres, as early as the 2-cell stage, adopt restricted developmental potentials (Sulston et al. 1983). Importantly, early embryonic differentiation events are driven by maternal factors accumulated in the cytoplasm of totipotent oocytes. These maternal factors must be dormant in the oocyte to prevent precocious differentiation, whereas shortly after fertilization, they must be activated in a temporally and spatially orchestrated manner to drive embryogenesis. Differential regulation of such developmental activities between oocyte and embryo, including orchestrated activation during oocyte-to-embryo transition, is a central question of developmental biology.

A previous study indicated that *oma-1* and *oma-2* are redundantly required for oocyte maturation (Detwiler et al. 2001). Consistent with their genetic requirement, OMA-1 and OMA-2 proteins are expressed in late oocytes (Detwiler et al. 2001). Their expression, interestingly, persist through the 1-cell stage further beyond oocyte maturation (Lin 2003). This persistence is not likely due to the lack of general ubiquitin-proteasome activity at the 1-cell stage because at least three proteins are degraded in a proteasome-dependent manner before OMA protein degradation, shortly after meiosis II (Srayko et al. 2000; Liu et al. 2004; Sonneville and Gonczy 2004). Thus their persisting expression at the 1-cell stage implies a potential function for OMA-1 and OMA-2 in the 1-cell embryo. However, genetic dissection of OMA function in the 1-cell embryo has been hampered by the fully penetrant sterility of *oma-1(-); oma-2(-)* mutant (Detwiler et al. 2001).

The notion for the embryonic function of *oma-1/2* was further supported by the isolation of *oma-1(zu405)* mutation. *oma-1(zu405)* is a temperature sensitive, semi-dominant mutation that causes embryonic lethality, but not an oocyte maturation defect (Lin 2003). *oma-1(zu405)* homozygotes produce only dead embryos at 25°C, whereas *oma-1(zu405)* or *oma-1(zu405); oma-2(RNAi)* animals do not exhibit an oocyte maturation defect (Lin 2003). *oma-1(zu405)* is a strict maternal effect lethal mutation because wild-type sperm cannot rescue the embryonic lethality (Lin 2003). On the other hand, sperm from *oma-1(zu405)* homozygote can fully viable progeny when fertilized with wild-type eggs (Lin 2003). *zu405* embryonic lethality is fully suppressed by the depletion of *oma-1* by RNAi or an intragenic loss-of-function mutation, indicating that *oma-1*(*zu405)* is a gain-of-function mutation (Lin 2003).

oma-1(zu405) embryos exhibit certain cell fate transformations and never hatch (Lin 2003). Molecular characterizations revealed that *oma-1(zu405)* embryos mislocalize various cell fate determinants at early embryonic stages (Lin 2003). Previous analyses observed overabundance and mislocalization of the maternally provided cell fate determinants: PIE-1, MEX-1, POS-1, MEX-5, MEX-3, and SKN-1 (Lin 2003). Of these, the misregulation of SKN-1 was linked to the apparent C-to-EMS transformation observed in the mutant embryo (Lin 2003). On the other hand, the contributions of the other early defects to the terminal *zu405* phenotype and lethality are not clear (Lin 2003).

A prominent defect of *oma-1(zu405)* mutant is a delay in OMA-1 protein degradation, which normally happens at the end of 1-cell stage (Lin 2003). *oma-1(zu405)* changes P_{240} of OMA-1 protein to leucine (Lin 2003). My analysis revealed that *zu405*/P_{240}L mutation interferes with MBK-2 and likely GSK-3 phosphorylation on OMA-1, which is required for OMA-1 degradation (see Chapter 2). It was previously reasoned that the delay in OMA-1 degradation is causal to the early defects, cell fate transformations, and lethality of *oma-1(zu405)* mutant (Lin 2003). However, the contribution of this mutation to the property of OMA-1 protein has not been addressed previously. I began to address this possibility via yeast two-hybrid analysis in Chapter 5, and showed that certain interactions are attenuated by *oma-1(zu405)*/P_{240}L mutation. The change OMA-1 protein property might be due to attenuated MBK-2 and GSK-3 phosphorylation in the 1-cell stage. MBK-2 and GSK-3 phosphorylation might contribute to OMA-1 function in the 1-cell stage and *zu405* mutation might cause defects via the interference of MBK-2 and GSK-3 phosphorylation.

In this chapter, I describe my genetic analysis to obtain insights into the function of OMA proteins in embryogenesis, mainly through characterizations of *oma-1(zu405)* mutant embryos. My analysis identified multiple embryonic processes that might be targets of OMAs. These processes include 1) PAR polarity, 2) expression of translational regulator, GLD-1, 3) ZIF-1-mediated protein degradation, 4) germline precursor division, and 5) silencing of zygotic transcription. First, I discovered that *oma-2* depletion greatly enhances *oma-1(zu405)* lethality. Characterization of *oma-1(zu405); oma-2(RNAi)* embryos revealed two novel defects that were not previously seen in *oma-1(zu405)* embryos: 1) abnormal PAR polarity and 2) apparent additional divisions of germline precursors. On the other hand, a previously reported defect, ZIF-1-mediated protein degradation was further enhanced by *oma-2* depletion. Additionally, I discovered two novel *oma-1(zu405)* defects, diminishment of embryonic GLD-1 expression and ectopic silencing of zygotic transcription. Whereas the diminishment of GLD-1 expression was diminished was not enhanced by *oma-2* depletion, the silencing of zygotic transcription was greatly enhanced by *oma-2* depletion.

Some of these defects are not simply due to the delay in OMA-1 degradation because 1) PAR localization defect occurs in the 1-cell stage before the normal OMA-1 degradation timing, and 2) ZIF-1 degradation defect correlates with compromised MBK-2 and GSK-3 phosphorylation, not degradation delay. These results suggest that change(s) in OMA protein property due to $P_{240}L$ mutation and OMA-1 degradation delay both contribute to *oma-1(zu405)* phenotype, and that the changes of OMA protein property include their inability to be efficiently phosphorylated by MBK-2 and GSK-3.

I further tested whether or not *oma-1(zu405)* defects are mis-regulated in *oma-1/2* hypomorphic mutants. Indeed, GLD-1 and ZIF-1-mediated protein degradation were precociously expressed in early *oma-1(rof); oma-2(rof)* embryos, and *oma-1/2* RNAi gonad respectively. Combined with a previously published result that additional germline precursor divisions occurred in embryos weakly depleted of *oma-1/2*, my results suggest that some of the processes misregulated in *oma-1(zu405)* are physiological targets of OMA-1/2. In summary, my analyses in this chapter identified likely candidate OMA-1/2 target processes for embryogenesis.

EXPERIMENTAL PROCEDURES

Strains

Bristol strain N2 was used as the wild-type strain (Brenner 1974). Genetic markers used are: LGIV: *oma-1 (zu405), oma-1 (te21),* LGIV: *oma-2(te50)*, *nT1(IV;V),* LGX: *axIs36* [pJH1.16 ($P_{pes\text{-}10}$*pes-10::gfp*)], LGextrachromosomal and LG unknown: *axEx73*[pJH3.92 ($P_{pie\text{-}1}$*pie-1::gfp*), pRF4], *axEx1120* [pKR1.58 ($P_{pie\text{-}1}$*gfp::pie-1* ^{ZF1}), pRF4], *itIs153* [pMW1.03 ($P_{pie\text{-}1}$*gfp::par-2*), pRF4]. An transgenic strain, SS747 ($P_{pie\text{-}1}$*gfp::pgl-1,* a gift from Susan Strome) was used for RNAi analysis.

Plasmid construction

oma-2 feeding RNAi clone, pRL451 was constructed by inserting the entire coding sequence from a cDNA into pPD129.36. *spn-4* RNAi clone was constructed by inserting the entire spliced coding region into the feeding RNAi vector pDONRdT7 (Reddien et al. 2005). *mex-*

3 RNAi clone was isolated from the Ahringer library and sequence verified (Kamath and Ahringer 2003).

RNA interference

oma-2, spn-4, and *mex-3* RNAi was performed using the feeding method (Timmons and Fire 1998). Briefly, overnight saturated culture of HT115 transformant was induced with 0.4mM IPTG at room-temperature for 3 hr and spun concentrated 10-fold before placed onto NGM plates containing 1mM IPTG. Worms were fed with the dsRNA-expression bacteria from L1 stage to adulthood at 25C.

Immunofluorescence and imaging

Immunofluorescence and imaging were performed essentially as previously described (Albertson 1984; Lin et al. 1998). Briefly, three methods were employed. Methanol fixation: Embryos were released from gravid adults by dissection on the polylysine-coated glass slide. Embryos were squished by placing a coverslip over samples and wicking off H_2O between the glass slide and coverslip to crack the eggshell. After flash freezing the slide on dry ice, the coverslip was flicked off in order to remove eggshell. Slides were immediately immersed in methanol at -20°C for 10 minutes for fixation, re-hydrated in PBS-T (PBS containing 0.1% Tween20) for 10 minutes, then incubated with Landon blocking solution (Lin et al. 1998) for 30 minutes at a room-temperature. Slides were incubated with primary antibodies prepared in PBS overnight at 4°C. After 3 times of PBS-T washes, samples were incubated with fluorophore-conjugated secondary antibodies for 1 hour at a room-

temperature. After 3 times of PBS-T washes, the samples were mounted and analyzed. Methanol-acetone fixation: essentially the same as the methanol fixation except that samples were treated with acetone for 10 minutes at -20°C after methanol fixation, then re-hydrated by acetone/PBS series (90%, 60%, 30%, 10%, and 0% acetone), and that 1% non-fat milk in PBS-T was used as a blocking reagent instead of Landon blocking solution. PFA/DMF fixation: After dissecting worms on the glass slide, H_2O was replaced with 2% paraformaldehyde (PFA)-containing fixative (Lin et al. 1998) and embryos were squished as described for methanol fixation. The squished embryos were incubated in the PFA fixative for 15 minutes at a room-temparature to allow fixation to proceed before flash frozen on dry ice. After the coverslip was flicked off, the slide was immersed in dimethylformamide (DMF) for 5 minutes at -20°C. The rest of the procedure was identical to methanol fixation. Antibody dilutions and fixation method used: rabbit anti-OMA-1 1/2, PFA/DMF (Detwiler et al. 2001); mouse anti-PIE-1 (a gift from James Priess) 1/50, PFA/DMF; mouse anti-MEX-5 (a gift from James Priess) no dilution, PFA/DMF; rabbit anti-PGL-1 (a gift from Susan Strome) 1/10,000, PFA/DMF; rabbit anti-SPN-4 (a gift from Yuji Kohara) 1/10,000, methanol/acetone; rabbit anti-GLD-1 (a gift from Tim schedl) 1/10 or 1/25, methanol; mouse anti-MEX-3, no dilution, PFA/DMF, goat anti-mouse IgG-Alexa 568 (Molecular Probes) 1:250, goat anti-rabbit IgG-Alexa 488 (Molecular Probes) 1:250.

RESULTS

oma-1(zu405) is a maternal effect embryonic lethal mutation. All my analyses for *oma-1(zu405)* were performed on embryos derived from homozygous *oma-1(zu405)* animals. For simplicity, I refer to these embryos as "*oma-1(zu405)* embryos".

It has been proposed that OMA-1 degradation defect is likely to be causal to the defects seen in *oma-1(zu405)* embryos (Lin 2003). However, *zu405*/P_{240}L substitution might also change the property of OMA-1. For example, MBK-2 and GSK-3 phosphorylation might contribute to the function of OMA-1 in the 1-cell embryo. P_{240}L mutation would disturb such phosphorylation-dependent function. Such qualitative alteration of OMA-1 might contribute to the phenotype of *oma-1(zu405)*. Alternatively, the consequences of a qualitative alteration might be revealed only when OMA-1's redundant partner, OMA-2 is depleted (Detwiler et al. 2001). Analysis of OMA-1 P_{240}L property might provide us with insights into OMA proteins' function, particularly in the 1-cell embryo, and particularly in relation to MBK-2 and GSK-3 phosphorylation.

In order to dissect the consequence of P_{240}L mutation to OMA-1 protein property, I took two approaches. The first is to characterize *oma-1(zu405); oma-2(RNAi)* embryos. This analysis revealed 3 classes of early embryonic defects that are described below: 1) defects that are revealed only when *oma-2* is depleted, 2) *oma-1(zu405)* defects that are further enhanced by *oma-2* depletion, 3) an *oma-1(zu405)* defect that is not enhanced by *oma-2(RNAi)*. The second is to genetically manipulate phosphorylation and/or degradation of OMA proteins. This analysis suggested that phosphorylation, but not degradation delay itself, contribute to certain defects of *oma-1(zu405)* embryos.

I. Characterization of *oma-1(zu405); oma-2(RNAi)* embryos

1. *oma-2* RNAi enhances *oma-1(zu405*) lethality without delaying OMA-1 degradation

I reasoned that by depleting *oma-1*'s redundant homolog, *oma-2*, the impact of $P_{240}L$ mutation on OMA-1 protein property might be unveiled. A previous study has shown that OMA-2 protein expression level and pattern are unaltered by *oma-1(zu405)* mutation (Lin 2003). Conversely, I showed that *oma-2* depletion does not change the OMA-1 expression level nor enhance OMA-1 degradation delay in *oma-1(zu405)* mutant embryos (Figure 3.1). Thus *oma*-2 depletion would reveal the impact of $P_{240}L$ on OMA-1 protein property in the oocyte and 1-cell embryo, where OMA-2 is expressed (Detwiler et al. 2001). Whereas all *oma-1(zu405)* mutant embryos are lethal at 25°C, 50% of them are viable at 15°C (Lin 2003). Indeed, I showed that RNAi depletion of *oma-2* enhanced the embryonic lethality of *oma-1(zu405)* from 50% to 100% at 15°C. *oma-2* RNAi in the wild-type strain does not produce any phenotype (Detwiler et al. 2001). *oma-2* RNAi at the same condition causes fully penetrant oocyte maturation defect phenotype in *oma-1(-)* animals (Detwiler et al. 2001). On the other hand, *oma-1(zu405); oma-2(RNAi)* animals did not show a defect in oocyte maturation at 16°C or 25°C, indicating that OMA-1 $P_{240}L$ protein is functional for oocyte maturation. This result is consistent with the notion that $P_{240}L$ mutation affects embryonic function, but not oocyte maturation function, of OMA-1. To understand the molecular basis of this observation, *oma-1(zu405); oma-2(RNAi)* embryos were further analyzed utilizing markers for early embryogenesis.

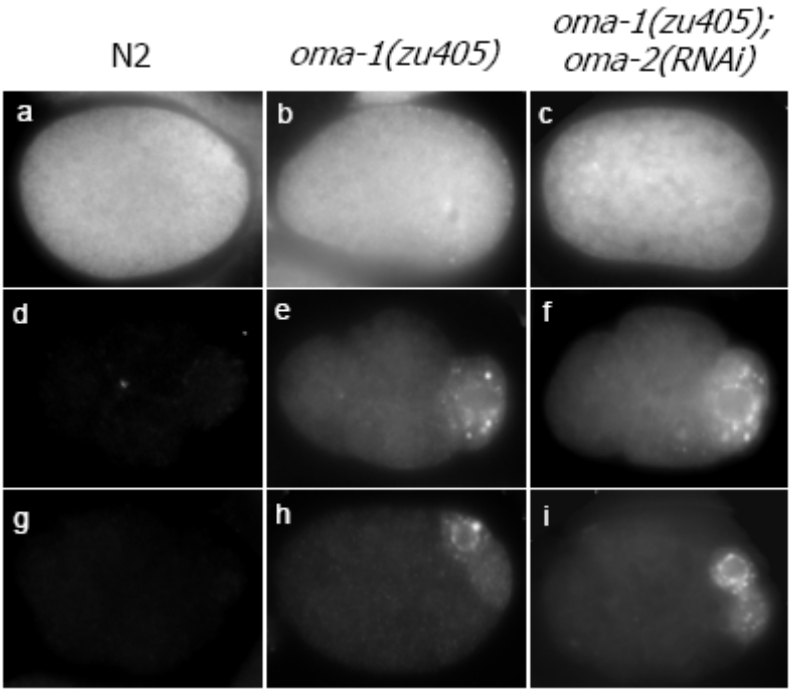

Figure 3.1 *oma-2* depletion does not alter OMA-1 expression in *oma-1(zu405)* embryos
Early embryos of N2 (left column), *oma-1(zu405)* (middle column), and *oma-1(zu405); oma-2(RNAi)* (right column) were stained with anti-OMA-1 antibody. (a-c) 1-cell stage (d-f) 4-cell stage (g-i) 28-cell stage

2. Novel defects revealed by *oma-2* RNAi

2-1. Abnormal early embryonic polarity

PAR proteins are important for asymmetric cell division and cell polarity in many different organisms (Doe 2001). Whereas PARs localize asymmetrically along the anterior-posterior axis in germline precursors shortly before their divisions, they exhibit basolateral versus apical polarity in somatic blastomeres in early *C. elegans* embryos (Nance and Priess 2002)(Figure 3.2j). In order to analyze the embryonic polarity of *oma-1(zu405)* embryos, I

examined PAR-localization utilizing GFP::PAR-2 transgene (Cuenca et al. 2003). Whereas *oma-1(zu405)* embryos did not exhibit an abnormality in PAR-2 localization, *oma-1(zu405); oma-2(RNAi)* embryos exhibited disruptions in PAR-2 distribution at early embryonic stages (Figure 3.2). Specifically, at the 1-cell stage, a persisting patch of cortical PAR-2 was frequently observed in the anterior, where PAR-2 is normally absent, or present only transiently (Boyd et al. 1996; Cuenca et al. 2003)(Figure 3.2f). PAR-2 is expressed exclusively in the P1 blastomere in the wild-type 2-cell stage embryo (Boyd et al. 1996; Cuenca et al. 2003)(Figure 3.2g). In *oma-1(zu405); oma-2(RNAi)* embryos, PAR-2 was laterally expressed on the cortex of the AB and P1 blastomeres (Figure 3.2i). At the 4-cell stage in wild-type, all 3 somatic blastomeres express PAR-2 only on the baso-lateral cortex (Nance and Priess 2002)(Figure 3.2j). In many *oma-1(zu405); oma-2(RNAi)* embryos, the EMS blastomere ectopically expressed PAR-2 on the apical cortex (Figure 3.2l). In summary, PAR-2 assumes abnormal localizations in early *oma-1(zu405); oma-2(RNAi)* embryos, but not *oma-1(zu405)* embryos. Importantly, the PAR-2 localization defect was observed as early as early 1-cell stage, when OMA-1 degradation has not been initiated in wild-type. In addition, the PAR-2 localization defect was uncovered only when *oma-2* was depleted. *oma-2* depletion did not enhance OMA-1 degradation delay (Figure 3.1). Thus the observed PAR-2 defect, at least at the 1-cell stage, is independent of OMA-1 degradation delay.

2-2. Extra P-granule containing blastomeres

P-granule is the germ-granule of *C. elegans* thought to be critical for germline identity (Strome and Wood 1982; Strome and Wood 1983). Consistently, P-granule is restricted to the germline lineage throughout the lifecycle of *C. elegans* (Strome and Wood 1982; Strome and Wood 1983). Up to the 100-cell stage during embryogenesis, only single germline precursor is present in the embryo, and P-granule is restricted to this single germline precursor, although shortly after germline precursor divisions, low levels of P-granule are observed in the somatic daughter (Strome and Wood 1982). At the 100-cell stage, the germline precursor P4 divides symmetrically to give rise to two germline progenitors, and throughout the rest of embryogenesis, these two blastomeres remain the only blastomeres containing P-granule (Strome and Wood 1982). Although P-granule distribution was apparently normal in *oma-1(zu405)*, nearly 100% of *oma-1(zu405)*; *oma-2(RNAi)* embryos contained extra blastomeres containing P-granule before the 100-cell stage. Up to 4 P-granule-expressing blastomeres were observed before the 100-cell stage, and 6 blastomeres after the 100-cell stage. These blastomeres were clustered at the posterior pole of the embryo, where the germline precursor normally resides (Sulston et al. 1983). Importantly, no P-granule mis-expression was observed at or before the 28-cell stage (data not shown). P4 is generated by the 28-cell stage, in the wild-type and apparently in *oma-1(zu405)* embryo (Sulston et al. 1983; Lin 2003). P4 does not divide again until the 100-cell stage (Sulston et al. 1983). These observations suggest that the increased number of P-granule-containing blastomeres in *oma-1(zu405); oma-2(RNAi)* embryos is likely due to additional divisions of germline precursors after the 28-cell stage, not due to mis-segregation of P-granules during cell divisions, although a lineage analysis is required to confirm this notion.

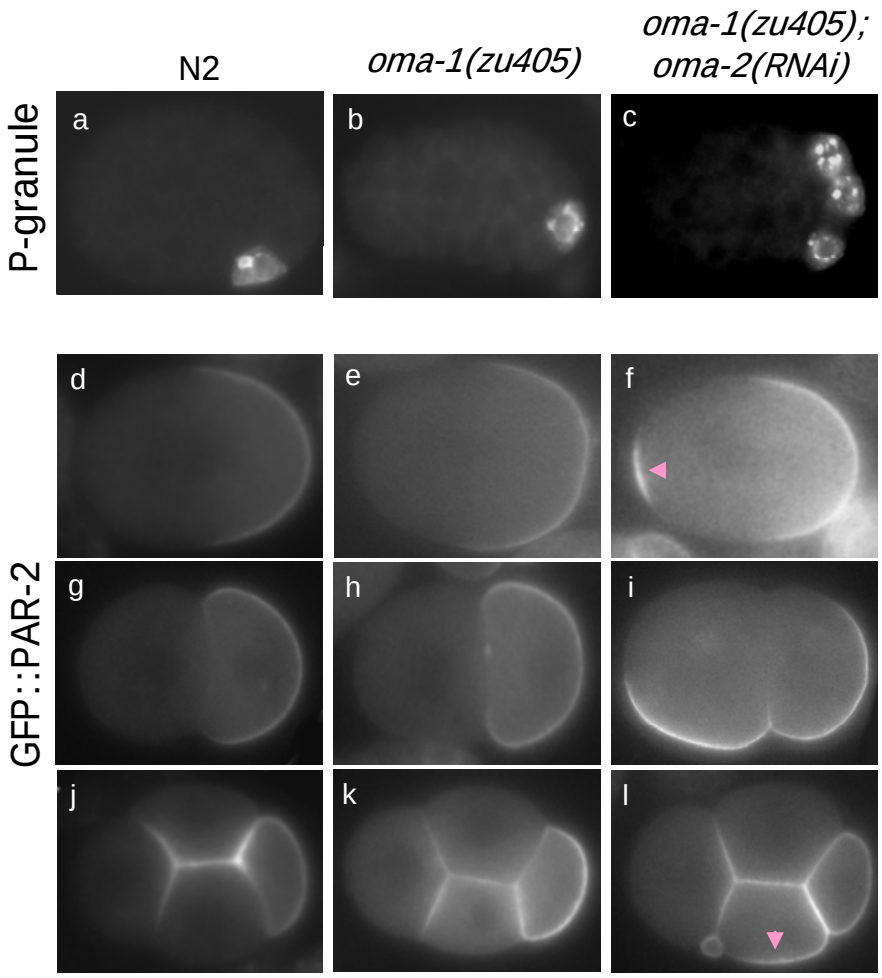

Figure 3.2 P-granule and PAR-2 are mislocalized in *oma-1(zu405); oma-2(RNAi)* embryos
(a-c) 50-cell stage embryos stained with anti-PGL-1 (P-granule component) antibody. (d-l) embryos carrying GFP::PAR-2 reporter. (d-f) 1-cell pronuclear migration stage, (g-i) 2-cell stage, (j-l) 4-cell stage. Arrowheads indicate anterior cortex of 1-cell stage embryo (f), and apical cortex of the EMS blastomere (l),where PAR-2 is ectopically localized.

3. *oma-1(zu405)* defects enhanced by *oma-2* RNAi

3-1. ZIF-1-mediated CCCH zinc finger protein degradations in soma

A previous study showed mis-localizations of several maternally provided proteins in *oma-1(zu405)* mutant embryos, including PIE-1 and MEX-5 (Lin 2003). They are germline

precursor-restricted and -enriched factors important for the germline fate and embryonic patterning (Mello et al. 1996; Schubert et al. 2000). Their patterned expression is thought to be mediated by at least two separate mechanisms. The first mechanism involves polarization in the germline precursor shortly before cell divisions. PIE-1 distribution becomes strongly polarized in germline precursors shortly before divisions through an unknown mechanism (Mello et al. 1996; Reese et al. 2000). Consequently, the majority of PIE-1 is inherited to the germline daughter, however a small proportion of PIE-1 protein is segregated to the somatic daughter (Mello et al. 1996; Reese et al. 2000). The second mechanism is known to involve proteasomal protein degradation in somatic blastomeres. The small amount of PIE-1 protein inherited to somatic blastomeres is targeted to degradation by ZIF-1 E3 ligase (Reese et al. 2000; DeRenzo et al. 2003). In *zif-1* depleted embryos, PIE-1 accumulates in somatic blastomeres (DeRenzo et al. 2003). MEX-5 localization similarly relies on a pre-division polarization and ZIF-1-mediated protein degradation although the localization pattern of MEX-5 is distinct from PIE-1 (Mello et al. 1996; Schubert et al. 2000; DeRenzo et al. 2003). Importantly, ZIF-1 appears to play a major part in shaping the proper MEX-5 localization as *zif-1* depletion results in a dramatic mislocalization of MEX-5 (DeRenzo et al. 2003).

I examined PIE-1 and MEX-5 expression in *oma-1(zu405); oma-2(RNAi)* embryos. The pre-division polarization of PIE-1 and MEX-5 at the 1- and 2-cell stages was not affected in *oma-1(zu405)* or *oma-1(zu405); oma-2(RNAi)* embryos, suggesting that the pre-division polarization of PIE-1 and MEX-5 in the germline precursor is unaffected (Figure 3.3 a-c and g-i). This notion was supported for later germline precursor divisions as well, at least for PIE-1, because the majority of PIE-1 protein was segregated to a single blastomere like in

wild-type (Figure 3.3 d-f). On the other hand, both PIE-1 and MEX-5 showed ectopic expression in the somatic blastomeres of *oma-1(zu405)* at and after the 4-cell stage as reported before (Lin 2003) (Figure 3.3 e and k). Interestingly, the PIE-1 and MEX-5 mislocalization was further exacerbated by RNAi depletion of *oma-2* (Figure 3.3 f and l). The ectopic expression of PIE-1 and MEX-5 in *oma-1(zu405); oma-2(RNAi)* embryos was strikingly reminiscent of embryos depleted of *zif-1*, the E3 ligase responsible for the degradation of PIE-1 and MEX-5 in somatic blastomeres (DeRenzo et al. 2003). This observation prompted me to examine the expression of GFP::PIE-1^{ZF1}, a specific marker for the ZIF-1-mediated degradation of PIE-1 and MEX-5 (Reese et al. 2000; DeRenzo et al. 2003). Indeed, GFP::PIE-1^{ZF1} exhibited a severe degradation delay in *oma-1(zu405)* (Figure 3.3n). Consistent with the ectopic expression of PIE-1 and MEX-5 enhanced by *oma-2* depletion, the delay in GFP::PIE-1^{ZF1} degradation was also exacerbated by *oma-2* depletion (Figure 3.3o). In summary, my results suggest that *oma-1(zu405)* mutation specifically compromise the ZIF-1 E3 ligase-mediated degradation of PIE-1 and MEX-5 in soma, but not the pre-division polarization of PIE-1 and MEX-5, and that *oma-2* depletion exacerbate the degradation defect.

3-2. mis-localizations of OMA-1 binding proteins, MEX-3 and SPN-4

MEX-3 and SPN-4 are RNA binding translational regulators expressed in early embryos (Draper et al. 1996; Ogura et al. 2003). In Chapter 5, I show that both MEX-3 and SPN-4 physically interact with OMA-1 in a yeast two-hybrid system. MEX-3 is a KH domain protein expressed in the cytoplasm of developing oocytes and early embryos (Draper et al.

1996). In the early embryo, MEX-3 is enriched in anterior blastomeres, however, starting around the 8- to 16-cell stage, its expression becomes restricted to the posterior in the germline lineage (Draper et al. 1996). The molecular mechanism regulating this MEX-3 expression pattern is currently unknown. As previously reported, MEX-3 was mislocalized in *oma-1(zu405)* embryos (Lin 2003)(Figure 3.4h). Although initial embryonic MEX-3 pattern appeared normal in *oma-1(zu405)*, MEX-3 expression was less restricted to germline precursors in later *oma-1(zu405)* embryos (Lin 2003) (Figure 3.4h and data not shown). This defect was further exacerbated by the depletion of *oma-2* (Figure 3.4i). MEX-3 expression level and pattern in the gonad did not change by *oma-2* RNAi in *oma-1(zu405)* mutant (data not shown).

Like MEX-3, SPN-4 protein is expressed in developing oocytes and shows patterned expression in early embryos (Ogura et al. 2003). The patterned embryonic expression is thought to be important for SPN-4 to translationally regulate its target in a blastomere-specific manner (Ogura et al. 2003). Consistent with its importance in embryogenesis, *spn-4* mutants show fully penetrant embryonic lethality (Gomes et al. 2001; Ogura et al. 2003). In wild-type, SPN-4 expression is enriched in posterior blastomeres and eventually becomes restricted to the germline precursors (Ogura et al. 2003). Although initial expression pattern appeared normal in *oma-1(zu405)* at the 2- to 6-cell stages, SPN-4 was less restricted to the posterior embryos at the 8- to 28-cell stage (Figure 3.4b and data not shown). Although *oma-2* depletion did not alter SPN-4 expression in early stages (4- to 28-cell stages, Figure 3.4c), SPN-4 was less strictly restricted to the germline precursor in later embryos (Figure 3.4f).

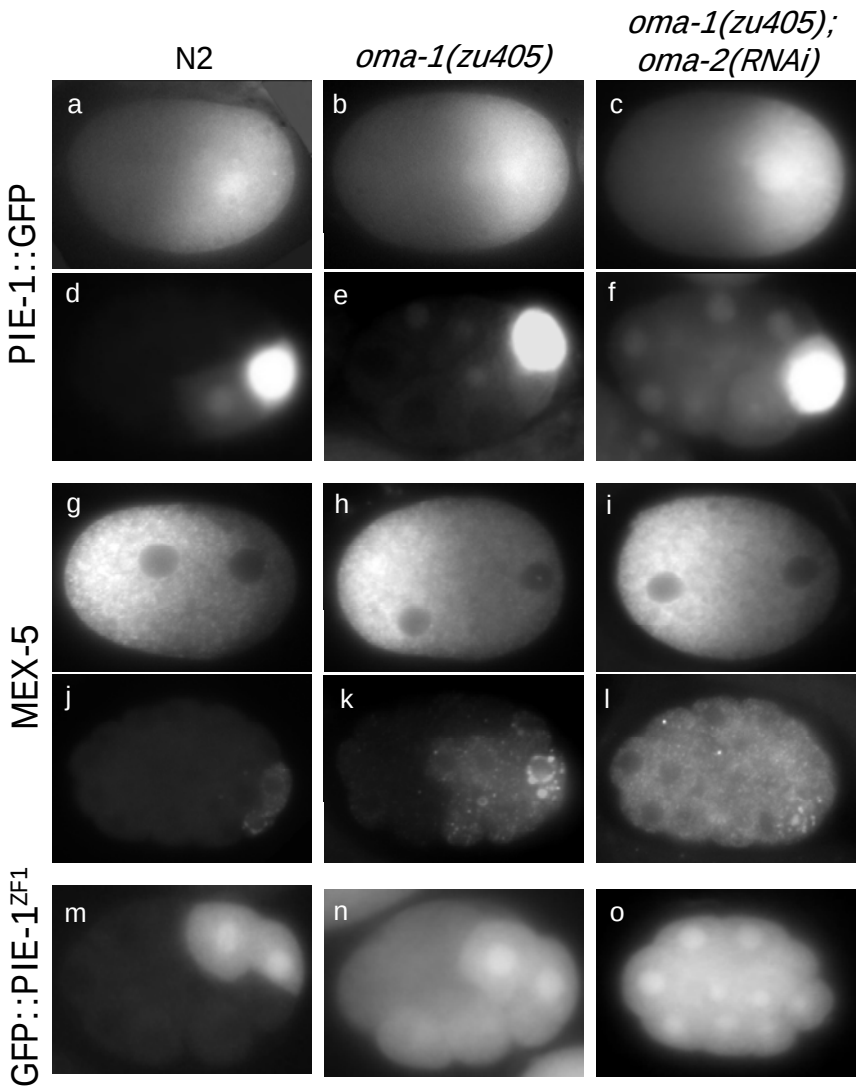

Figure 3.3 *oma-2* depletion exacerbates ZIF-1 mediated degradation delay of *oma-1(zu405)*

(a-c, g-i) 1-cell stage, (d-f, m-o) 16-cell stage (j-l), 28-cell stage embryos carrying PIE-1::GFP reporter (a-f) or GFP::PIE-1^{ZF1} reporter (m-o), or stained with anti-MEX-5 (g-l) from N2 (left comulm), *oma-1(zu405)* (middle column), and *oma-1(zu405); oma-2(RNAi)* animals

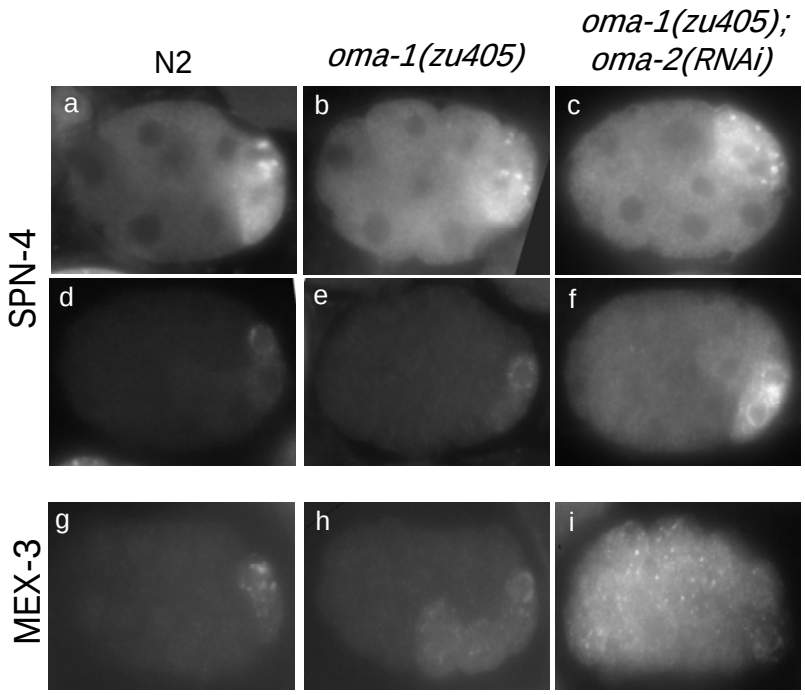

Figure 3.4 *oma-2* depletion exacerbates SPN-4 and MEX-3 mis-localization defects of *oma-1(zu405)*
Embryos of indicated genotypes at the 8-cell stage (a-c) and 50-cell stage (d-i) stained with anti-SPN-4 antibody (a-f) or anti-MEX-3 antibody (g-i).

3.3 ectopic transcriptional silencing in soma

In early *C. elegans* early embryos, transcription is inactive in the germline lineage (Seydoux and Fire 1994). This transcriptional quiescence is thought to be essential for germline precursors to retain the properties of germline such as totipotency (Seydoux et al. 1996; Seydoux and Dunn 1997). PIE-1 is known to mediate the transcriptional quiescence in the early embryo. Specifically, the transcriptional quiescence in the germline precursor at and after the 4-cell stage depends on PIE-1 (Seydoux et al. 1996). The 1-cell embryo and the P1

blastomere at the 2-cell stage are germline precursors and transcription is inactive. However, the mechanism responsible for the transcriptional quiescence at these stages was unknown.

I investigated the transcriptional activity of *oma-1(zu405)* and *oma-1(zu405); oma-2(RNAi)* embryos using PES-10::GFP reporter (a gift from Geraldine Seydoux). This GFP reporter robustly expresses all blastomeres but the germline precursor at and after the 28-cell stage. As shown for PIE-10::lacZ reporter previously, the absence of the PES-10::GFP signal in the germline precursor depends on PIE-1, because *pie-1(RNAi)* embryos express PES-10::GFP in all blastomeres including the germline precursor (Figure 3.5b) (Seydoux et al. 1996). I showed that PIE-1 is ectopically expressed in early *oma-1(zu405)* and *oma-1(zu405); oma-2(RNAi)* embryos (Figure 3.3). Thus, *oma-1(zu405)* and *oma-1(zu405); oma-2(RNAi)* embryos are expected to exhibit transcriptional silencing due to PIE-1 mis-expression. However, in this study, I specifically asked whether or not *oma-1(zu405)* mutant shows *pie-1*-independent transcriptional silencing in the early embryo by depleting *pie-1* by RNAi. As mentioned above, *pie-1* RNAi results in the expression of PES-10::GFP reporter in the germline precursor in wild-type (Figure 3.5b). Interestingly, in *oma-1(zu405)* mutant embryos depleted of *pie-1*, PES-10::GFP signal was weaker in the posterior in and around the germline precursors (Figure 3.5c). Strikingly, the depletion of *oma-2*, in addition to *pie-1*, resulted in a severe reduction in PES-10::GFP signal throughout the embryo (Figure 3.5d). These results suggest that *oma-1(zu405)* results in PIE-1-independent transcriptional silencing in the early embryo, and *oma-2* depletion strongly enhances this phenotype.

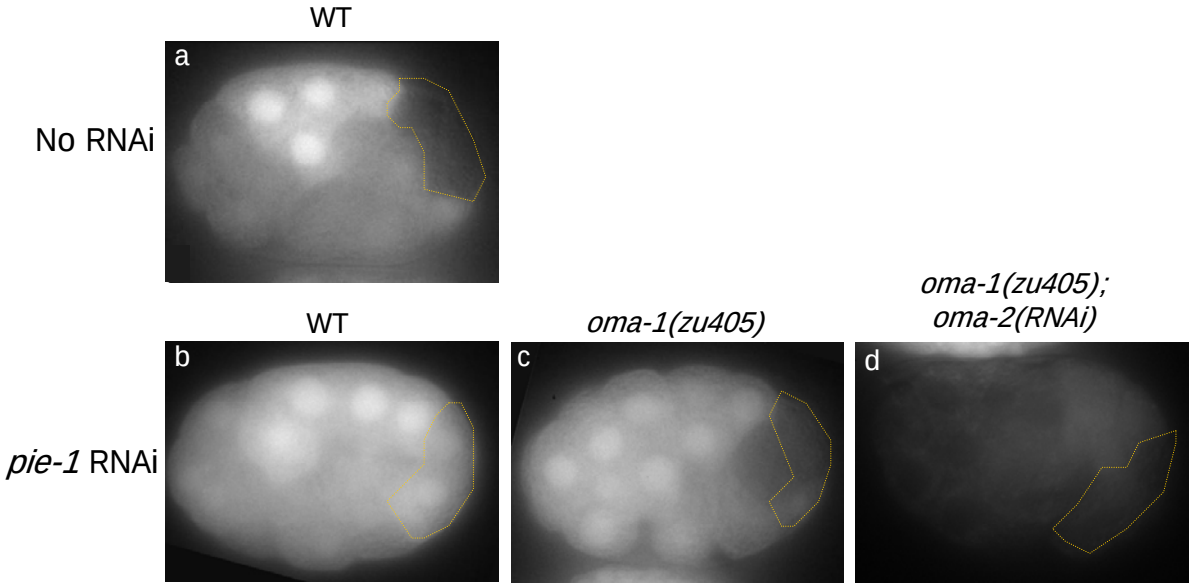

Figure 3.5 *oma-1(zu405)* shows PIE-1-independent downregulation of PES-10::GFP
PES-10::GFP signal without *pie-1* RNAi (a) or with *pie-1* RNAi (b-d) at the 28-cell stage. (a and b) wild-type, (c) *oma-1(zu405)*, and (d) *oma-1(zu405)* depleted of *oma-2* (in addition to *pie-1*). The germline precursor and its sister are outlined with dashed line in yellow.

4. *oma-2* independent *oma-1(zu405)* defect

4.1 GLD-1 is diminished in early oma-1(zu405) embryos

GLD-1 is a KH domain protein known as a translational repressor expressed in the distal gonad as well as in the early embryo (Jones et al. 1996). GLD-1 expression is nearly reciprocal to that of OMA-1/2 both in the gonad and early embryo. In the gonad, GLD-1 is highly expressed in the distal region, whereas in the embryo, GLD-1 is expression at and after 4-cell stage (Jones et al. 1996). On the other hand, OMA-1/2 are expressed in the proximal gonad and 1-cell stage embryo (Detwiler et al. 2001; Lin 2003). In the distal gonad, GLD-1 represses the translation of OMA-1/2 (Lee and Schedl 2001b). In the

proximal gonad, GLD-1 level is lowered through an unknown mechanism, allowing OMA-1/2 proteins to accumulate (Lee and Schedl 2001b; Lee and Schedl 2004). OMA-1/2 proteins remain expressed until the end of the 1-cell stage, at which they become degraded by the phosphorylation and ubiquitination events (See Chapter 2). GLD-1 expression resumes soon after the degradation of OMA proteins, at the 4-cell stage (Jones et al. 1996; Lin 2003). The underlying mechanism controlling GLD-1 expression in the embryo is unknown. In addition to OMA-1/2, GLD-1 is known to translationally repress many factors in the distal gonad (Lee and Schedl 2001b; Lee and Schedl 2004). *gld-1*, together with *mex-3*, is required to prevent germ cells from taking somatic fates (Ciosk et al. 2006). Thus it has been proposed that GLD-1 protects the totipotency of germ cells via translational repression (Ciosk et al. 2006). In the early embryo, GLD-1 is thought to repress the translation of a developmental regulator, GLP-1/Notch (Marin and Evans 2003).

To characterize *oma-1(zu405)* mutant further, I analyzed GLD-1 expression in *oma-1(zu405)* mutant embryos. In wild-type, GLD-1 is expressed at as early as the 4-cell stage, robustly in the germline precursor and weakly in its sister (Jones et al. 1996)(Figure 3.6). GLD-1 remains associated with the germline precursor and the primordial germ cells throughout embryonic development (Jones et al. 1996). Strikingly, in *oma-1(zu405)* embryos, GLD-1 expression is greatly diminished at early embryonic stages (2- to 28-cell stages) (Figure 3.6 and data not shown). Embryos at later stages expressed GLD-1 in the correct pattern at comparable levels as wild-type (data not shown). Notably, the onset of GLD-1 expression around 28-cell stage coincides with the disappearance of OMA-1 protein in *oma-1(zu405)* embryos, consistent with the notion that the ectopic

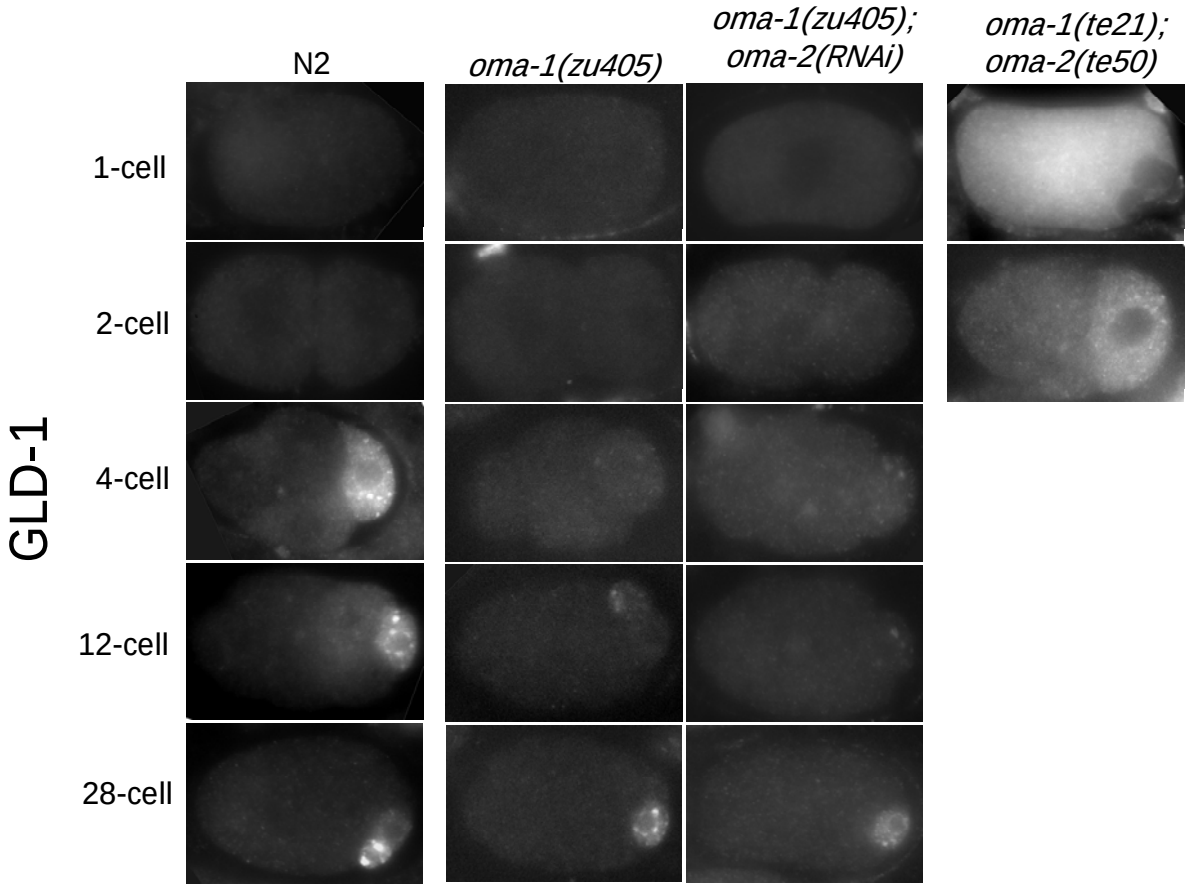

Figure 3.6 GLD-1 is downregulated in *oma-1(zu405)* and upregulated in *oma-1(te21); oma-2 (te50)* embryos
Embryos of the indicated genotypes and stages were stained with anti-GLD-1 antibody [*oma-1(te21); oma-2(te50)* analysis was performed by Rueyling Lin].

presence of OMA-1 represses GLD-1 expression in *oma-1(zu405)* mutant embryos (Lin 2003). *oma-2* depletion did not result in a notable alteration of GLD-1 expression in *oma-1(zu405)* embryos (Figure 3.6). These results suggest that OMA-1 degradation delay, not a change in OMA-1 protein property, is responsible for the observed GLD-1 diminishment in *oma-1(zu405)*.

4.2 Embryonic GLD-1 expression might be regulated by OMAs

Both in wild-type and *oma-1(zu405)* mutant, OMA-1/2 and GLD-1 are expressed in nearly reciprocal patterns in the embryo. This raised a possibility that OMA-1/2 normally repress GLD-1 expression in the early embryo. To test this notion, embryos from a double mutant of *oma-1/2* reduction alleles, *oma-1(te21); oma-2(te50)* were analyzed for GLD-1 expression. *oma-1(te21); oma-2(te50)* animals exhibit an impenetrant oocyte maturation defect and produce embryos (Nishi and Lin 2005). The embryos from *oma-1(te21); oma-2(te50)* animals are lethal with severe defects in early development (Nishi and Lin 2005). In *oma-1(te21); oma-2(te50)* mutant embryos, higher levels of GLD-1 were observed at the 1- and 2-cell stages, suggesting that OMA-1/2 normally represses GLD-1 expression (Experiment conducted by Rueyling Lin, Figure 3.6). On the other hand, GLD-1 expression in the gonad was not altered significantly in *oma-1(te21); oma-2(te50)* mutant, suggesting that OMA-1/2 repress GLD-1 specifically in the embryo (data not shown).

II. Potential role of phosphorylation in embryonic functions of OMA proteins

oma-1(zu405) mutation interferes with OMA-1 phosphorylation at T_{239} and causes a delay in OMA-1 protein degradation (see Chapter 2). Although OMA-1 degradation delay was speculated to account for the embryonic defects of *oma-1(zu405)*, attenuated OMA-1 phosphorylation could contribute to *oma-1(zu405)* defects as well (Lin 2003). In order to assess this possibility, I have examined a process defective in *oma-1(zu405)*, ZIF-1-mediated protein degradation (Figure 3.3).

I showed that MBK-2 and GSK-3 both directly phosphorylate OMA-1 (see Chapter 2). I and another group showed that *mbk-2* and *gsk-3* are both required for OMA-1 degradation at

the first mitosis (Pellettieri et al. 2003)(Chapter 2). Thus *mbk-2* and *gsk-3* RNAi will result in both compromised OMA protein phosphorylation and a delay in OMA protein degradation. On the other hand, candidate E3 ligases for OMAs are not expected to affect phosphorylation of OMA proteins (See Chapter 2). Rather, they are likely to execute OMA protein degradation in response to MBK-2 and GSK-3 phosphorylation.

I examined GFP::PIE-1 ^{ZF1} degradation pattern in *gsk-3*, *cul-1*, and *skr-1* RNAi embryos. *mbk-2* RNAi was previously shown to result in delays in both OMA-1 and GFP::PIE-1 ^{ZF1} degradation (Pellettieri et al. 2003). Interestingly, *gsk-3* RNAi similarly resulted in a severe delay in GFP::PIE-1^{ZF1} degradation, whereas *cul-1* and *skr-1* RNAi did not alter GFP::PIE-1^{ZF1} degradation pattern (Figure 3.7 and data not shown). On the other hand, *gsk-3*, *cul-1*, and *skr-1* RNAi all delayed OMA-1 degradation to similar extents (Figure 3.7 and data not shown). These results suggest that compromised phosphorylation of OMA proteins, but not OMA-1 degradation delay alone, is responsible for the delay in ZIF-1-mediated protein degradation in *oma-1(zu405)* mutant.

III. ZIF-1-mediated degradation might be regulated by OMAs

I showed that GLD-1 is diminished in *oma-1(zu405)*, whereas GLD-1 is precociously expressed in 1- and 2-cell embryos of *oma-1/2* hypomorphic mutant (Figure 3.6). This result is consistent with GLD-1 expression being repressed by OMA-1/2 at the 1- and 2-cell stages in wild-type. Furthermore, a recent study showed that additional divisions of germline precursors occur in embryos weakly depleted of *oma-1/2* (Shimada et al. 2006). Additional germline precursor divisions were observed in *oma-1(zu405); oma-2(RNAi)* embryos in my

analysis (Figure 3.2). Thus the processes mis-regulated in *oma-1(zu405)* embryos are likely to be good candidates for physiological targets of OMA-1/2. In this section, I describe my analysis of another process misregulated in *oma-1(zu405)*, ZIF-1-mediated proteasomal degradation. My data shows that ZIF-1-mediated degradation precociously occur in *oma-1/2* depleted goand and the repression of ZIF-1-mediated degradation in *oma-1(zu405)* embryo is *mex-3* and *spn-4* dependent, thus OMA proteins might translationally repress ZIF-1-mediated degradation in the gonad and 1-cell embryo.

GFP::PIE-1^{ZF1} reporter is expressed in a patterned fashion in early embryos (Reese et al. 2000). This patterned expression is thought to reflect ZIF-1 E3 ligase activity. The fragment fused to GFP in the reporter (PIE-1^{ZF1}) physically interacts with ZIF-1, and the depletion of *zif-1* results in ubiquitous expression of GFP::PIE-1^{ZF1} in early embryos (DeRenzo et al. 2003). In order to ask whether OMA-1/2 regulate ZIF-1-mediated protein degradation, GFP::PIE-1^{ZF1} expression was analyzed in *oma-1(RNAi); oma-2(RNAi)* gonad. In *oma-1(zu405)* embryos, the degradation of GFP::PIE-1^{ZF1} was delayed (Figure 3.3n). In contrast, in the gonad of *oma-1(RNAi); oma-2(RNAi)* animals, GFP signal was greatly diminished (Figure 3.8). On the other hand, the same RNAi condition did not result in a change in the expression level of GFP::PGL-1 transgene (Figure 3.8). The GFP::PGL-1 transgene was controlled by the same 5' and 3' elements as the GFP::PIE-1^{ZF1} transgene, suggesting that the diminishment of GFP::PIE-1^{ZF1} signal was post-translational. These results suggest that ZIF-1-mediated proteasomal degradation is ectopically expressed in *oma-1(RNAi); oma-2(RNAi)* oocytes. Thus OMA-1/2 might normally repress ZIF-1-mediated proteasomal degradation in the gonad and 1-cell embryo.

To further investigate the mechanism of the repression, I took a candidate approach to test two factors that physically interact with OMA-1, MEX-3 and SPN-4. MEX-3 and SPN-4 are translational regulators that are expressed in late oocytes and early embryos (Draper et al. 1996; Ogura et al. 2003). I show that OMA-1 physically interact with MEX-3 and SPN-4 via the first zinc finger domain (see Chapter 5). As also shown in Figure 3.3, GFP::PIE-1^{ZF1} shows a delayed degradation in *oma-1(zu405)* (Figure 3.9). Interestingly, both *mex-3* and *spn-4* RNAi suppressed this degradation delay pheynotype of *oma-1(zu405)* (Figure 3.9). Note that although MEX-3 and SPN-4 show mislocalization at later embryonic stages, they localize normally at the 4-cell stage, at which the suppression was assayed for (data not shown). These results suggest that OMA-1/2 repress ZIF-1-mediated degradation with MEX-3 and SPN-4. Because MEX-3 and SPN-4 are both known translational regulators, this repression might be at translational level.

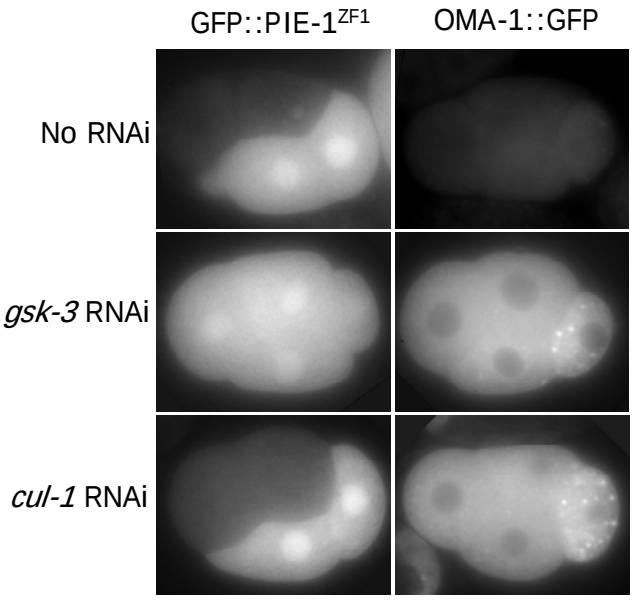

Figure 3.7 GSK-3, but not SCF E3 ligase, is required for ZIF-1 mediated degradation
gsk-3 and *cul-1* RNAi was performed in a strain carrying GFP:PIE-1^{ZF1} or OMA-1::GFP reporter.

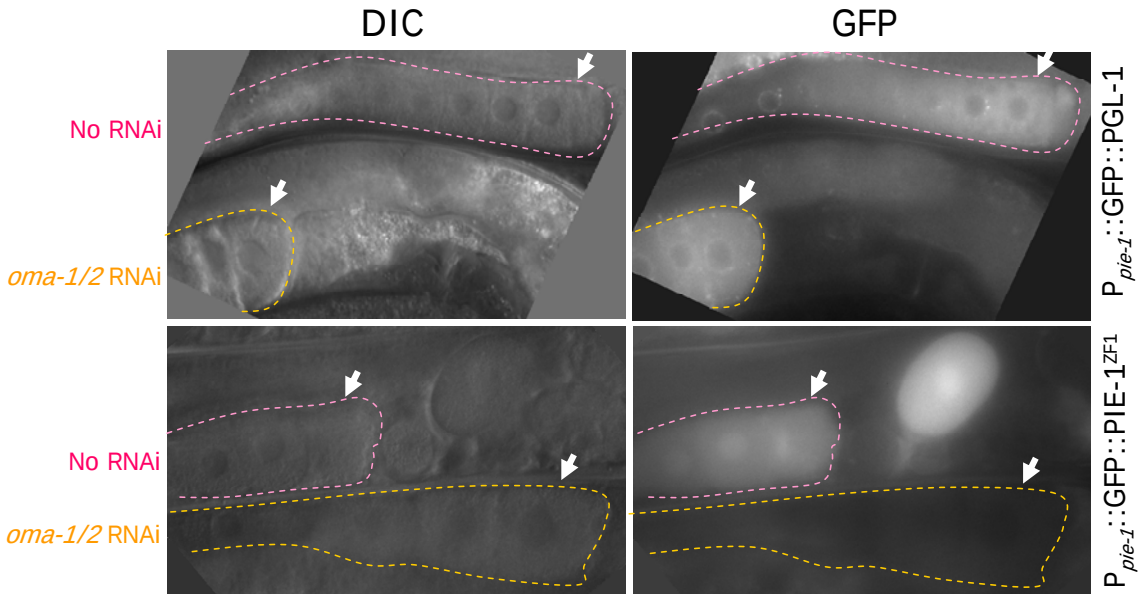

Figure 3.8 ZIF-1-mediated protein degradation precociously occurs in *oma-1/2* RNAi oocytes.
oma-1 and *oma-2* were simultaneously depleted by RNAi in a strain carrying GFP::PGL-1 or GFP::PIE-1^{ZF1} transgene. Both transgenes were expressed using identical 5' and 3' elements, thus observed differences are likely to be post-translational. No-RNAi control and *oma-1/2* RNAi animals were laid next to each other and photographed together. No-RNAi and *oma-1/2* RNAi gonads are outlined with dashed line in magenta and yellow, respectively. Arrows point at the most proximal oocytes immediately next to the spermatheca.

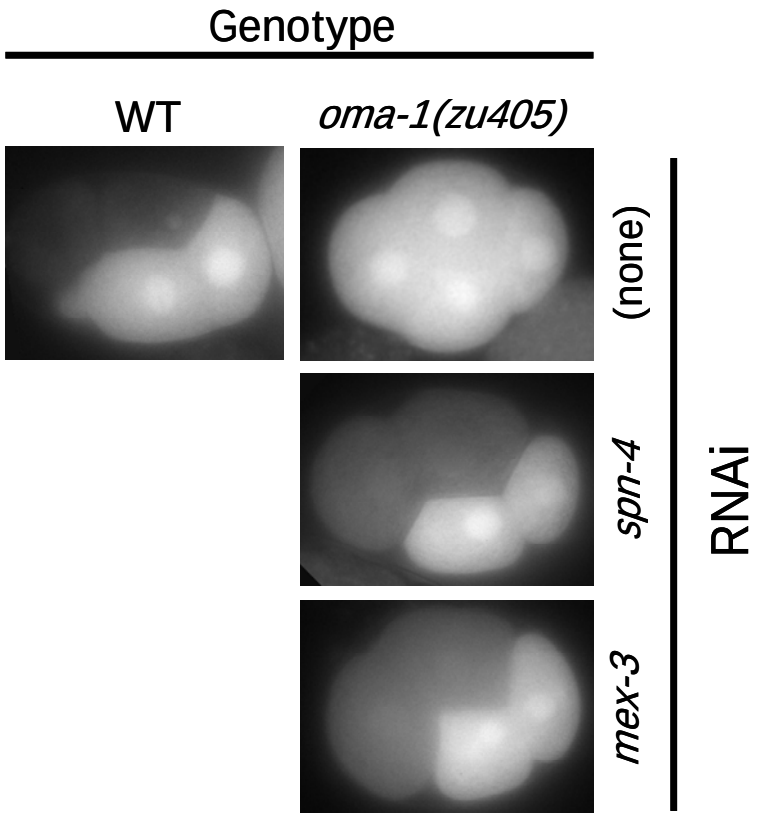

Figure 3.9 *mex-3* and *spn-4* RNAi suppresses the delay in ZIF-1 mediated proetasomal degradation in *oma-1(zu405)* mutant
Embyors of indicated genotypes carrying GFP::PIE-1^{ZF1} reporter transgene was treated with indicated RNAi.

DISCUSSION

Phosphorylation might regulate 1-cell embryonic function of OMAs

oma-1(zu405) provides a unique and useful genetic tool to probe the function of *oma-1/2*, particularly in embryogenesis. A striking phenotype of *oma-1(zu405)* is a delay in OMA-1 degradation (Lin 2003). The mutant embryos also exhibit mis-localizations of several maternally-provided cell fate determinants, which are likely to contribute to the observed cell fate transformation and ultimate death (Lin 2003). Reasonably, it has been speculated that the defects of *oma-1(zu405)* are caused by the OMA-1 degradation delay (Lin 2003). My analyses, however, suggest that change(s) in OMA-1 protein property and OMA-1 degradation delay both contribute to *oma-1(zu405)* mutant phenotypes. The changes in OMA-1 property include its inability to be efficiently phosphorylated by MBK-2 and likely by GSK-3. In Chapter 2, I showed that *zu405*/$P_{240}L$ mutation interferes with MBK-2/DYRK2 phosphorylation of OMA-1 at T_{239} at the 1-cell stage. My data further suggested that the MBK-2 phosphorylation facilitates GSK-3 phosphorylation of OMA-1, thus *zu405* mutation likely compromises GSK-3 phosphorylation as well (see Chapter 2). My analyses suggested that these phosphorylation events are critical for the degradation of the protein (see Chapter 2). On the other hand, the impact of these phosphorylation events on OMA-1/2 protein function was unknown.

In this chapter, I uncovered novel PAR-2 and P-granule mis-localization defects by depleting *oma-2* in *oma-1(zu405)* mutant embryos (Figure 3.2). I also discovered enhancements of other protein mis-localization defects (PIE-1 and MEX-5, MEX-3, and SPN-4) by *oma-2* RNAi (Figure 3.3 and 3.4). Importantly, *oma-2* depletion did not

exacerbate OMA-1 degradation delay (Figure 3.1). In addition, PAR-2 localization defect was seen as early as the 1-cell stage, before the stage when OMA-1 is normally degraded (Figure 3.2). These results suggest that some *oma-1(zu405)* defects are independent of OMA-1 degradation delay. These results suggest that change(s) of OMA-1 protein property caused by *oma-1(zu405)*/P_{240}L mutation contribute to these defects. One obvious candidate for such change is the lack or compromised phosphorylation by MBK-2 and GSK-3. I tested this possibility by genetically altering OMA-1 phosphorylation status and/or degradation (Figure 3.7). Combined with previously published results, this analysis revealed that the delay in ZIF-1-mediated protein degradation correlates with compromised phosphorylation of OMA-1, not OMA-1 degradation delay itself (DeRenzo et al. 2003; Pellettieri et al. 2003; Shirayama et al. 2006). Furthermore, a previous study showed that PAR-2 assumes an abnormal localization in an *mbk-2* mutant (Pang et al. 2004). The PAR-2 localization in the *mbk-2* mutant is strikingly reminiscent of that in *oma-1(zu405); oma-2(RNAi)* embryos, suggesting that compromised OMA-1 phosphorylation is responsible for the PAR-2 localization defect of the *mbk-2* and *oma-1(zu405)* mutant embryos (Pang et al. 2004). In parallel, as speculated previously, OMA-1 degradation delay is likely to contribute to some of the defects of *oma-1(zu405)*. Particularly, GLD-1 diminishment was not enhanced by *oma-2* depletion, and the GLD-1 and OMA-1 P_{240}L localizations in *oma-1(zu405)* mutant and in wild-type embryos show nearly reciprocal patterns. Thus the GLD-1 diminishment phenotype is likely due to the OMA-1 degradation delay. Further systematic analyses would assign contributions of phosphorylation and degradation delay to each defect of *oma-1(zu405)* mutant in the future.

Genetics of *oma-1(zu405)* allele

It is currently unclear how *oma-2* depletion causes enhanced as well as novel phenotypes without exacerbating OMA-1 degradation delay. One plausible explanation is that $P_{240}L$ mutation affects certain embryonic function of OMA-1. In *oma-1(zu405)* single mutant, the $P_{240}L$-sensitive embryonic functions proceed normally because OMA-2 is present, however, the depletion of OMA-2 might result in the failure in such functions. Consistent with the idea that OMA-1 $P_{240}L$ has an attenuated embryonic function, a recent study showed that weak *oma-1/2* depletion results in extra divisions of the germline precursor lineage, very similar *oma-1(zu405); oma-2(RNAi)* embryos (Shimada et al. 2006). Importantly, unlike *oma-1(te31 lof); oma-2(RNAi*) mutant, *oma-1(zu405); oma-2(RNAi)* mutant shows no sign of sterility (Detwiler et al. 2001). This indicates that OMA-1 $P_{240}L$ mutant protein is functional for oocyte maturation. As discussed above, this embryo-specific deficit of OMA-1 function could be explained by compromised phosphorylation by MBK-2 and GSK-3. Consistently, my analyses in Chapter 2 suggest that these phosphorylation events happen only after oocyte maturation (see Figure 2.2).

Although the redundancy between *oma-1* and *oma-2* and an attenuated embryonic OMA-1 function of *oma-1(zu405)* allele can explain the novel *zu405* phenotypes uncovered only upon *oma-2* depletion, it cannot explain why some *oma-1(zu405)* defects are further exacerbated by *oma-2* depletion. A predicted *oma-1* null allele does not exhibit any decernable phenotype (Detwiler et al. 2001). This is not due to compensation by an increase in OMA-2 expression because OMA-2 expression was not affected by *oma-1(te33)* mutation

(Detwiler et al. 2001). In addition, OMA-2 expression level and pattern are not altered in *oma-1(zu405)* mutant gonad and embryos (Lin 2003). These results indicate that simple reduction of OMA function in the 1-cell stage does not account for *oma-1(zu405)* phenotypes. One possibility is that both OMA-1 degradation and phosphorylation independently contribute to these defects. In this scenario, the degrees of defects seen in *oma-1(zu405)* are due to OMA-1 degradation delay, and the increase in the expressivity by the depletion of *oma-2* is due to compromised embryonic OMA-1 function. Another possibility is that OMA-1 $P_{240}L$ behaves as a dominant negative protein that affects OMA-2 function at the 1-cell stage. In this scenario, OMA-dependent embryonic processes that are more sensitive to the level of OMA function show partial defects in *oma-1(zu405)* mutant even without *oma-2* depletion. Alternative scenario is that OMA-2 protein masks the toxicity of OMA-1 $P_{240}L$ protein. Again, processes that are more sensitive to the toxicity would be affected even without *oma-2* depletion.

OMAs might regulate GLD-1 expression and ZIF-1-mediated proteasomal degradation

GLD-1 expression pattern in wild-type is nearly reciprocal to that of OMA proteins. GLD-1 is expressed in the distal gonad and is absent in the proximal gonad (Jones et al. 1996). OMA-1/2 are absent in the distal gonad and present in the proximal gonad (Detwiler et al. 2001). In the embryo, OMA-1/2 are expressed at the 1-cell stage and rapidly decline thereafter, whereas GLD-1 is absent at the 1-cell stage and expression resumes at the 4-cell stage, shortly after the degradation of OMAs (Jones et al. 1996; Lin 2003). GLD-1 is known to be a repressor of OMA protein translation. Although *oma-1/2* transcripts are expressed in

the distal gonad, OMA-1/2 proteins do not express until GLD-1 level declines (Lee and Schedl 2001a). How GLD-1 protein level declines in the proximal gonad, and how its expression returns in the early embryo are both unknown. I showed that GLD-1 is diminished in *oma-1(zu405)* embryos (Figure 3.6). GLD-1 eventually becomes expressed around when OMA-1 protein is degraded in *oma-1(zu405)* mutant. Conversely, precocious GLD-1 expression was observed in the 1- and 2-cell embryo from *oma-1(te21); oma-2(te50)* homozygotes (Figure 3.6). These results suggest that OMA proteins repress GLD-1 expression at the 1- and 2-cell stage in wild-type. Because *gld-1* transcript is present at the 1- and 2-cell stage, the return of GLD-1 expression is likely to be post-transcriptional. OMA-1/2 are predicted to be translational regulators, thus it is a likely possibility that OMA-1/2 repress *gld-1* translation. On the other hand, OMA-1 physically interacts with GLD-1 protein, thus protein-level downregulation also is a possibility (see Chapter 5). It should be noted that the downregulation of GLD-1 by OMA proteins does not exclude the possibility that OMA-1 and GLD-1 function together as proposed in Chapter 5. Certain protein complexes become degraded in an activity dependent manner, thus the downregulation of GLD-1 could be a consequence of OMA-1/GLD-1 activity.

Another process that might be regulated by OMAs is ZIF-1 E3 ligase-mediated proteasomal degradation. I showed that a marker of ZIF-1-mediated degradation, GFP::PIE-1^{ZF1} shows a delayed degradation in *oma-1(zu405)*. On the other hand, GFP::PIE-1^{ZF1} is diminished in *oma-1(RNAi); oma-2(RNAi)* gonad, suggesting that ZIF-1-mediated degradation is repressed by OMA proteins in the gonad. However, the situation is not very simple. *oma-2* depletion enhances the GFP::PIE-1^{ZF1} degradation delay in *oma-1(zu405)*

embryos without enhancing the OMA-1 degradation delay. Furthermore, my RNAi analysis suggest that compromised OMA phosphorylation, not OMA degradation delay itself, correlates with the GFP::PIE-1^{ZF1} degradation delay phenotype. Thus qualitative change of OMAs, particularly, compromised phosphorylation is likely to contribute to the regulation of ZIF-1. How then phosphorylation of OMA-1/2 affects ZIF-1-mediated protein degradation? As shown in Chapter 2, OMA protein phosphorylation is initiated at the 1-cell stage, after meiosis II. Phosphorylated OMA-1/2 persist for a short period until the end of the 1-cell stage, at which it becomes quickly degraded by the proteasome. Perhaps, unphosphorylated OMA proteins function as repressors of ZIF-1-mediated degradation. Phosphorylated OMAs might simply unable to repress ZIF-1-mediated protein degradation, or alternatively, actively participate in the activation of ZIF-1-mediated degradation at the 1-cell stage. How do OMAs regulate ZIF-1-mediated protein degradation? An attractive model is that OMA-1/2 regulate the expression of ZIF-1, particularly by translational control. *zif-1* transcript is maternally supplied in the germlilne gonad and early embryos based on an *in situ* analysis (NEXTDB http://nematode.lab.nig.ac.jp/, yk570e9). However, it is not known when the transcript is translated to produce ZIF-1 protein. I show that translational regulators, MEX-3 and SPN-4 physically intract with OMA-1 (see Chapter 5). In this chapter, I showed that *mex-3* and *spn-4* RNAi suppresses the degradation delay of GFP::PIE-1^{ZF1} in *oma-1(zu405)* embryos (Figure 3.9). This result suggests that OMA-1/2 regualte ZIF-1-mediated degradation with MEX-3 and SPN-4. Because MEX-3 and SPN-4 are both translational regulators expressed in late oocytes and early embryos, they might translationally repress ZIF-1-mediated degradation with OMAs. This analysis was performed in the embryo,

however, it also is interesting to know whether or not depletion of *mex-3* and *spn-4*, and other OMA-1/*oma-1*-interacting translational regulators (*gld-1, puf-3*, *puf-5*, and *cpb-3*) result in a precocious degradation of GFP::PIE-1^{ZF1} in the gonad (see Chapter 4 and 5). The repression of ZIF-1-mediated protein degradation in the gonad and 1-cell stage embryo is thought to be important for embryogenesis as the targets of ZIF-1 include essential cell fate determinants that are supplied maternally as protein, such as PIE-1 and MEX-5 (DeRenzo et al. 2003). Precocious expression of ZIF-1 activity would lead to precocious destructions of these cell fate determinants, which is deterious to embryogenesis.

CHAPTER FOUR

GENOME-WIDE RNAi SCREEN FOR SUPPRESSORS OF *oma-1(zu405)*

INTRODUCTION

My analysis in the previous chapter identified likely OMA target processes by examining previously characterized embryonic events. On the other hand, an unbiased search for OMA target processes would further expand our understanding of OMA function. In this chapter, I describe my genome-wide RNAi screen for suppressors of *oma-1(zu405)*. The screen identified suppressor clones targeting 135 genes in various processes. Major suppressors isolated were: 1) cell cycle regulators, 2) DNA replication factors, 3) nuclear transport machinery, and 4) translational regulators. A secondary screen revealed that 11 of them genetically interact with *oma-1* and/or *oma-2* loss-of-function mutation, making them promising candidates. These 11 include pumilio/FBF-type translational regulators, PUF-3 and PUF-5, and their partner, CPB-3/CPEB, suggesting OMAs in translational regulation. In summary, this screen provides a rich resource to understand embryonic OMA functions, and suggests OMAs in translational regulation.

EXPERIMENTAL PROCEDURES

Strains

Bristol strain N2 was used as the wild-type strain (Brenner 1974). Genetic markers used are: LGIV: *oma-1 (zu405), oma-1(te33),* LGV: *oma-2(te51).*

Library screen

The library screen was conducted essentially as described before (Labbe et al. 2006). Briefly, the Ahringer library of dsRNA-producing bacterial transformants was first replica plated onto LB/agar plates. The library bacteria were inoculated from the LB plates into 500µl LB/ampicillin on 96-well deep-well plates and grown overnight at 37°C (Kamath and Ahringer 2003). dsRNA production was induced the following day by 1mM IPTG at 37°C for 1-2 hr with shaking. Cells were then spun down and re-suspended in 160µl of suppression test buffer (50mM potassium phosphate pH6.0, 150mM NaCl, 5µl/ml Cholesterol, ampicillin and 1mM IPTG). 30µl of the resulting bacterial suspension was transferred to flat-bottom 96-well tissue culture plates for suppression test. *oma-1(zu405)* were grown in a large quantity until starvation at 16°C. Newly starved animals were collected with M9 buffer and adults were removed by gravity to obtain mainly L1 population. Worms were washed twice with suppression test buffer. The 96-well RNAi test plates were inoculated with average 15 *oma-1(zu405)* larvae per well and were incubated at 20°C in a humidifier chamber for 6 days before being scored. Duplicated screens were performed for most part of the library screen to eliminate false positives due to minute temperature changes within the incubator. Bacteria that resulted in an outstandingly higher number of progeny than background in only one of two plates, and ones that consistently resulted in more progeny than background on both duplicates, were re-tested in the 96-well liquid culture format. Because cross-contamination of the library is not uncommon, re-tests were performed on the original population of bacteria from positive wells as well as cultures re-cloned from each well via streaking. After suppression was confirmed by re-streaked

clones, their inserts were analyzed by sequencing with M13-21 primer followed by BLAST search. Indeed, approximately 24% (31/128) of total hits were caused by contaminating bacteria mostly from neighboring wells.

Characterization of suppressor clones

RNAi in *oma-1(te33 lof)* and *oma-2(te51 lof)* strains was performed on solid NGM/agar support. RNAi bacteria were grown as the liquid test in the 96-well deep well plate, spun down, and resuspended in 50µl suppression test buffer. 25µl of the bacterial suspension was put onto NGM/agar in 24-well tissue culture plates. The RNAi test plates were inoculated with 15 L1 animals and incubated at 20°C. Sterility was scored for soon after inoculated animals reached adulthood, and embryonic lethality was scored for 1 day later. Some of the positive clones were re-tested to determine hatching rate in a similar condition.

Imaging

Imaging live embryos was performed as described previously (Rogers et al. 2002). The filter wheels (Ludl Electronic Product) and shutter controller were driven by a custom software package (*os4d 1.0*, freely available upon request to jwaddle@mail.smu.edu).

RESULTS

I. RNAi screen results

In parallel with the above molecular analyses using known markers, I attempted to genetically characterize *oma-1(zu405)* mutant via an unbiased, genome-wide RNAi-based

suppressor screen. Previous forward genetic screen as well as RNAi analyses identified 6 suppressors of *oma-1(zu405)*, indicating that the mutation is suppressible (3 uncloned likely extragenic recessive mutations, and *mex-3*, *mex-5,* and *mex-6*, Detwiler and Rueyling Lin, unpublished results). Importantly, this screen will not only help us understand *oma-1(zu405)* mutant, but also provide us with insights into the normal functions of *oma-1 and oma-2,* because previous studies have established that a reduction of *oma-1* level and/or activity results in an efficient suppression of *oma-1(zu405)* lethality (Detwiler et al. 2001; Lin 2003). Thus this *oma-1(zu405)* RNAi suppressor screen is a very sensitive assay to identify positive regulators of *oma-1* function and/or expression.

The RNAi screen utilized a bacteria-feeding RNAi technique and a genome-wide library of dsRNA producing bacterial strains (Timmons and Fire 1998; Kamath and Ahringer 2003; Labbe et al. 2006). The library individually targets approximately 85% of the predicted open reading frames in the *C. elegans* genome (Kamath and Ahringer 2003). Briefly, *oma-1(zu405)* animals were fed with clonal library bacteria at semi-restrictive temperature, 20°C, at which approximately 1% of the eggs hatch (Experimental Procedure). Individual assay well was visually inspected to identify clones producing higher number of progeny than background. Suppressor candidate clones were retested and sequenced to confirm reproducibility and RNAi target identify (Experimental Procedure). Although cross depletion, or off-target effect, is not an ignorable issue in this type of sensitive RNAi assays, I refer to primary targets of suppressing clones as suppressors or suppressor genes for the sake of simplicity in this manuscript (Ma et al. 2006).

The library screen yielded 135 clones that reproducibly suppressed *oma-1(zu405)* lethality (Table 4.1). Importantly, I isolated the two known RNAi suppressors of *oma-1(zu405)* lethality at this particular assay condition; *oma-1* itself and *mex-6*, validating the sensitivity of the screen (Detwiler et al. 2001)(Rueyling Lin, unpublished result). Thirty two of them (32/131 tested, 24%) also suppressed *oma-1(zu405)* lethality at 25°C (Table 4.1). The largest class was genes involved in DNA replication and cell cycle regulation. I have isolated 12 genes involved in DNA replication, and 17 genes involved in cell cycle regulation (Table 4.1). Second largest class of suppressors was genes encoding nuclear pore complex components and nuclear transport effectors. Indeed, I have isolated 9 out of the 22 predicted nuclear pore complex components (Table 4.1). Eight translational regulators as suppressors are particularly interesting considering predicted role of OMA-1/2 as translational regulators (Table 4.1). Consistent with functions in the germline and embryogenesis, the vast majority of the *zu405* suppressor clones were reported to result in either or both sterility and embryonic lethality in previous RNAi studies (Maeda et al. 2001; Kamath et al. 2003; Simmer et al. 2003; Rual et al. 2004; Sonnichsen et al. 2005). However, in my parallel RNAi assays using the wild-type strain, only a small fraction of them caused observable sterility or embryonic lethality, suggesting that in many cases, the target genes were only weakly depleted (data not shown).

II. Some *oma-1(zu405)* suppressors genetically interact with *oma-1/2* loss-of-function mutations

In order to better understand the mechanisms of *zu405* suppressions, I characterized all suppressors by testing them for genetic interactions with *oma-1* and *oma-2* loss-of-function mutations. *oma-1* and *oma-2* function redundantly in oocyte maturation because *oma-1(lof); oma-2(lof)* mutant exhibits a specific defect in oocyte maturation (Detwiler et al. 2001). In addition, *oma-1* and *oma-2* might be redundant in embryogenesis because *oma-1(rof); oma-2(rof)* mutant exhibits embryonic lethality (Nishi and Lin 2005). Some clones might suppress *oma-1(zu405)* lethality via specifically reducing *oma-1* (but not *oma-2*) expression or function. Thus I reasoned that depletion of such suppressors in the absence of *oma-2* activity might result in the reduction of *oma*-dependent function, thus germline or embryonic defects. Additionally, suppressors that affect both *oma-1* and *oma-2* expression/function might also be sensitive to *oma-1* and/or *oma-2* loss-of-function.

I depleted all isolated suppressors individually in wild-type and *oma-1(te33 lof)* and *oma-2(te51 lof)* mutants (Experimental Procedure). In parallel, *oma-1(zu405)* was cultured on the same bacterial preparation at the same temperature to monitor suppression activity. In a control experiment, I showed that RNAi of *ama-1* (RNA polymerase II) results in similar embryonic lethality rate in *oma-1(te33), oma-2(te51),* and wild-type (N2: 91%, *te33*: 79%, and *te51*: 87%), indicating that *oma-1(te33)* and *oma-2(te51)* have normal sensitivity to RNAi. The RNAi analysis in *oma-1/2* mutants revealed that 11 clones show enhanced embryonic lethality in *oma-2(te51)* single mutant compared to the wild-type N2 strain (Table 4.1). These 11 clones include 2 that showed enhanced embryonic lethality in *oma-1(te33)* mutant (Table 4.1). On the other hand, no clone showed enhanced lethality only in *oma-1(te33)* mutant. These results are consistent with the following 3 statements: 1) The 9 clones

which showed enhancement specifically with *oma-2(te51)* suppress *oma-1(zu405)* by specifically reducing *oma-1* activity and/or expression. 2) The 2 clones that showed enhancement with both *oma-1(te33)* and *oma-2(te51)* generally reduce both *oma-1* and *oma-2* activities/expressions. 3) No clone specifically reducing *oma-2* activity was isolated because the original screen was designed to identify suppressors of *oma-1(zu405)*, not of *oma-2* gain-of-function mutation.

Of the 9 clones that showed enhanced embryonic lethality in *oma-2(te51),* I performed quantitative and phenotypic characterizations for *puf-3*, *puf-5*, and *cpb-3* (Table 4.1). PUF proteins and CPB/CPEB are known to physically interact and function together in multiple systems including *C. elegans* and vertebrate (Luitjens et al. 2000; Nakahata et al. 2001). *puf-3* and *puf-5* encode Pumilio/FBF class RNA binding proteins (Wickens et al. 2002). *C. elegans* genome encodes at least 11 PUF family proteins that are implicated in various processes. Genetic and functional overlaps appear to exist among the *puf* genes, exemplified by the genetic redundancy between *fbf-1* and *-2* and among *puf-5/6/7* (Crittenden et al. 2002; Lublin and Evans 2007). PUF proteins are known to interact with their mRNA targets as well as their protein co-factors via different PUF repeats (Wickens et al. 2002). Of the 4 CPEBs in *C. elegans* genome, CPB-3 is the only member that is expressed in the adult female germline (Luitjens et al. 2000) (NEXTDB http://nematode.lab.nig.ac.jp). Consistently, *cpb-3* is required for female fertility and embryonic development (Luitjens et al. 2000). PUF-3, PUF-5, and CPB-3 are shown to be or expected to be expressed in the cytoplasm of the germline gonad and/or early embryos, thus they are likely to co-express with OMA-1/2 (Lublin and Evans 2007).

Quantitative analysis revealed that embryonic lethality of *cpb-3*, *puf-3*, and *puf-5* was greatly enhanced by *oma-2(te51)* mutation (Figure 4.1). Because it has been known that many *puf* family genes are genetically redundant, I further tested *puf-6/7*, *puf-8*, and *puf-9* for enhancement in *oma-1(te33)* and *oma-2(te51)* (Crittenden et al. 2002; Lublin and Evans 2007). None of them showed enhancement with *oma-1(te33)*, whereas *puf-8* showed weak enhancement of embryonic lethality by *oma-2(te51)* mutation (Figure 4.1 and data not shown).

Morphological analysis revealed that *oma-2(te51); puf-5(RNAi)* embryo, but not *oma-2(te51)* embryo or wild-type embryo depleted of *puf-5*, exhibits early embryonic defects (Figure 4.2). Embryonic *oma-2(te51); puf-5(RNAi)* defects include weak egg shell, nuclear division and cytokinesis defect (Figure 4.2). Superficially the appearance of *oma-2(te51); puf-5(RNAi)* embryos resemble that of combined *puf* RNAi (*puf-5/6/7* triple RNAi), suggesting that PUF function is compromised (Lublin and Evans 2007)(Figure 4.2).

gene name	description	Suupression at 25°C	Enhancement / synthetic	
			oma-1(te33)	*oma-2(te51)*
Cell cycle regulators				
apc-2	APC component	**yes**	no	no
emb-27	APC component	**yes**	no	no
emb-30	APC component	**yes**	no	**yes**
fzy-1	APC component (CDC20)	**yes**	no	**yes**
mat-3	APC component (CDC23)	**yes**	no	no
cye-1	cyclinE	no	no	no
cdk-2	cyclin dependent kinase	n/d	no	no
dom-6	cyclin dependent kinase cofactor (CDC28/cks-1)	**yes**	no	no
C34G6.5	cyclin dependent kinase (CDC7)	no	no	no
Y54G9A.6	mitotic check point protein BUB3	no	no	no
K10D2.2	S-M check point regulator	**yes**	no	no
Y47D3A.28	cell cycle regulator	no	no	no
K08F4.1	sister chromatid cohesion	no	no	no
mel-28	mitosis defect	no	no	no
mat-4	meta-ana tsn defect	**yes**	**yes**	**yes**

Y71H2AM.20	PP2A cell cycle regulator	no	no	no
sun-1	spindle localized protein	no	no	no
DNA replication / repair				
rfc-1	DNA replication factor	no	no	no
rfc-2	DNA replication factor	**yes**	no	no
rfc-3	DNA replication factor	**yes**	no	**yes**
M04F3.1	DNA replication factor	**yes**	no	**yes**
R53.6	DNA replication factor	no	no	no
ZC168.3	origin recognition complex	no	no	no
div-1	DNA polymerase alpha-primase.	**yes**	no	no
F08B4.5	DNA polymerase epsilon	**yes**	no	no
Y53F4B.3	DNA polymerase epsilon, subunit C	n/d	no	no
T26A5.8	DNA polymerase epsilon	**yes?**	no	no
F33H2.5	DNA polymerase epsilon	no	no	no
mus-101	DNA repair	**yes**	no	no
Nuclear pore complex				
nnp-22	nuclear pore complex	no	no	no
npp-12	nuclear pore complex	no	no	no
npp-14	nuclear pore complex	no	no	no
npp-15	nuclear pore complex	no	no	**yes**
npp-16	nuclear pore complex	no	no	no
npp-19	nuclear pore complex	no	no	no
npp-2	nuclear pore complex	no	no	no
npp-5	nuclear pore complex	no	no	no
npp-3 and *col-84*	nuclear pore complex and collagen	no	no	no
Nuclear transport				
ran-5	exportin	no	no	no
ima-3	importin	no	no	no
Translation				
cbp-3	CPEB	no	no	**yes**
puf-3	pumillo/FBF-class translational regulator	no	no	**yes**
puf-5	pumillo/FBF-class translational regulator	no	no	**yes**
gla-3	CCCH ZF. Negatively regulates MAPK signaling	no	no	no
mex-6	CCCH zinc finger protein	no	no	no
oma-1	CCCH zinc finger protein	**yes**	no	**yes**
F20D12.1	translation initiation factor	no	no	no
vig-1	RNA binding (vasa intronic protein)	no	no	no
lem-2	predicted translation initiation factor	no	no	no
General transcription factors				
F57C2.6	predicted transcription initiation factor	no	no	no
R10D12.14	GYF domain	no	no	no
Gene specific transcription factors				
lsl-1	C2H2 TXN factor	no	no	no
W03F9.1	C4 type zinc finger, likely nuclear hormone receptor	no	no	no
Signaling				
rskn-1	Acts downstream of MAPK in goand	no	no	no
smk-1	important for *daf-16* dependent processes	no	no	**yes**

T24F1.2	redundant with MAPK pathway	no	no	no
K08F4.2	predicted Ras GAP	no	no	no
F25H5.5	Claspin-related. Regulates Chk1	no	no	no
C36B1.8	potentially involved in MAPK signaling	no	no	no
T09B4.2	SH3 domain	no	no	no
Ubiquitination				
elb-1	elongin (TXN and ubiquitination)	no	no	no
ufd-2	E4 ligase (polyUb elongation)	no	no	no
innexin (gap junction)				
inx-8	inx-8 and -9 are nearly identical	no	no	no
inx-9	inx-8 and -9 are nearly identical	no	no	no
inx-14	innexin	**yes?**	no	no
inx-22 and Y47G6A.25	inx-22 and Y47G6A.25	no	no	no
Other cellular processes				
air-1	aurora kinase	no	no	no
T03F1.8	guanylate kinase	no	no	no
pak-8	p21 activated protein kinase	n/d	no	no
ZK856.8	Calmodulin regulated phosphatase	no	no	no
pph-5	protein phosphatase 2A catalytic subunit	no	no	no
C06H5.6	Synaptic vesicle transporter	no	no	no
vha-7	vacuolar H ATPase	no	no	no
T27E9.7 and T27E9.2	ABC transporter and mitochontrial	no	no	no
ooc-3	localized in ER and required for 1-cell polarity	no	no	no
Y49A3A.1	choline/ethanolaminephosphotransferase	no	no	no
Y19D10A.1 and C01B4.9	Monocarboxylate transporters	no	no	no
Y19D10A.12	Monocarboxylate transporter	no	no	no
dhs-5	steroid dehydrogenase	no	no	no
arl-1	ADP-ribosylation factor, membrane traffic	**yes**	no	no
Y45F10D.4	mitochondrial matrix component	no	no	no
T23B12.4	glucose repressive gene	no	no	no
ani-2	anillin (actin regulating protein)	no	no	no
T20B12.7	apoptosis inhibitor	no	no	no
math-33	math domain involved in apoptosis	no	no	no
T22H6.2	proline biogenesis	no	no	no
Unknown function				
F17C11.10	WD repeat protein	no	no	no
F33G12.4	leucine rich repeat	no	no	no
ddl-1	coiled-coil domain	no	no	no
pqn-14	prion Q/N rich protein	no	no	no
F59E12.11	uncharacterized conserved protein	**yes**	no	no
Y65B4BR.8	uncharacterized conserved protein	no	no	no
R07H5.11	uncharacterized worm specific gene	no	no	no
T12F5.1	uncharacterized worm specific gene	no	no	no
F31C3.5	uncharacterized worm specific gene	no	no	no
Y69A2AR.28	uncharacterized worm specific gene	no	no	no
F34D10.3	uncharacterized worm specific gene	no	no	no
F55H2.7	uncharacterized worm specific gene	no	no	no
T05H4.11	uncharacterized worm specific gene	no	no	no
K10D2.4	uncharacterized worm specific gene	**yes**	no	no
C24H12.5	uncharacterized worm specific gene	no	no	no

C31H1.8	uncharacterized worm specific gene	no	no	no
H02I12.5	uncharacterized worm specific gene	no	no	no
Y75B8A.25	uncharacterized worm specific gene	**yes**	no	no
C09H10.7	uncharacterized worm specific gene	**yes**	**yes**	**yes**
F11C7.5	uncharacterized worm specific gene	n/d	no	no

Table 4.1 List of RNAi suppressors of *oma-1(zu405)* lethality
RNAi assays were performed at 20°C otherwise indicated (see Experimental Procedures). Enhancement/synthetic: enhancement or synthetic sterility and/or embryonic lethality assayed in indicated genotype.

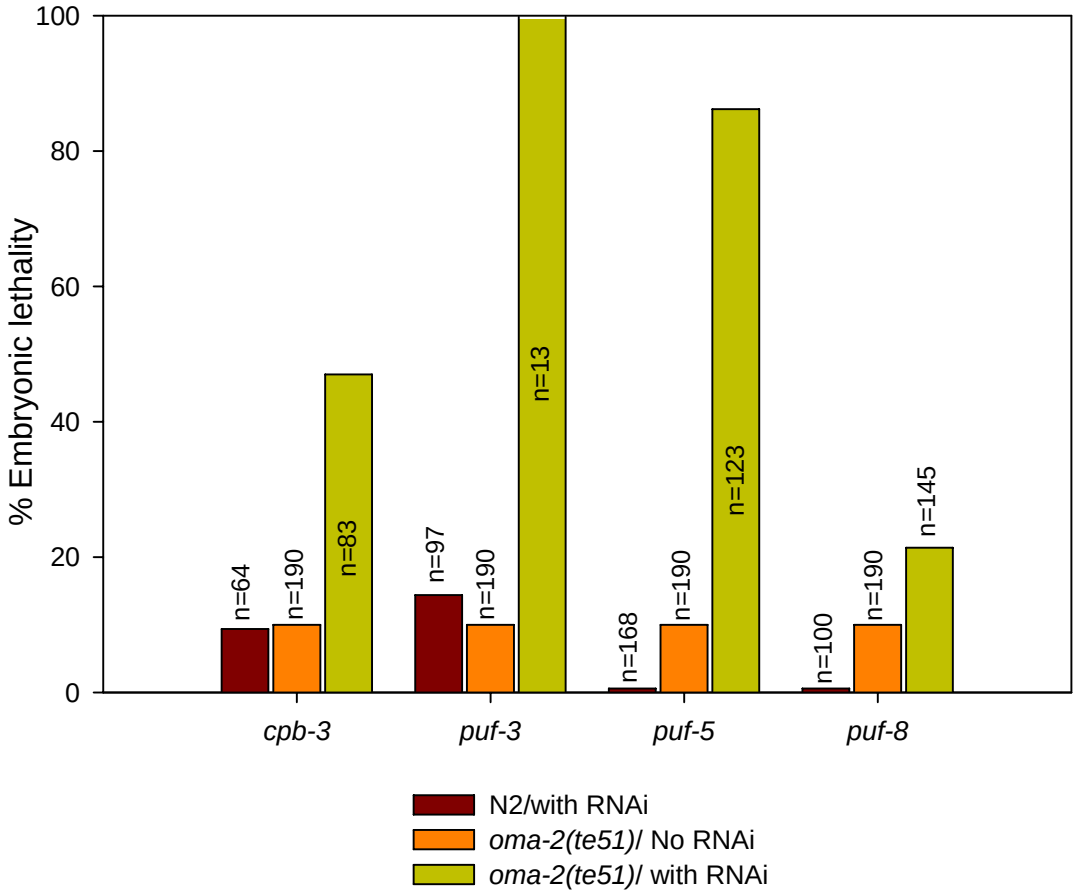

Figure 4.1 *puf-3*, *puf-5*, *puf-8*, and *cpb-3* RNAi result in higher lethality in *oma-2 (te51)*mutant

Embryonic lethality was scored as in text and Experimental Procedures. Note that "*oma-2(te51)* without RNAi" presented for each RNAi group is identical data repeatedly presented for the sake of easier comparison.

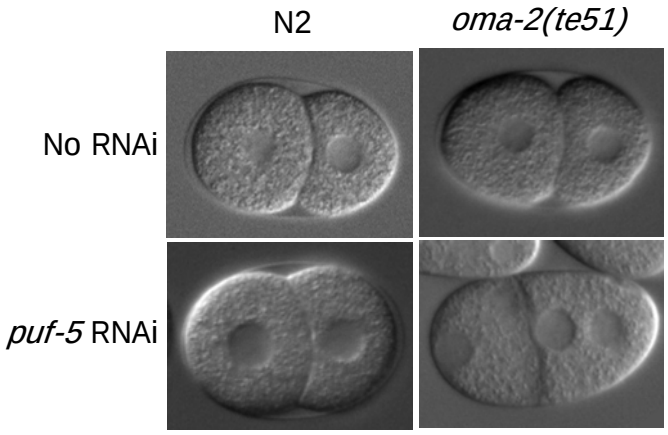

Figure 4.2 *puf-5* RNAi shows enhanced defects in *oma-2(te51)* background
DIC images of representative embryos with indicated genotype and RNAi treatment at 2-cell or comparable stage.

DISCUSSION

My genome-wide screen identified 135 candidate suppressors of *oma-1(zu405)*, however, actual number of individual processes interacting with *oma-1(zu405)* mutation is likely to be significantly lower because many clones target components of a common complex or process (Table 4.1). For example, the 9 subunits of nuclear pore complex might suppress *oma-1(zu405)* simply by lowering nuclear pore abundance or integrity. Additional examples are 11 DNA replication factors and 5 APC components.

Suppression via specific and non-specific downregulation of OMA-1 expression

Although this screen provides a rich resource to understand the functions of *oma-1/2,* interpretation of some of these interactions requires caution and further experiments. Specifically, previous studies and my own analyses indicate that the depletion of OMA-1

results in very efficient suppression of *oma-1(zu405)* lethality (Detwiler et al. 2001). Although this means that specific positive regulators of OMA-1 expression could be isolated through the screen, clones that non-specifically lowers OMA-1 expression might also be isolated. My analysis revealed that weak OMA-1 depletion that is undetectable by OMA-1::GFP reporter could cause very efficient suppression of *oma-1(zu405)* lethality in the library screen condition (data not shown). Thus distinguishing other informative classes of suppressors from non-specific downregulators of OMA-1 expression might be a challenge for some cases. Non-specific OMA-1 downregulators might include clones that target *oma-1* via off-target effect. Recent studies showed that RNAi off-target effect in *Drosophila* system is not an ignorable issue (Kulkarni et al. 2006; Ma et al. 2006). With our current knowledge, predicting all off-target effects is very difficult as a perfect nucleotide match might not be required to cause downregulation via miRNA pathway (Ambros 2003). In this regard, clones targeting different peptides functioning in a common process (such as nuclear pore components) are not likely to be off-target *oma-1* downregulators. Additionally, many off-target clones should be eliminated simply by targeting multiple non-overlapping regions of a gene of interest. True suppressors should suppress no matter which region is targeted for RNAi.

Suppression by alleviating *oma-1(zu405)* defects

Another class of suppressors is ones that alleviate embryonic defects of *oma-1(zu405)*. *oma-1(zu405)* mutant exhibit various embryonic defects. For example, various maternally supplied proteins show overabundance in early embryos (Lin 2003). Weak depletion of

factors abnormally upregulated in *oma-1(zu405)* might result in suppression of the lethality. Indeed, MEX-5 is overabundant in *oma-1(zu405)* due to compromised ZIF-1 mediated degradation (Lin 2003)(Figure 3.3). Weak depletion of *mex-5* suppresses *oma-1(zu405)* lethality, potentially due to the alleviation of the overabundance phenotype (Rueyling Lin, unpublished result). This class of suppressors might include normal targets of OMA-1 that are misregulated in *oma-1(zu405)*.

Supression by enhancement of MBK-2 and/or GSK-3 phosphorylation

My analyses in the previous chapter suggest that change(s) in OMA-1 property due to *zu405*/$P_{240}L$ mutation contributes to *oma-1(zu405)* phenotype, and likely, lethality. My analysis in chapter 2 showed that $P_{240}L$ mutation interferes with MBK-2 phosphorylation at T_{239}. The MBK-2 phosphorylation facilitates GSK-3 phosphorylation at T_{339}. Thus negative regulators of MBK-2 and GSK-3 might be identified through my screen. Such genes are particularly interesting knowing that the regulation of MBK-2 activity is unknown.

Suppression by general or embryo specific downregulation of OMA-1-dependent function

Another informative class of suppressors is positive regulators of OMA-dependent processes. As *oma-1* depletion efficiently suppresses *oma-1(zu405)* lethality, lowering of OMA-1-dependent processes, such as depletion of OMA-1 co-factor, is expected to suppress *oma-1(zu405)*. Depletion of factors specifically working with OMA-1 would result in an enhancement of RNAi effect in the absence of *oma-2* activity because *oma-1* and *oma-2* are

genetically redundant. Indeed, 9 suppressors showed enhanced lethality specifically in *oma-2* but not *oma-1* loss-of-function mutant. On the other hand, 2 additional suppressors resulted in higher embryonic lethality both in *oma-1* and *oma-2* loss-of-function mutants. These 2 suppressor genes might function both with *oma-1* and *oma-2*. However, enhancement of lethality by *oma-1* and *oma-2* loss-of-function mutations might be a too high threshold for some genes functioning with OMAs, thus I might have missed such factors. Additional genetic tests in a more sensitized background might identify weaker genetic interactions with *oma-1/2* hypomorphic mutations. For example, enhancement of impenetrant *oma-1(te21); oma-2(te50)* oocyte maturation defect and embryonic lethality might serve as a good reporter of OMA-dependent function.

*puf*s and *cpb-3* suggest OMAs in translation

Of the total 11 clones that show enhancement with *oma-2* loss-of-function mutant, I chose 3 genes, *puf-3*, *puf-5*, and *cpb-3* for quantitative and phenotypic analysis. Previous studies showed that PUF proteins and CPEB interact and function together to regulate translation in the cytoplasm. I showed that *puf-5(RNAi); oma-2(te51)* embryos show similar phenotype as *puf-5/6/7* triple RNAi (Lublin and Evans 2007). These results suggest that *oma-1* and *puf-5* together function in parallel with *oma-2*. *oma-2* might have its own *puf* partner to function in parallel with *oma-1*. Indeed, my preliminary result showed that *fbf-1/2* RNAi is enhanced by *oma-1(te33)* mutation. Thus OMA-1-PUF-3/5 and OMA-2-FBF-1/2 might redundantly regulate embryogenesis. My protein interaction analysis described in Chapter 5 revealed that OMA-1 interacts with 3 other translational regulators: GLD-1, MEX-3, and SPN-4. Our

preliminary result suggests that weak *mex-3* and *spn-4* RNAi causes suppression and enhancement of *oma-1(zu405)* lethality, respectively (Yuichi Nishi and Rueyling Lin, unpublished results). *mex-3* was not isolated as a suppressor in this screen, however, *mex-3* RNAi causes strong lethality in the screen condition, thus likely masked its suppressor activity. It will be interesting to determine how OMA proteins function together with these translational regulators. PUFs and CPB/CPEB are suggested in a common complex, whereas KH proteins (MEX-3 and GLD-1) and SPN-4 are proposed to function in a different type of processes. OMA proteins might form distinct complexes with PUF/CPEB and KH/SPN-4. Alternatively, OMAs might form a complex with PUFs, CPEB, KH, and SPN-4 to regulate common processes. The identification of OMA target transcripts would greatly progress our understanding of OMA function in 1-cell embryo as well as in the germline gonad.

CHAPTER FIVE

IDENTIFICATION AND CHARACTERIZATION OF OMA-1 PROTEIN INTERACTION PARTNERS

SUMMARY

My candidate and unbiased genetic approaches identified multiple processes that might be regulated by OMAs or function with OMAs (Chapter 3 and 4). In this chapter, I describe my complimentary approach to understand OMA function at 1-cell stage: identification and characterization of OMA binding proteins. Through yeast-two hybrid assay and *in vivo* analyses (GFP-reporter assay and RNAi analysis), I identified several additional processes that might be controlled by OMAs, or might function with OMAs. Such potential processes include: 1) regulation of transcriptional quiescence at the earliest stages of embryogenesis via a regulation of general transcription factor, TAF-4, 2) regulation of embryogenesis via a novel UBA and Q/N rich domain protein, PQN-59, and 3) translational regulation with KH proteins, GLD-1 and MEX-3, and RRM-protein, SPN-4. My study in this chapter and results from previous chapters together suggest that OMAs might be multi-functional proteins regulating various processes to assist the transition from oocyte to embryo.

INTRODUCTION

Biochemical functions of OMA-1 and OMA-2 are currently unknown. OMA-1/2 are expressed exclusively in the cytoplasm partly associated with RNA-rich organelle, P-granule, in dveloping oocytes and in 1-cell stage embryo (Detwiler et al. 2001; Lin 2003)(Figure 1.8). OMA-1/2 proteins contain two copies of Tis-11 like CCCH zinc fingers (Detwiler et al.

2001). Many Tis-11-like CCCH zinc finger proteins regulate translation in the cytoplasm via direct RNA binding (Lai et al. 1999; Ogura et al. 2003; Tenlen et al. 2006). Thus it is an attractive hypothesis that OMA-1/2 similarly regulate translation via RNA binding. Indeed, I detected genetic interaction between *oma-1/2* mutations and translational regulators, *puf-3/5/8*, and *cpb-3* in the previous chapter. However, the zinc finger domains are only small portions of OMA-1/2 coding sequence, and the regions outside of zinc fingers are generally poorly conserved among Tis-11 CCCH zinc finger protein family members, thus it is also tempting to speculate other biochemical functions for OMA-1/2.

In order to gain insights into the molecular functions of OMA-1/2, screens for OMA-1 binding proteins (OBP) were previously performed using yeast-two hybrid systems (Angela Collins and Rueyling Lin). These screens yielded multiple candidate OBPs some of which I characterized in this study. Analysis of these OBPs suggest that 1) OMA proteins might promote transcriptional quiescence by regulating nuclear localization of a general transcription factor, TAF-4, and 2) a novel UBA and Q/N rich domain protein, PQN-59 might function with OMAs for embryogenesis. Additionally, I have undertaken a candidate approach and detected interactions between OMA-1 and translational regulators, MEX-3, GLD-1, and SPN-4 (Huang et al. 2002; Marin and Evans 2003; Ogura et al. 2003). MEX-3, GLD-1, and SPN-4 are thought to control developmental programs via translationally regulating maternal transcripts (Ciosk et al. 2006). In summary, my data suggest that OMA proteins regulate multiple processes including transcriptional quiescence and translation to regulate oocyte-to-embryo transition.

EXPERIMENTAL PROCEDURES

Strains and transgenesis

Bristol strain N2 was used as the wild-type strain (Brenner 1974). Genetic markers used were: LGIII: *unc-119(ed3*), LGIV: *oma-1(zu405), oma-1(te21), oma-1(te33), teIs1* [*pRL475*($P_{oma\text{-}1}$*oma-1::gfp*)], LGV: *oma-2(te50), oma-2(te51),* LG unknown: *teIs85* [pRL1483(*Ppie-1gfp::taf-4*)] (Tugba Guven and Rueyling Lin, unpublished). Transgenics were generated by microparticle bombardment (Praitis et al. 2001) or complex array injection technique (Kelly et al. 1997) to allow for expression in the germline gonad. Most transgenics generated via the complex array technique were unstable, with the transgenes silenced typically by F4 generation. After consistency of GFP expression pattern was confirmed in multiple lines, the following representative lines were chosen for detailed analyses: *teEx301* [pRL1483(*Ppie-1gfp::taf-4*)], *teIs71* [pRL1650(*Ppie-1gfp::C27B7.2*)], *teEx332*[pRL1706(*Ppie-1gfp::DH11.4*)], *teIs92* [pRL1483(*Ppie-1::gfp::pqn-59*)].

Plasmid construction

All plasmids generated for this study were constructed using Gateway technology (Invitrogen).

For yeast two-hybrid analysis

High copy number (2μ replication origin) GAL4 two-hybrid destination vector, pRL1057 and pRL1058 are derivatives of pASII and pACTII (Clontech), respectively. Single copy-number (CEN replication origin) GAL4 two-hybrid destination vectors, pRL865 and pRL864

are derivatives of pDEST32 and pDEST22 (Invitrogen). Similarly, destination vectors for SRS assays, pRL1077 and pRL1070 are derived from pSOS and pMyr (Stratagene). Unless otherwise indicated, full-length spliced coding sequences were PCR cloned from a cDNA clone into a destination vector via BP followed by LR recombination reactions (Invitrogen).

Clone used were: **pGBKT7-derived [GAL4 DB fusion/high copy number]**: pRL575[OMA-1 N-terminus (aa.1-117)], **pRL865/pDEST32-derived [GAL4 DB fusion/low copy number]**: pRL1485(OMA-1 WT), pRL1996 (OMA-1T_{239}D), pRL2170 (OMA-1T_{239}A), pRL2141 (OMA-1P_{240}L) , pRL2277 (OMA-1E_{141}K), pRL2278 (OMA-1E_{141}K P_{240}L), pRL2278 (OMA-1S_{331}A S_{335}A T_{339}A), pRL2032 (OMA-2), **pRL1057/pASII-derived [GAL4 DB fusion/high copy number]:** pRL1883 (OMA-1 zinc fingers, aa.111-188), **pRL1058/pACTII-derived [GAL4 AD fusion/high copy number]**: pRL2063 (SPN-4), pRL2027 (MEX-3), pRL2022 (GLD-1), pRL1368 (TAF-4), pRL976 (C27B7.2), pRL938 (DH11.4), **pRL864/pDEST22-derived [GAL4 AD fusion/low copy number]**: pRL1909 (PQN-59 full-length), pRL1918 [PQN-59 C-terminus (a.a.407-712)], pRL1936 [PQN-59 N-terminus (a.a.1-406)], **pRL1077/pSOS-derived [hSOS fusion]**: pRL1158 (OMA-1 WT), pRL1830 (OMA-1T_{239}A), pRL1344 (OMA-1T_{239}D), pRL1831 (OMA-1T_{239}E), pRL1359 (OMA-1P_{240}L), pRL1834 (OMA-1S_{302}D), pRL1832 (OMA-1S_{331}D S_{335}D T_{339}E), pRL2031 (OMA-1T_{239}D S_{331}D S_{335}D T_{339}E), **pRL1070/pMyr-derived [myristoylation signal fusion]**: pRL1435 [PQN-59 C-terminus (a.a.407-712)], pRL1829 (PQN-59 FL), pRL1440 (Y47G6A.9).

For RNAi

Feeding RNAi clones were generated by inserting full-length coding sequences from cDNAs into pDONRdT7 via BP recombination (Reddien et al. 2005)

For transgenesis

Full-length coding sequences were PCR amplified from cDNAs and individually recombined into pID3.01 by BP followed by LR recombination reactions (Invitrogen). Resulting clones produce N-terminal GFP fusion under the control of *pie-1* promoter and *pie-1* 3'UTR. *pie-1* promoter and *pie-1* 3'UTR together drive expression in the germline gonad (Reese et al. 2000).

Yeast two-hybrid assay

For GAL4-based assays, growths of AH109 (Clontech) transformants were assessed on SD–Trp–Leu–His plates containing 3AT (3-amino-1,2,4-triazole) at concentrations ranging from 10mM to 50mM. For SRS [SOS recruitment system (Cytotrap, Stratagene)] assay, cdc25H strain (Stratagene) was transformed and interaction was assayed based on specific growth on galactose-containing plate at 37°C according to manufacturer's instruction.

RNA interference

RNAi interference was performed using feeding technique at 25°C as described in previous chapters.

RESULTS

I. Yeast two-hybrid screens for OMA-1 binding proteins (OPB)

Previously, two types of yeast-two hybrid screens were conducted to identify binding partners of OMA-1 (OMA-1 binding protein, OBP) in order to gain insights into the molecular function(s) of OMA-1 (Angela Collins and Rueyling Lin). The first screen was conducted using GAL4-based system with the first 117 amino acids of OMA-1 as GAL4 DNA binding domain fusion. The truncated protein does not contain either the zinc finger domains or the MBK-2 and GSK-3 phosphorylation sites. The second screen was conducted in SOS-recruitment system (SRS) using full-length OMA-1 harboring threonine to aspartate substitution at one of the MBK-2 phosphorylation sites, T_{239}, aiming to identify phosphorylation-dependent interactions. Whereas GAL4-based system detects protein-protein interactions in the nucleus, interactions occur on the plasma membrane in SRS (Fields and Song 1989; Aronheim et al. 1997). In SRS, protein-protein interactions are detected via genetic rescue of a temperature-sensitive lethal mutation in ras-MAPK pathway in the host strain (Aronheim et al. 1997). The two screens identified multiple candidate OBPs, some of which I characterized in this study.

Of the in-frame clones isolated from the GAL4-based screen using the first 117 amino acids of OMA-1, I confirmed specific interactions for C12B7.2, DH11.4, and TAF-4. This screen isolated 2 clones for C27B7.2, 2 clones for DH11.4, and 2 clones for TAF-4. On the other hand, I identified 1 clone each for Y47G6A.9 and PQN-59 from the SRS screen that are in-frame and shows reproducible interaction with OMA-1.

1. TAF-4 (general transcription factor)

An important aspect of oocyte-to-embryo transition is transcriptional quiescence and zygotic genome activation. In *C. elegans*, maternal transcription ceases in maturing oocyte and in 1-cell embryo, followed by the activation of zygotic transcription at 4-cell stage (Seydoux and Fire 1994; Seydoux and Dunn 1997). The transcriptional quiescence appears to be important for the switch from maternal to zygotic transcriptional programs and is thought to be a universal phenomenon covering broad phyla (Thompson et al. 1998). However, the underlying mechanism for this transcriptional quiescence is currently unknown (Thompson et al. 1998).

TBP (TATA binding protein) associated factors, TAFs, are general transcription factors conserved from yeast to human (Green 2000). They were initially identified as components of TBP-containing TFIID complex and subsequently shown to be genetically required for a number of transcriptional events (Green 2000). In *C. elegans*, total 17 TAFs have been identified (Walker et al. 2001). Whereas some of these TAFs, such as *C. e*TAF-5, are required for a subset of transcriptional events, *C. e*TAF-4 appears to be required for zygotic transcription universally (Walker et al. 2001).

TAF-4 was initially identified as an OBP though a GAL4-based screen using the N-terminus of OMA-1 (amino acids 1-117). Subsequently, I showed that full-length OMA-1 and full-length TAF-4 interact in the GAL4 Y2H system (Table 5.1). Via truncations and internal deletions, the interaction domain of TAF-4 was mapped to amino acids 333-382 (Tugba Guven and Rueyling Lin, unpublished data). Amino acids 333-382 of TAF-4 was sufficient to interact with OMA-1, whereas the internal deletion of aa. 333-382 in full-length

OBP \ OMA-1	WT	$T_{239}A$	$T_{239}D$	$P_{240}L$	$E_{141}K$	$E_{141}K\ P_{240}L$	$S_{331}A\ S_{335}A\ T_{339}A$
TAF-4	++	+	++	+	-	-	-
PQN-59	++	++	++	++	-	-	++
Y47G6A.9	++	n/d	++	n/d	n/d	n/d	n/d
C27B7.2	+++++	+++++	+++++	+++++	+++++	++++	+++++
DH11.4	+++++	+++++	+++++	+++++	+++++	++++	+++++
MEX-3	+++	+	++	+	-	-	-
SPN-4	+++	++	++	+	-	-	-
GLD-1	++	-	++	-	-	-	-

Table 5.1 Mutational analysis of OMA-1 for OMA-1/OBP interactions
Various mutant forms of OMA-1 was tested for interaction with OBP. Interaction assays were performd using GAL4 yeast two-hybrid system, except for Y47G6A.9, whose interaction was assayed in SRS (Cytotrap) system. Binding strength was determined based on growth on + galactose plate at 37°C (Y47G6A.9) or –His plate containing varying amount of 3-AT (all other).

TAF-4 abolished the interaction with OMA-1 (Tugba Guven and Rueyling Lin, unpublished data). OMA-1 interacts with only TAF-4 out of 8 TAFs tested in the yeast two-hybrid system (TAF-1, -4, -5, -6, -8, -9, -10, and -12, Tugba Guven and Rueyling Lin, unpublished data). It was further shown that aa.45-80 of OMA-1 was sufficient for TAF-4 binding (Tugba Guven and Rueyling Lin, unpublished data).

I performed a series of mutational analysis to ask 1) effects of phosphorylation and 2) importance of CCCH zinc finger domain, in OMA-1/TAF-4 interaction. I identified OMA-1 phosphorylation at specific sites (see Chapter 2). Using phosphorylation abolishing and phosphorylation mimicking mutations, I asked whether or not phosphorylation at these sites affects TAF-4 interaction. *oma-1(te21)* is a reduction-of-function allele that changes a conserved residue in the first zinc finger domain (E_{141}-to-K mutation) (Detwiler et al. 2001). *te21* does not seem to affect the expression level or pattern of OMA-1 *in vivo* based on

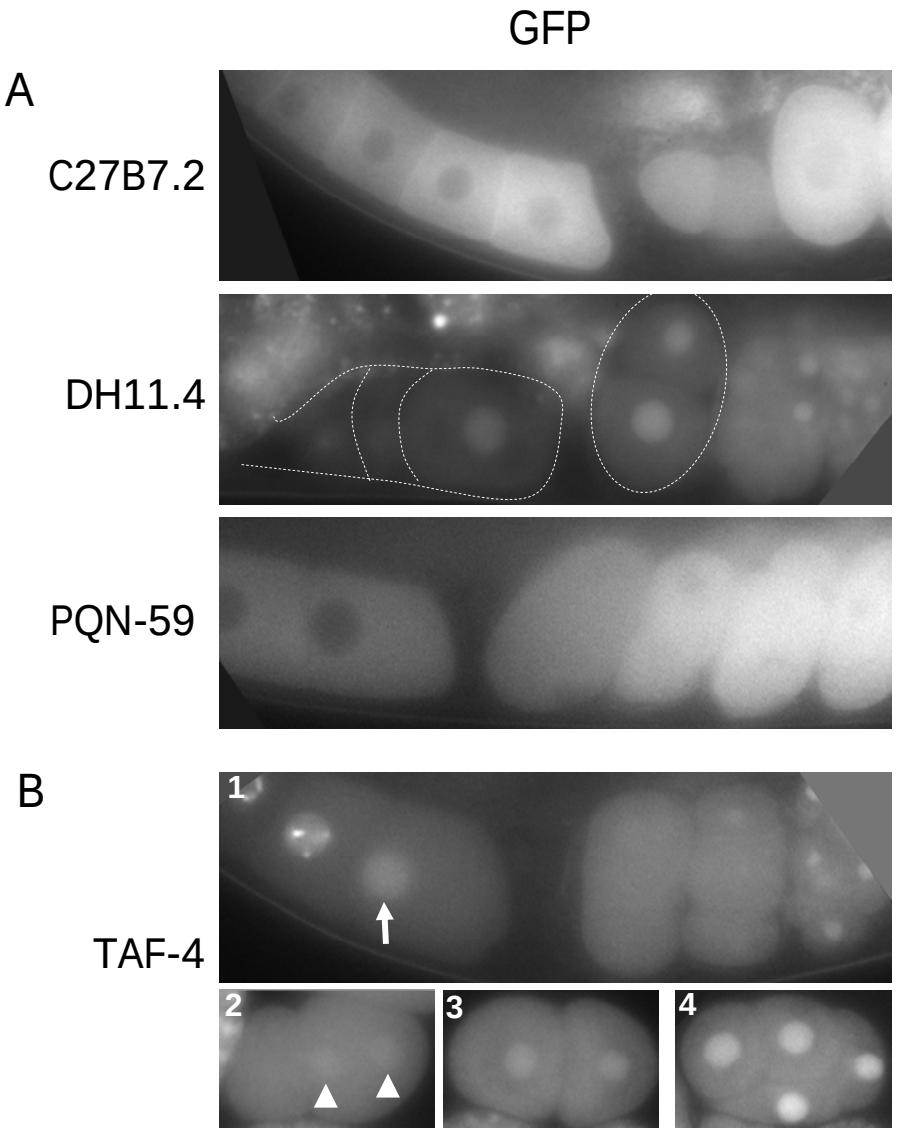

Figure 5.1 Localization of GFP::OBP driven by a germline promoter
OBPs were expressed as GFP-fusion under the control of *pie*-1 transcriptional (promoter) and translational element (3'UTR). (A) GFP signal of gonad (left) and embryos in the uterus (right) are shown. For DH11.4, late oocytes and 2-cell embryo are outlined with dotted line. (B) 1. GFP::TAF-4 in late oocytes and early embryos. The nucleus of maturing oocyte is indicated by an arrow. (2-4) Ex utero embryos at pronuclear migration stage (2), late 2-cell stage (3), and 4-cell stage (4). Paternal and maternal pronuclei are marked by arrowheads in (2).

western blot and immunofluorescence analyses (Detwiler et al. 2001)(immunofluorescence data not shown). CCCH zinc finger domain is suggested in RNA binding and is thought to be essential for the function of many CCCH zinc finger proteins, thus the *te21* mutation is predicted to disrupt RNA-regulating function of OMA-1 (if any) (Blackshear 2002).

My analysis summarized in Table 3.1 showed that whereas a phospho-mimicking mutation at an MBK-2 site, $T_{239}D$ did not alter His reporter activation, phosphorylation abolishing and diminishing mutations, $T_{239}A$ and $P_{240}L$ resulted in a severe reduction in the reporter activity. In chapter 2, I also identified a cluster of GSK-3 phosphorylation sites, S_{331} S_{335} T_{339}. Although I was unable to test $T_{339}E$ or $S_{331}D$ $S_{335}D$ $T_{339}E$ mutant due to strong self-activation of the HIS3 reporter, $S_{331}A$ $S_{335}A$ $T_{339}A$ resulted in a great reduction in the reporter gene activation (Table 5.1). These results are consistent with the notion that these sites are phosphorylated in the yeast and the phosphorylation at the MBK-2 and GSK-3 sites is important for OMA-1/TAF-4 interaction.

Additionally, *te21* mutation $E_{141}K$ resulted in a great reduction in His reporter activity (Table 5.1). This result suggests that the integrity of the first CCCH zinc finger domain is important for OMA-1/TAF-4 interaction.

In order to probe the *in vivo* role of TAF-4, its localization pattern was analyzed by expressing GFP::TAF-4 translational fusion. *pie-1* promoter and 3'UTR were chosen for this purpose because they together drive expression in the germline gonad and early embryo. PIE-1 expression covers the stages in which OMA-1 is expressed, *ie*. the stages in which TAF-4 localization is to be analyzed in the context of OMA-1 interaction. As expected for a general transcription factor required broadly for transcription, GFP::TAF-4 was detected in

the oocyte nuclei and in the nuclei of most embryonic blastomeres (Figure 5.1B). However, an interesting exception was 1-cell and early 2-cell stages. At these stages, nuclear GFP::TAF-4 levels were significantly lower (Figure 5.1B, 2 and 3). GFP::TAF-4 also was detected in the cytoplasm, and the cytoplasmic signal in 1- and 2-cell stages was not lower than oocyte or later embryonic stages, suggesting that the lower nuclear level at 1- and early 2-cell stages is not due to general absence of the protein (Figure 5.1B). The nucleus started regaining GFP::TAF-4 at late 2-cell stage, and by 4-cell stage, the nuclear GFP intensity was comparable to later stages or oocytes (Figure 5.1B). These observations agree with a previous report by immunofluorescence (Walker et al. 2001). Additionally, GFP::TAF-4 formed apparently chromosomal puncta in most oocyte nucleus (Figure 5.1). The only exception was maturing oocyte. Although chromosomes remain condensed in the maturing oocyte, these apparent chromosomal foci disappeared in the maturing oocyte (Figure 5.1B). .

2. C27B7.2 (small protein encoded in *oma-1* operon)

C27B7.2 was initially isolated as an interaction partner of OMA-1 aa.1-117 in a GAL4-based screen. I subsequently showed that full-length OMA-1 interacts with full-length C27B7.2. Mutational analysis revealed that the phospho-mimicking and phospho-abolishing MBK-2 site mutants, and the phospho-abolishing GSK-3 site mutant all result in HIS3 reporter activation at similar strength, suggesting that phosphorylation at these sites are not important for OMA-1/C27B7.2 interaction (Table 5.1). *te21* ($E_{141}K$) mutant also showed at comparable HIS3 reporter activity as wild-type, suggesting that OMA-1/C27B7.2 does not rely on the integrity of the first zinc finger (Table 5.1).

C27B7.2 is a previously uncharacterized gene. The majority of its predicted 196 amino acid-long coding sequence is an evolutionarily conserved domain of unknown function. Very interestingly, C27B7.2 belongs to *oma-1* operon. Currently, the *oma-1* operon is predicted to contain 4 genes. Unlike most other eukaryotes, many of the *C. elegans* genes are organized in operons (Spieth et al. 1993; Blumenthal et al. 2002; Blumenthal and Gleason 2003). Although different from prokaryotic operons in mechanism, *C. elegans* operons are also believed to contain genes functioning in common processes (Blumenthal and Gleason 2003). Thus the occurrence of *oma-1* and C27B7.2 in the same operon implies *in vivo* significance of their physical interaction.

In order to gain insights into the *in vivo* function of C27B7.2, I have generated transgenics expressing GFP::C27B7.2 translational fusion under the control of the *pie-1* promoter and 3'UTR (Experimental Procedures). In both oocytes and embryos, GFP::C27B7.2 signal was observed in the cytoplasm excluded from the nucleus with enrichment on the cortex (Figure 5.1). The distribution did not exhibit asymmetry in the oocyte or in the embryo. C27B7.2 remained expressed after 1-cell stage, at which OMA-1 protein becomes degraded, until many stages later. No change in distribution was observed upon oocyte maturation and fertilization. The intracellular distribution of GFP::C27B7.2 suggests that it could form a complex with OMA-1 in the cytoplasm, since OMA-1 also resides in the cytoplasm.

To probe the genetic role of C27B7.2, I have performed a systematic RNAi analysis. Previous 4 sets of published genome-wide RNAi studies and my own preliminary RNAi analysis produced no observable, specific phenotype for C27B7.2 in wild-type or *rrf-3* RNAi sensitive mutant background (Maeda et al. 2001; Kamath et al. 2003; Rual et al. 2004;

Sonnichsen et al. 2005). Thus I modified the assay to include various *oma-1* and *oma-2* mutants and OMA-1::GFP reporter aiming to detect genetic interactions between C27B7.2 and *oma* mutations and deviation in OMA-1 expression pattern, particularly OMA-1 degradation pattern. First, C27B7.2 RNAi was performed in *oma-1(te33)* and *oma-2(te51)* single mutants and sterility and embryonic lethality were scored for. *te33* and *te51* are predicted loss-of-function alleles. Whereas *oma-1(te33); oma-2(te51)* shows fully penetrant sterility due to an oocyte maturation defect, *oma-1(te33)* and *oma-2(te51)* single mutants do not cause a defect (Detwiler et al. 2001). I expected that reducing an *oma*-dependent function in a single mutant might result in a synthetic phenotype. Second assay was to detect suppression of embryonic lethality of *oma-1 (zu405).* As described in detail in Chapter 4, suppression of this gain-of-function mutation is a sensitive assay to detect *oma*-dependent function (Lin 2003). Third, enhancement of *oma-1(te20 rof); oma-2(te50 rof)* mutation was sought. Compared to *oma-1(te33 lof); oma-2(te51lof)* mutant, *oma-1(te21 rof); oma-2(te50 rof)* mutant shows less penetrant oocyte maturation defect, likely due to residual activities of *oma-1* and *oma-2* (Nishi and Lin 2005). Thus again, an enhancement of the oocyte maturation phenotype in *oma-1(te21); oma-2(te50)* strain will indicate a reduction in *oma*-dependent activity. However, in all three assays, C27B7.2 failed to show any genetic interaction. Additionally, C27B7.2 did not alter OMA-1::GFP expression or distribution (including the degradation pattern) in a detectable manner.

3. DH11.4 (nuclear C2 domain protein)

DH11.4 was identified as an OBP in the GAL4-based screen using the N-terminal OMA-1 fragment (aa 1-117). I showed that full-length OMA-1 interacts with DH11.4. My mutational analysis showed that the phosphorylation site mutants and the zinc finger mutants resulted in no or only weak deviation in HIS3 reporter activity, suggesting that neither the phosphorylation nor zinc finger integrity is important for OMA-1/DH11.4 interaction (Table 3.1). DH11.4 is a 374 amino acid protein containing a C2 domain. C2 domain is generally thought to be a Ca^{2+} dependent lipid binding domain for membrane targeting (Rizo and Sudhof 1998). Previous analyses of DH11.4 were limited to genome-wide RNAi studies (Kamath et al. 2003; Rual et al. 2004; Sonnichsen et al. 2005). None of these studies or my analysis generated a detectable phenotype in the wild-type or in *rrf-3* RNAi sensitive strain (Kamath et al. 2003; Rual et al. 2004; Sonnichsen et al. 2005). I performed the same set of RNAi analysis as C27B7.2, using the *oma-1/2* mutations and OMA-1::GFP reporter. However, none of the RNAi test showed in a genetic interaction with the *oma* mutations or a deviation in OMA-1 localization.

To gain insights into the function of DH11.4, I analyzed intracellular localization of the protein using *pie-1* promoter and *pie-1* 3'UTR. To my surprise, GFP::DH11.4 was localized to the nucleus, but apparently not on the membrane (Figure 5.1). Cytoplasmic signal was also detectable (Figure 5.1). This localization pattern was unexpected knowing the protein contains membrane targeting C2 domain (Rizo and Sudhof 1998). The GFP signals showed no asymmetry in the embryo at any stage. No significant change in localization was observed during oocyte-to-embryo transition. DH11.4 remained detectable essentially in the

same manner for many stages later. This result suggests that DH11.4 might have a function in the nucleus.

4. Y47G6A.9 (similarity with DNA pol III)

Y47G6A.9 was identified initially as an interaction partner of full-length OMA-1 harboring $T_{239}D$ mutation in an SRS screen. Later, I showed that Y47G6A.9 interacts with OMA-1 wild-type and $T_{239}D$ mutant with comparable binding strengths (Table 5.1).

Y47G6A.9 shows statistically significant similarity with a subunit of mammalian DNA-dependent RNA polymerase III (E-value 1.1e-27 with mouse homolog) throughout 93% of its 230 amino acid coding sequence. RNAi depletion of Y47G6A.1 failed to detect any detectable phenotype in wild-type or *rrf-3* RNAi sensitive strain. The RNAi tests using *oma-1/2* mutants and OMA-1::GFP reporter detected no genetic interaction nor a deviation in GFP pattern.

5. PQN-59 (prion-like Q/N-rich protein with ubiquitin association motif)

PQN-59 similarly was identified as an OBP in an SRS screen using OMA-1 $T_{239}D$. I subsequently showed that OMA-1 wild-type as well as OMA-2 wild-type interacts with PQN-59 in SOS system at similar interaction strengths (data not shown for OMA-2). The original clone isolated from the screen contained a C-terminal half of 712 amino acid coding sequence (aa.407-712). I showed that full-length OMA-1 and full-length PQN-59 interact both in SRS and GAL4 systems (Table 5.1 and data not shown). The reciprocal N-terminal region of PQN-59 (aa.1-406) failed to show an interaction with OMA-1 in neither SRS nor

GAL4 system, suggesting that the OMA-1 interaction region lies within the C-terminus (data not shown). Mutational analysis in OMA-1 in SRS and GAL4 system collectively showed that phospho-interfering or –mimicking mutation at MBK-2 ($T_{239}A$, $T_{239}D$, $P_{240}L$, $S_{302}A$, and $S_{302}D$) or GSK-3 site ($S_{331}A$ $S_{335}A$ $T_{339}A$ and $S_{331}D$ $S_{335}D$ $T_{339}E$) has no effect on HIS3 reporter activity, suggesting that PQN-59/OMA-1 interaction is MBK-2 or GSK-3 phosphorylation-independent (Table 5.1 and data not shown).

PQN-59 contains an UBA motif near the N-terminus. UBA motif is suggested in ubiquitin-involving processes (Buchberger 2002). Toward C-terminus lies an extensive prion-like glutamine and asparagine (Q/N)-rich stretch. This type of glutamine/asparagine-rich stretches are suggested in various processes and associated with self-aggregation (Soto et al. 2006). However, OMA-1/PQN-59 interaction is not likely due to a mere protein aggregation because PQN-59 showed two-hybrid interaction with only a small subset of proteins tested (data not shown). This is consistent with a previously conducted genome-wide yeast two-hybrid analysis, in which only 4 proteins were identified as PQN-59-interactors (Li et al. 2004).

In order to genetically analyze the role of *pqn-59*, RNAi analysis for *pqn-59* was performed. RNAi depletion of *pqn-59* in wild-type caused pleiotropic defects consistent with previous genome-wide RNAi analyses (Simmer et al. 2003; Rual et al. 2004; Fernandez et al. 2005; Sonnichsen et al. 2005). Strong RNAi caused maternal sterility, whereas attenuated RNAi resulted in embryos showing various defects, suggesting that *pqn-59* is an essential gene. The sterile phenotype did not resemble that of *oma-1(-); oma-2(-)* animals (Detwiler et al. 2001). Eggs very often showed irregular shapes and sizes. Cytokinesis as well as

nuclear division was often abnormal, producing blastomeres at aberrant positions and shapes with polyploid nuclei. Although embryonic lethality suggest that *pqn-59* is essential for embryogenesis, analyses of early embryonic markers failed to pinpoint a primary defect to this point, partly because strong depletion causes sterility (data not shown).

In order to determine the localization of PQN-59, GFP::PQN-59 was expressed in the germline gonad and early embryo using *pie-1* promoter and *pie-1* 3'UTR (Experimental Procedures). PQN-59::GFP was localized uniformly in the cytoplasm of germline gonad and early embryos. The GFP signal was essentially uniform in the embryo with each blastomere expressed similar density of PQN-59::GFP, although signals in early germline precursors appeared to be consistently, yet only slightly, lower than somatic blastomeres at 2-4 cell stages (data not shown). GFP expression was maintained until many stages later and gradually faded.

II. Candidate Approach for OBPs – translational regulators interact with OMA-1

Tis11-like CCCH zinc finger proteins are generally known as sequence-specific RNA binding translational regulators (Chen and Varani 2005). Indeed, 3 out of the 6 Tis11-like CCCH zinc finger proteins suggested in *C. elegans* early embryogenesis have also been proposed to translationally regulate their targets in the embryo (Tenenhaus et al. 2001; Huang et al. 2002; Ogura et al. 2003; D'Agostino et al. 2006). Two of them, MEX-6 and POS-1 are shown to interact with SPN-4, GLD-1 and MEX-3 previously (Huang et al. 2002; Marin and Evans 2003; Ogura et al. 2003). SPN-4 is an RRM domain protein shown to interact with mRNA (Ogura et al. 2003). GLD-1 and MEX-3 contain RNA binding domain, KH domain

(Jones and Schedl 1995; Draper et al. 1996). Indeed, GLD-1 has been reported to interact with various mRNAs in the distal gonad (Lee and Schedl 2001a). Genetic data support the notion that MEX-6/SPN-4/MEX-3 and POS-1/SPN-4/GLD-1 translationally repress their target transcripts (Huang et al. 2002; Ogura et al. 2003).

The expressions of SPN-4 and MEX-3 overlap with that of OMA-1/2 in the cytoplasm in late oocytes and in 1-cell embryo (Draper et al. 1996; Ogura et al. 2003). GLD-1 is a repressor of OMA-1/2 translation, and consistently, GLD-1 and OMA-1/2 expressions are nearly reciprocal (Jones et al. 1996; Detwiler et al. 2001; Lee and Schedl 2001a). However, there might be low levels of GLD-1 and OMA proteins co-expressed at their expression boundaries. Thus, it is a very attractive hypothesis that the Tis11-like CCCH proteins OMA-1/2 function with SPN-4, GLD-1, and/or MEX-3 to regulate translation.

In order to test this possibility, I examined the physical interactions between OMA-1 and SPN-4, MEX-3 and GLD-1 individually using a GAL4-based yeast-two hybrid system, and showed that OMA-1 and GLD-1, MEX-3, and SPN-4 interact in this system (Table 5.1). I further showed that the two zinc fingers of OMA-1 (aa.111-188) are sufficient to interact with GLD-1, MEX-3, and SPN-4 (data not shown). Conversely, *oma-1(te21)* mutation $E_{141}K$, changing a conserved residue in the first zinc finger, abolished the interactions (Table 5.1). These results suggest that OMA-1 interact with SPN-4, MEX-3, and GLD-1 via CCCH zinc finger domains. In order to further characterize these interactions, I tested various point mutants of OMA-1 (Table 5.1). Intriguingly, phosphorylation-interfering mutations at MBK-2 site: $T_{239}A$ and $P_{240}L$ resulted in weaker HIS3 reporter activation, whereas phosphorylation-mimicking mutation, T239D lowered only slightly (Table 5.1).

Phosphorylation abolishing mutations at GSK-3 site: $S_{331}A$ $S_{335}A$ $T_{339}A$ similarly resulted in a severe diminishment of HIS3 reporter activity (Table 5.1). These phosphorylation sites lie outside of the zinc finger domains. These results suggest that OMA-1 interaction with SPN-4, MEX-3, and GLD-1 are likely to happen via CCCH zinc finger domains, however the phosphorylation of OMA-1 outside of the domain influences interaction affinity.

DISCUSSION

I identified and characterized several OMA-1 binding proteins using yeast two-hybrid system, through non-biased screens as well as a candidate approach. Tis-11-like CCCH zinc finger protein, OMA-1 is predicted to be an RNA binding protein. Consistent with this notion, I showed that three RNA binding translational regulators, GLD-1, MEX-3, and SPN-4 interact with OMA-1 via zinc finger domains. Thus OMA-1/2 might function together with these factors to regulate translation. On the other hand, the majority of OMA proteins are not similar to any other *C. elegans* or non-*C. elegans* CCCH zinc finger proteins. This implies that OMA proteins might have non-RNA binding functions. Consistent with this notion, my analysis identified several OMA-1 binding proteins that are not previously characterized or predicted as RNA binding proteins. Interactions with two of these proteins, DH11.4 and C27B7.2 indeed were independent of the integrity of the CCCH zinc finger domains (Table 5.1). In addition, my analysis of an OMA-1 binding partner, TAF-4 suggests OMA proteins in transcriptional regulation. Thus OMA proteins might be a multi-functional proteins exerting RNA-binding and non-RNA binding functions.

PQN-59 as a partner of OMAs for embryogenesis

PQN-59 is a previously uncharacterized protein containing UBA domain at the N-terminus and Q/N-rich stretch at the C-terminus. UBA domain is often involved in ubiquitin-mediated processes, whereas Q/N-rich stretch is associated with various processes (Buchberger 2002; Soto et al. 2006). Depletion of *pqn-59* resulted in maternal sterility and embryonic lethality, suggesting that *pqn-59* is essential for embryogenesis. *pqn-59* sterility does not resemble *oma-1(-); oma-2(-)* sterility, thus the cause of sterility might be different from *oma-1(-); oma-2(-)*. Alternatively, additional defects might mask *Oma* gonadal phenotype in *pqn-59* RNAi gonad. Further analysis of the sterility and embryonic phenotype is necessary to understand the function of PQN-59. UBA domain is associated with ubiquitination. Particularly, in some cases, UBA domain-containing proteins prevent poly-ubiquitin chain elongation of its target proteins. As OMAs and PQN-59 physically interact, PQN-59 might be a negative regulator of OMA protein degradation. However, my analysis suggest that this might not be the case because *pqn-59* RNAi did not result in a premature degradation of OMA-1::GFP (data not shown). *oma-1(zu405)* shows defective degradation of several maternally supplied proteins (Chapter 3)(Lin 2003). Interestingly, PQN-59 contains a DYRK/MBK phosphorylation consensus toward the N-terminus at S_{255} (RSL**S**P, between UBA motif and Q/N rich stretch). An interesting possibility is that its activity is modulated at oocyte-to-embryo transition by MBK-2 phosphorylation, like OMA-1/2. However, unlike OMA-1/2 this potential phosphorylation might not cause a degradation of PQN-59 since GFP::PQN-59 does not degrade at or shortly after 1-cell stage.

Potential function as regulators of transcriptional quiescence

Earliest stages of embryogenesis lack polII-mediated transcription. In *C. elegans*, transcription is inactive in 1- and 2-cell stage then become activated at 4-cell stage (Seydoux and Dunn 1997). This transcriptional quiescence at the beginning of embryogenesis is evolutionarily highly conserved. The evolutionary conservation suggests an essential nature of the phenomenon, however, the underlying mechanism is largely unknown (Bultman et al. 2006). TAF-4 is a general transcription factor broadly required for zygotic transcription in *C. elegans* (Walker and Blackwell 2003). I have characterized OMA-1 and TAF-4 interaction in yeast two-hybrid system and showed that TAF-4 nuclear level is lowered in 1-cell and early 2-cell stage in the embryo. As TAF-4 is broadly required for embryonic transcription, the lower nuclear level of TAF-4 at 1- and 2-cell stages might be causal to the transcriptional quiescence. Recent analysis revealed that a depletion of *oma-1/2* results in high nuclear TAF-4 and coincidental rise of a transcriptional marker in 1- and 2-cell stages (Tugba Guven and Rueyling Lin, unpublished data). These results together suggest that OMA-1/2 contribute to transcriptional quiescence of 1- and 2-cell stage via directly regulating TAF-4 nuclear localization.

But then how is TAF-4 localization temporally regulated by OMA-1/2? Both OMA-1/2 and TAF-4 are expressed in late ooctyes, however TAF-4 is strongly localized to the nucleus and transcription is active at these stages (Figure 5.1). One model is that nuclear envelope breakdown during oocyte maturation is required for OMA/TAF-4 interaction. TAF-4 is expressed likely ubiquitously, whereas OMA-1 accumulates only in late oogenesis. Thus OMA-1/2 accumulate in the cytoplasm after TAF-4 is made and localized to the nucleus. As

a consequence, OMA-1/2 might not have an access to nuclear TAF-4. The nuclear boundary remains integral throughout oogenesis until oocyte maturation. Upon oocyte maturation nuclear envelope breaks down and nucleo- and cyto-plasm are mixed, resulting in OMA-1/TAF-4 interaction. Because OMA-1/2 are excluded from the nucleus, OMA-1/2 tether TAF-4 in the cytoplasm, thereby counteracting nuclear localization of TAF-4 when pronclei form at late 1-cell stage.

An alternative possibility is temporally regulated phosphorylation of OMA-1/2. A cascade of phosphorylation events marks OMA-1/2 for degradation at the end of 1-cell stage (see Chapter 2). I showed that MBK-2 and GSK-3 phosphorylate OMA-1 and OMA-2. Importantly, MBK-2 phosphorylation occurs shortly after the completion of meioses, before DNA decondensation (Figure 2.2). MBK-2 phosphorylation distantly primes GSK-3 phosphorylation, although the onset of GSK-3 phosphorylation has not been determined (see Chapter 2). An interesting possibility is that MBK-2 (and perhaps GSK-3) phosphorylation happening after meiosis II enhances the affinity of OMA/TAF-4 interaction thereby allowing OMA-mediated tethering of TAF-4 in the cytoplasm. DNA remains highly condensed in late oogenesis as well as early 1-cell stage until DNA decondensation/pronuclear formation (Figure 1.3). Highly condensed DNA is generally viewed as transcriptionally inactive, thus, transcription is not likely to happen even without a preventive mechanism (such as OMA-mediated mechanism). However, decondensed pronuclei might be structurally permissive to transcription. Undesired transcription might be prevented by binding of phosphorylated OMA-1/2 with TAF-4. Indeed, my yeast two-hybrid analysis suggest that MBK-2 and GSK-3 phosphorylation sites in OMA-1/2 are important for TAF-4 interaction, consistent with

MBK-2 and GSK-3 phosphorylation contributing to TAF-4 interaction (Table 5.1). The degradation of OMA-1/2 (also mediated by MBK-2/GSK-3 phosphorylation) frees TAF-4 at the end of 1-cell stage, resulting in re-accumulation of TAF-4 in the nucleus and higher transcriptional activity. In this scenario, TAF-4 can (but does not have to) freely shuttle between the nucleus and cytoplasm, however until MBK-2 phosphorylation, TAF-4 is not captured by OMAs in the cytoplasm.

Why transcription needs to be inactive in 1-cell embryo? 1-cell embryo can be seen as a germline precursor. Previous studies suggest that transcriptional quiescence is important for germline potential. Germline precursors of *C. elegans* and *Drosophila* early embryos are inactive in polII-mediated transcription (Seydoux and Dunn 1997). In *C. elegans*, this transcriptional quiescence of early germline lineage is mediated by a transcriptional repressor, PIE-1 (Seydoux et al. 1996; Batchelder et al. 1999). The depletion of *pie-1* results in polII-mediated transcription and somatic differentiation in normally germline blastomeres (Mello et al. 1996; Seydoux et al. 1996). Importantly, PIE-1-dependent transcriptional repression starts at 4-cell stage. 1- and 2-cell embryos appear to be transcriptionally inactive in the absence of PIE-1, indicating that PIE-1-indepednet transcriptional repression must exist in 1- and 2-cell stages. My data suggest that OMAs repress polII-dependent transcription via regulating TAF-4 nuclear localization. This OMAs-mediated mechanism might serve to maintain the germline potential of 1-cell and 2-cell embryo.

OMA-1/2 as translational regulators

Lastly, OMA-1's interaction with SPN-4, MEX-3 and GLD-1 provides a clue for another function of OMA-1/2: translational regulation. Previous localization analyses show that SPN-4 and MEX-3 co-localize with OMA proteins in the cytoplasm of oocytes as well as 1-cell embryo (Huang et al. 2002; Ogura et al. 2003). Although GLD-1 and OMA proteins show nearly reciprocal pattern in the gonad and early embryos, it is possible that they co-exist at their expression boundaries (*i.e.* at the end of pachytene and 1-cell stage) (Jones et al. 1996; Detwiler et al. 2001). Since a well known function for CCCH zinc finger proteins is translational regulation, particularly, translational repression, an interesting possibility is that OMA-1/2 and SPN-4, MEX-3, and/or GLD-1 repress mRNA translation in late oocytes and 1-cell embryo. Repression of developmental regulators is a particularly important issue in late oocytes and 1-cell stage as their expression might differentiate oocyte and 1-cell nuclei. An interesting possibility is that OMAs repress such developmental factors with SPN-4, MEX-3, and GLD-1. Indeed, MEX-3 and GLD-1 have been previously suggested in repressing somatic fates in the germline gonad (Ciosk et al. 2006). It will be interesting to ask whether OMAs participate in this MEX-3/GLD-1-mediated somatic fate repression in the germline gonad. Molecularly, identification of OMA-1/2 mRNA binding targets would provide us insights into the function of OMA proteins in the gonad as well as in 1-cell embryo. The founding member of Tis-11-like CCCH zinc finger proteins, mammalian Tis-11, exhibits high RNA binding specificity (Carballo et al. 1998). Interestingly, a recent study predicted that OMA-1/2 would possess less stringent RNA specificity, based on amino acid sequences at critical adenine recognition pocket (Pagano et al. 2007). Thus OMA-1 and OMA-2 might have multiple targets. Association with MEX-3, GLD-1 and SPN-4 might

result in higher binding specificity as RNA binding partner would need to possess binding signature for each protein.

It should be noted here that my genetic data presented in Chapter 3 suggest that GLD-1 expression might be negatively regulated by OMAs. Thus an alternative explanation for GLD-/OMA-1 interaction is that OMAs downregulate GLD-1 expression via physical interaction.

The interaction of OMA-1 with a transcription factor: TAF-4 and translational regulators: SPN-4, GLD-1, and MEX-3 raise an interesting possibility that OMAs maintain totipotency of the germline and 1-cell embryo by both translational and transcriptional repression. Further genetic analysis and the identification of OMAs' mRNA targets will likely to answer this possibility.

CHAPTER SIX
Conclusions and Recommendations

Regulation of OMA protein degradation

My studies revealed that OMA protein degradation is controlled by direct phosphorylation by two kinases, MBK-2/DYRK2 and GSK-3 and further showed that these phosphorylation events are likely sequential. My genetic analysis suggests that SCF and/or ECS E3 ligase and proteasome are likely to execute OMA protein degradation. Currently, the substrate binding subunit of E3 ligase for OMAs has not been identified. The identification of such a subunit is essential to understand the molecular mechanisms by which the phosphorylation leads to ubiquitination and proteasomal degradation. The requirement of phosphorylation favors the involvement of SCF over ECS, as SCF is known to be phosphorylation dependent (Deshaies 1999). The signature motif of the SCF substrate binding subunit is F-box domain, which was identified in over 300 proteins encoded in *C. elegans* genome previously (Kipreos and Pagano 2000). With the genome-wide library and OMA-1::GFP reporter, these F-box encoding genes can be screened with a reasonable amount of effort. A broader screen for regulators of OMA protein degradation would likely identify key steps of oocyte-to-embryo transition, in addition to direct regulators of OMA protein degradation.

Molecular functions of OMAs

Interestingly, the phosphorylation events appear to be important for embryonic functions of OMAs. Phosphorylation-abolishing mutations affect several OMA-1 interactions in yeast two-hybrid assays and genetic interference of phosphorylation phenocopies a defect of *oma-*

1(zu405). My analysis of *oma-1(zu405)* and *oma-1(zu405); oma-2(RNAi)* implicated several processes that OMAs might be involved in the 1-cell embryo. In addition, I identified physical and genetic interactors of OMAs/*oma*s. In the future, efforts should be made to establish genetic relationships with *oma*s for physical interactors. Conversely, for genetic interactors, molecular links would be very valuable and informative. Through both approaches, I have obtained supportive evidence for OMAs as translational regulators. Specifically, GLD-1, MEX-3, and SPN-4 physically interact with OMA-1 and *puf-3/5/8*, and *cpb-3* genetically interact with *oma-1/2*. As next step, not only the characterization of these interactions but also identification of translational targets will be essential. A recent study predicts that OMA-1/2 would show somewhat relaxed substrate specificity, thus they are likely to have multiple targets (Pagano et al. 2007). At this point, *zif-1* and *gld-1* are likely candidates, since mis-regulation of their translational repression could explain observed mis-expression of their products and activity in *oma-1/2* mutants. In addition, a non-biased, molecular screen such as reverse yeast three-hybrid and/or biochemical identification for RNA binding targets would likely to provide key insights into the function of OMAs in 1-cell embryo and oocytes, as well as the regulation of oocyte-to-embryo transition.

BIBLIOGRAPHY

Aberle, H., Bauer, A., Stappert, J., Kispert, A., and Kemler, R. 1997. beta-catenin is a target for the ubiquitin-proteasome pathway. *Embo J* **16**(13): 3797-3804.

Albertson, D.G. 1984. Formation of the first cleavage spindle in nematode embryos. *Dev Biol* **101**(1): 61-72.

Alessi, D.R., Saito, Y., Campbell, D.G., Cohen, P., Sithanandam, G., Rapp, U., Ashworth, A., Marshall, C.J., and Cowley, S. 1994. Identification of the sites in MAP kinase kinase-1 phosphorylated by p74raf-1. *Embo J* **13**(7): 1610-1619.

Altafaj, X., Dierssen, M., Baamonde, C., Marti, E., Visa, J., Guimera, J., Oset, M., Gonzalez, J.R., Florez, J., Fillat, C., and Estivill, X. 2001. Neurodevelopmental delay, motor abnormalities and cognitive deficits in transgenic mice overexpressing Dyrk1A (minibrain), a murine model of Down's syndrome. *Hum Mol Genet* **10**(18): 1915-1923.

Ambros, V. 2003. MicroRNA pathways in flies and worms: growth, death, fat, stress, and timing. *Cell* **113**(6): 673-676.

An, J.H., Vranas, K., Lucke, M., Inoue, H., Hisamoto, N., Matsumoto, K., and Blackwell, T.K. 2005. Regulation of the Caenorhabditis elegans oxidative stress defense protein SKN-1 by glycogen synthase kinase-3. *Proc Natl Acad Sci U S A* **102**(45): 16275-16280.

Aronheim, A., Zandi, E., Hennemann, H., Elledge, S.J., and Karin, M. 1997. Isolation of an AP-1 repressor by a novel method for detecting protein-protein interactions. *Mol Cell Biol* **17**(6): 3094-3102.

Batchelder, C., Dunn, M.A., Choy, B., Suh, Y., Cassie, C., Shim, E.Y., Shin, T.H., Mello, C., Seydoux, G., and Blackwell, T.K. 1999. Transcriptional repression by the Caenorhabditis elegans germ-line protein PIE-1. *Genes Dev* **13**(2): 202-212.

Berleth, T., Burri, M., Thoma, G., Bopp, D., Richstein, S., Frigerio, G., Noll, M., and Nusslein-Volhard, C. 1988. The role of localization of bicoid RNA in organizing the anterior pattern of the Drosophila embryo. *Embo J* **7**(6): 1749-1756.

Blackshear, P.J. 2002. Tristetraprolin and other CCCH tandem zinc-finger proteins in the regulation of mRNA turnover. *Biochemical Society transactions* **30**(Pt 6): 945-952.

Blumenthal, T., Evans, D., Link, C.D., Guffanti, A., Lawson, D., Thierry-Mieg, J., Thierry-Mieg, D., Chiu, W.L., Duke, K., Kiraly, M., and Kim, S.K. 2002. A global analysis of Caenorhabditis elegans operons. *Nature* **417**(6891): 851-854.

Blumenthal, T. and Gleason, K.S. 2003. Caenorhabditis elegans operons: form and function. *Nature reviews* **4**(2): 112-120.

Bowerman, B., Draper, B.W., Mello, C.C., and Priess, J.R. 1993. The maternal gene skn-1 encodes a protein that is distributed unequally in early C. elegans embryos. *Cell* **74**(3): 443-452.

Bowerman, B., Eaton, B.A., and Priess, J.R. 1992. skn-1, a maternally expressed gene required to specify the fate of ventral blastomeres in the early C. elegans embryo. *Cell* **68**(6): 1061-1075.

Boyd, L., Guo, S., Levitan, D., Stinchcomb, D.T., and Kemphues, K.J. 1996. PAR-2 is asymmetrically distributed and promotes association of P granules and PAR-1 with the cortex in C. elegans embryos. *Development* **122**(10): 3075-3084.

Brenner, S. 1974. The genetics of Caenorhabditis elegans. *Genetics* **77**(1): 71-94.

Brown, R.S. 2005. Zinc finger proteins: getting a grip on RNA. *Current opinion in structural biology* **15**(1): 94-98.

Brunet, S. and Maro, B. 2005. Cytoskeleton and cell cycle control during meiotic maturation of the mouse oocyte: integrating time and space. *Reproduction* **130**(6): 801-811.

Buchberger, A. 2002. From UBA to UBX: new words in the ubiquitin vocabulary. *Trends in cell biology* **12**(5): 216-221.

Bultman, S.J., Gebuhr, T.C., Pan, H., Svoboda, P., Schultz, R.M., and Magnuson, T. 2006. Maternal BRG1 regulates zygotic genome activation in the mouse. *Genes Dev* **20**(13): 1744-1754.

Campbell, L.E. and Proud, C.G. 2002. Differing substrate specificities of members of the DYRK family of arginine-directed protein kinases. *FEBS Lett* **510**(1-2): 31-36.

Carballo, E., Lai, W.S., and Blackshear, P.J. 1998. Feedback inhibition of macrophage tumor necrosis factor-alpha production by tristetraprolin. *Science* **281**(5379): 1001-1005.

Carroll, J., Jones, K.T., and Whittingham, D.G. 1996. Ca2+ release and the development of Ca2+ release mechanisms during oocyte maturation: a prelude to fertilization. *Rev Reprod* **1**(3): 137-143.

Cheeks, R.J., Canman, J.C., Gabriel, W.N., Meyer, N., Strome, S., and Goldstein, B. 2004. C. elegans PAR proteins function by mobilizing and stabilizing asymmetrically localized protein complexes. *Curr Biol* **14**(10): 851-862.

Chen, Y. and Varani, G. 2005. Protein families and RNA recognition. *The FEBS journal* **272**(9): 2088-2097.

Ciosk, R., DePalma, M., and Priess, J.R. 2004. ATX-2, the C. elegans ortholog of ataxin 2, functions in translational regulation in the germline. *Development* **131**(19): 4831-4841.

Ciosk, R., DePalma, M., and Priess, J.R. 2006. Translational regulators maintain totipotency in the Caenorhabditis elegans germline. *Science* **311**(5762): 851-853.

Clandinin, T.R. and Mains, P.E. 1993. Genetic studies of mei-1 gene activity during the transition from meiosis to mitosis in Caenorhabditis elegans. *Genetics* **134**(1): 199-210.

Clark-Maguire, S. and Mains, P.E. 1994. Localization of the mei-1 gene product of Caenorhaditis elegans, a meiotic-specific spindle component. *J Cell Biol* **126**(1): 199-209.

Coux, O., Tanaka, K., and Goldberg, A.L. 1996. Structure and functions of the 20S and 26S proteasomes. *Annu Rev Biochem* **65**: 801-847.

Crittenden, S.L., Bernstein, D.S., Bachorik, J.L., Thompson, B.E., Gallegos, M., Petcherski, A.G., Moulder, G., Barstead, R., Wickens, M., and Kimble, J. 2002. A conserved RNA-binding protein controls germline stem cells in Caenorhabditis elegans. *Nature* **417**(6889): 660-663.

Cuenca, A.A., Schetter, A., Aceto, D., Kemphues, K., and Seydoux, G. 2003. Polarization of the C. elegans zygote proceeds via distinct establishment and maintenance phases. *Development* **130**(7): 1255-1265.

D'Agostino, I., Merritt, C., Chen, P.L., Seydoux, G., and Subramaniam, K. 2006. Translational repression restricts expression of the C. elegans Nanos homolog NOS-2 to the embryonic germline. *Dev Biol* **292**(1): 244-252.

De Robertis, E.M., Larrain, J., Oelgeschlager, M., and Wessely, O. 2000. The establishment of Spemann's organizer and patterning of the vertebrate embryo. *Nature reviews* **1**(3): 171-181.

Deb, K., Sivaguru, M., Yong, H.Y., and Roberts, R.M. 2006. Cdx2 gene expression and trophectoderm lineage specification in mouse embryos. *Science* **311**(5763): 992-996.

DeRenzo, C., Reese, K.J., and Seydoux, G. 2003. Exclusion of germ plasm proteins from somatic lineages by cullin-dependent degradation. *Nature* **424**(6949): 685-689.

Deshaies, R.J. 1999. SCF and Cullin/Ring H2-based ubiquitin ligases. *Annu Rev Cell Dev Biol* **15**: 435-467.

Detwiler, M.R., Reuben, M., Li, X., Rogers, E., and Lin, R. 2001. Two zinc finger proteins, OMA-1 and OMA-2, are redundantly required for oocyte maturation in C. elegans. *Dev Cell* **1**(2): 187-199.

Dickinson, M.E. and McMahon, A.P. 1992. The role of Wnt genes in vertebrate development. *Curr Opin Genet Dev* **2**(4): 562-566.

DiNardo, S., Kuner, J.M., Theis, J., and O'Farrell, P.H. 1985. Development of embryonic pattern in D. melanogaster as revealed by accumulation of the nuclear engrailed protein. *Cell* **43**(1): 59-69.

Doe, C.Q. 2001. Cell polarity: the PARty expands. *Nat Cell Biol* **3**(1): E7-9.

Draper, B.W., Mello, C.C., Bowerman, B., Hardin, J., and Priess, J.R. 1996. MEX-3 is a KH domain protein that regulates blastomere identity in early C. elegans embryos. *Cell* **87**(2): 205-216.

Driever, W. and Nusslein-Volhard, C. 1988. A gradient of bicoid protein in Drosophila embryos. *Cell* **54**(1): 83-93.

Elinson, R.P. and Rowning, B. 1988. A transient array of parallel microtubules in frog eggs: potential tracks for a cytoplasmic rotation that specifies the dorso-ventral axis. *Dev Biol* **128**(1): 185-197.

Evans, T.C., Crittenden, S.L., Kodoyianni, V., and Kimble, J. 1994. Translational control of maternal glp-1 mRNA establishes an asymmetry in the C. elegans embryo. *Cell* **77**(2): 183-194.

Fernandez, A.G., Gunsalus, K.C., Huang, J., Chuang, L.S., Ying, N., Liang, H.L., Tang, C., Schetter, A.J., Zegar, C., Rual, J.F., Hill, D.E., Reinke, V., Vidal, M., and Piano, F. 2005. New genes with roles in the C. elegans embryo revealed using RNAi of ovary-enriched ORFeome clones. *Genome research* **15**(2): 250-259.

Ferrell, J.E., Jr. 1999. Xenopus oocyte maturation: new lessons from a good egg. *Bioessays* **21**(10): 833-842.

Fields, S. and Song, O. 1989. A novel genetic system to detect protein-protein interactions. *Nature* **340**(6230): 245-246.

Fiol, C.J., Mahrenholz, A.M., Wang, Y., Roeske, R.W., and Roach, P.J. 1987. Formation of protein kinase recognition sites by covalent modification of the substrate. Molecular mechanism for the synergistic action of casein kinase II and glycogen synthase kinase 3. *J Biol Chem* **262**(29): 14042-14048.

Fotaki, V., Dierssen, M., Alcantara, S., Martinez, S., Marti, E., Casas, C., Visa, J., Soriano, E., Estivill, X., and Arbones, M.L. 2002. Dyrk1A haploinsufficiency affects viability and causes developmental delay and abnormal brain morphology in mice. *Mol Cell Biol* **22**(18): 6636-6647.

Frame, S., Cohen, P., and Biondi, R.M. 2001. A common phosphate binding site explains the unique substrate specificity of GSK3 and its inactivation by phosphorylation. *Mol Cell* **7**(6): 1321-1327.

Fraser, A.G., Kamath, R.S., Zipperlen, P., Martinez-Campos, M., Sohrmann, M., and Ahringer, J. 2000. Functional genomic analysis of C. elegans chromosome I by systematic RNA interference. *Nature* **408**(6810): 325-330.

Frigerio, G., Burri, M., Bopp, D., Baumgartner, S., and Noll, M. 1986. Structure of the segmentation gene paired and the Drosophila PRD gene set as part of a gene network. *Cell* **47**(5): 735-746.

Furukawa, M., He, Y.J., Borchers, C., and Xiong, Y. 2003. Targeting of protein ubiquitination by BTB-Cullin 3-Roc1 ubiquitin ligases. *Nat Cell Biol* **5**(11): 1001-1007.

Goldstein, B. 1992. Induction of gut in Caenorhabditis elegans embryos. *Nature* **357**(6375): 255-257.

Goldstein, B. 1995. Cell contacts orient some cell division axes in the Caenorhabditis elegans embryo. *J Cell Biol* **129**(4): 1071-1080.

Goldstein, B. and Hird, S.N. 1996. Specification of the anteroposterior axis in Caenorhabditis elegans. *Development* **122**(5): 1467-1474.

Gomes, J.E., Encalada, S.E., Swan, K.A., Shelton, C.A., Carter, J.C., and Bowerman, B. 2001. The maternal gene spn-4 encodes a predicted RRM protein required for mitotic spindle orientation and cell fate patterning in early C. elegans embryos. *Development* **128**(21): 4301-4314.

Gosden, R., Krapez, J., and Briggs, D. 1997. Growth and development of the mammalian oocyte. *Bioessays* **19**(10): 875-882.

Green, M.R. 2000. TBP-associated factors (TAFIIs): multiple, selective transcriptional mediators in common complexes. *Trends Biochem Sci* **25**(2): 59-63.

Guo, S. and Kemphues, K.J. 1995. par-1, a gene required for establishing polarity in C. elegans embryos, encodes a putative Ser/Thr kinase that is asymmetrically distributed. *Cell* **81**(4): 611-620.

Gwack, Y., Sharma, S., Nardone, J., Tanasa, B., Iuga, A., Srikanth, S., Okamura, H., Bolton, D., Feske, S., Hogan, P.G., and Rao, A. 2006. A genome-wide Drosophila RNAi screen identifies DYRK-family kinases as regulators of NFAT. *Nature* **441**(7093): 646-650.

Hao, Y., Boyd, L., and Seydoux, G. 2006. Stabilization of cell polarity by the C. elegans RING protein PAR-2. *Dev Cell* **10**(2): 199-208.

Hershko, A. and Ciechanover, A. 1998. The ubiquitin system. *Annu Rev Biochem* **67**: 425-479.

Himpel, S., Tegge, W., Frank, R., Leder, S., Joost, H.G., and Becker, W. 2000. Specificity determinants of substrate recognition by the protein kinase DYRK1A. *J Biol Chem* **275**(4): 2431-2438.

Huang, N.N., Mootz, D.E., Walhout, A.J., Vidal, M., and Hunter, C.P. 2002. MEX-3 interacting proteins link cell polarity to asymmetric gene expression in Caenorhabditis elegans. *Development* **129**(3): 747-759.

Hulskamp, M., Schroder, C., Pfeifle, C., Jackle, H., and Tautz, D. 1989. Posterior segmentation of the Drosophila embryo in the absence of a maternal posterior organizer gene. *Nature* **338**(6217): 629-632.

Hunter, C.P. and Kenyon, C. 1996. Spatial and temporal controls target pal-1 blastomere-specification activity to a single blastomere lineage in C. elegans embryos. *Cell* **87**(2): 217-226.

Irish, V., Lehmann, R., and Akam, M. 1989. The Drosophila posterior-group gene nanos functions by repressing hunchback activity. *Nature* **338**(6217): 646-648.

Ivan, M., Kondo, K., Yang, H., Kim, W., Valiando, J., Ohh, M., Salic, A., Asara, J.M., Lane, W.S., and Kaelin, W.G., Jr. 2001. HIFalpha targeted for VHL-mediated destruction by proline hydroxylation: implications for O2 sensing. *Science* **292**(5516): 464-468.

Jaakkola, P., Mole, D.R., Tian, Y.M., Wilson, M.I., Gielbert, J., Gaskell, S.J., Kriegsheim, A., Hebestreit, H.F., Mukherji, M., Schofield, C.J., Maxwell, P.H., Pugh, C.W., and Ratcliffe, P.J. 2001. Targeting of HIF-alpha to the von Hippel-Lindau ubiquitylation complex by O2-regulated prolyl hydroxylation. *Science* **292**(5516): 468-472.

Jamnongjit, M. and Hammes, S.R. 2005. Oocyte maturation: the coming of age of a germ cell. *Seminars in reproductive medicine* **23**(3): 234-241.

Jenkins, N., Saam, J.R., and Mango, S.E. 2006. CYK-4/GAP provides a localized cue to initiate anteroposterior polarity upon fertilization. *Science* **313**(5791): 1298-1301.

Jones, A.R., Francis, R., and Schedl, T. 1996. GLD-1, a cytoplasmic protein essential for oocyte differentiation, shows stage- and sex-specific expression during Caenorhabditis elegans germline development. *Dev Biol* **180**(1): 165-183.

Jones, A.R. and Schedl, T. 1995. Mutations in gld-1, a female germ cell-specific tumor suppressor gene in Caenorhabditis elegans, affect a conserved domain also found in Src-associated protein Sam68. *Genes Dev* **9**(12): 1491-1504.

Kamath, R.S. and Ahringer, J. 2003. Genome-wide RNAi screening in Caenorhabditis elegans. *Methods* **30**(4): 313-321.

Kamath, R.S., Fraser, A.G., Dong, Y., Poulin, G., Durbin, R., Gotta, M., Kanapin, A., Le Bot, N., Moreno, S., Sohrmann, M., Welchman, D.P., Zipperlen, P., and Ahringer, J. 2003. Systematic functional analysis of the Caenorhabditis elegans genome using RNAi. *Nature* **421**(6920): 231-237.

Kelly, W.G., Xu, S., Montgomery, M.K., and Fire, A. 1997. Distinct requirements for somatic and germline expression of a generally expressed Caernorhabditis elegans gene. *Genetics* **146**(1): 227-238.

Kemphues, K. 2000. PARsing embryonic polarity. *Cell* **101**(4): 345-348.

Kile, B.T., Schulman, B.A., Alexander, W.S., Nicola, N.A., Martin, H.M., and Hilton, D.J. 2002. The SOCS box: a tale of destruction and degradation. *Trends Biochem Sci* **27**(5): 235-241.

Kipreos, E.T., Lander, L.E., Wing, J.P., He, W.W., and Hedgecock, E.M. 1996. cul-1 is required for cell cycle exit in C. elegans and identifies a novel gene family. *Cell* **85**(6): 829-839.

Kipreos, E.T. and Pagano, M. 2000. The F-box protein family. *Genome Biol* **1**(5): REVIEWS3002.

Kleckner, N. 1996. Meiosis: how could it work? *Proc Natl Acad Sci U S A* **93**(16): 8167-8174.

Kosinski, M., McDonald, K., Schwartz, J., Yamamoto, I., and Greenstein, D. 2005. C. elegans sperm bud vesicles to deliver a meiotic maturation signal to distant oocytes. *Development* **132**(15): 3357-3369.

Krek, W. 1998. Proteolysis and the G1-S transition: the SCF connection. *Curr Opin Genet Dev* **8**(1): 36-42.

Kulkarni, M.M., Booker, M., Silver, S.J., Friedman, A., Hong, P., Perrimon, N., and Mathey-Prevot, B. 2006. Evidence of off-target effects associated with long dsRNAs in Drosophila melanogaster cell-based assays. *Nature methods* **3**(10): 833-838.

Labbe, J.C., Pacquelet, A., Marty, T., and Gotta, M. 2006. A Genomewide Screen for Suppressors of par-2 Uncovers Potential Regulators of PAR Protein-Dependent Cell Polarity in Caenorhabditis elegans. *Genetics* **174**(1): 285-295.

Lai, W.S., Carballo, E., Strum, J.R., Kennington, E.A., Phillips, R.S., and Blackshear, P.J. 1999. Evidence that tristetraprolin binds to AU-rich elements and promotes the deadenylation and destabilization of tumor necrosis factor alpha mRNA. *Mol Cell Biol* **19**(6): 4311-4323.

Latham, K.E., Solter, D., and Schultz, R.M. 1992. Acquisition of a transcriptionally permissive state during the 1-cell stage of mouse embryogenesis. *Dev Biol* **149**(2): 457-462.

Lee, K., Deng, X., and Friedman, E. 2000. Mirk protein kinase is a mitogen-activated protein kinase substrate that mediates survival of colon cancer cells. *Cancer Res* **60**(13): 3631-3637.

Lee, M.-H. and Schedl, T. 2001a. Identification of in vivo mRNA targets of GLD-1, a maxi-KH motif containing protein required for C. elegans germ cell development. *Genes Dev* **15**(18): 2408-2420.

Lee, M.H. and Schedl, T. 2001b. Identification of in vivo mRNA targets of GLD-1, a maxi-KH motif containing protein required for C. elegans germ cell development. *Genes Dev* **15**(18): 2408-2420.

Lee, M.H. and Schedl, T. 2004. Translation repression by GLD-1 protects its mRNA targets from nonsense-mediated mRNA decay in C. elegans. *Genes Dev* **18**(9): 1047-1059.

Lehmann, R. and Nusslein-Volhard, C. 1991. The maternal gene nanos has a central role in posterior pattern formation of the Drosophila embryo. *Development* **112**(3): 679-691.

Li, S., Armstrong, C.M., Bertin, N., Ge, H., Milstein, S., Boxem, M., Vidalain, P.O., Han, J.D., Chesneau, A., Hao, T., Goldberg, D.S., Li, N., Martinez, M., Rual, J.F., Lamesch, P., Xu, L., Tewari, M., Wong, S.L., Zhang, L.V., Berriz, G.F., Jacotot, L.,

Vaglio, P., Reboul, J., Hirozane-Kishikawa, T., Li, Q., Gabel, H.W., Elewa, A., Baumgartner, B., Rose, D.J., Yu, H., Bosak, S., Sequerra, R., Fraser, A., Mango, S.E., Saxton, W.M., Strome, S., Van Den Heuvel, S., Piano, F., Vandenhaute, J., Sardet, C., Gerstein, M., Doucette-Stamm, L., Gunsalus, K.C., Harper, J.W., Cusick, M.E., Roth, F.P., Hill, D.E., and Vidal, M. 2004. A map of the interactome network of the metazoan C. elegans. *Science* **303**(5657): 540-543.

Lin, R. 2003. A gain-of-function mutation in oma-1, a C. elegans gene required for oocyte maturation, results in delayed degradation of maternal proteins and embryonic lethality. *Dev Biol* **258**(1): 226-239.

Lin, R., Hill, R.J., and Priess, J.R. 1998. POP-1 and anterior-posterior fate decisions in C. elegans embryos. *Cell* **92**(2): 229-239.

Liu, J., Vasudevan, S., and Kipreos, E.T. 2004. CUL-2 and ZYG-11 promote meiotic anaphase II and the proper placement of the anterior-posterior axis in C. elegans. *Development* **131**(15): 3513-3525.

Logan, C.Y. and Nusse, R. 2004. The Wnt signaling pathway in development and disease. *Annu Rev Cell Dev Biol* **20**: 781-810.

Lublin, A.L. and Evans, T.C. 2007. The RNA-binding proteins PUF-5, PUF-6, and PUF-7 reveal multiple systems for maternal mRNA regulation during C. elegans oogenesis. *Dev Biol* **303**(2): 635-649.

Luitjens, C., Gallegos, M., Kraemer, B., Kimble, J., and Wickens, M. 2000. CPEB proteins control two key steps in spermatogenesis in C. elegans. *Genes Dev* **14**(20): 2596-2609.

Lyczak, R., Gomes, J.E., and Bowerman, B. 2002. Heads or tails: cell polarity and axis formation in the early Caenorhabditis elegans embryo. *Dev Cell* **3**(2): 157-166.

Ma, Y., Creanga, A., Lum, L., and Beachy, P.A. 2006. Prevalence of off-target effects in Drosophila RNA interference screens. *Nature* **443**(7109): 359-363.

Maduro, M.F., Meneghini, M.D., Bowerman, B., Broitman-Maduro, G., and Rothman, J.H. 2001. Restriction of mesendoderm to a single blastomere by the combined action of SKN-1 and a GSK-3beta homolog is mediated by MED-1 and -2 in C. elegans. *Mol Cell* **7**(3): 475-485.

Maeda, I., Kohara, Y., Yamamoto, M., and Sugimoto, A. 2001. Large-scale analysis of gene function in Caenorhabditis elegans by high-throughput RNAi. *Curr Biol* **11**(3): 171-176.

Marin, V.A. and Evans, T.C. 2003. Translational repression of a C. elegans Notch mRNA by the STAR/KH domain protein GLD-1. *Development* **130**(12): 2623-2632.

McCarter, J., Bartlett, B., Dang, T., and Schedl, T. 1999. On the control of oocyte meiotic maturation and ovulation in Caenorhabditis elegans. *Dev Biol* **205**(1): 111-128.

McNally, K.L. and McNally, F.J. 2005. Fertilization initiates the transition from anaphase I to metaphase II during female meiosis in C. elegans. *Dev Biol* **282**(1): 218-230.

McNatty, K.P., Moore, L.G., Hudson, N.L., Quirke, L.D., Lawrence, S.B., Reader, K., Hanrahan, J.P., Smith, P., Groome, N.P., Laitinen, M., Ritvos, O., and Juengel, J.L. 2004. The oocyte and its role in regulating ovulation rate: a new paradigm in reproductive biology. *Reproduction* **128**(4): 379-386.

Mehlmann, L.M. 2005. Stops and starts in mammalian oocytes: recent advances in understanding the regulation of meiotic arrest and oocyte maturation. *Reproduction* **130**(6): 791-799.

Mello, C.C., Draper, B.W., Krause, M., Weintraub, H., and Priess, J.R. 1992. The pie-1 and mex-1 genes and maternal control of blastomere identity in early C. elegans embryos. *Cell* **70**(1): 163-176.

Mello, C.C., Schubert, C., Draper, B., Zhang, W., Lobel, R., and Priess, J.R. 1996. The PIE-1 protein and germline specification in C. elegans embryos [letter]. *Nature* **382**(6593): 710-712.

Miller, C.T., Aggarwal, S., Lin, T.K., Dagenais, S.L., Contreras, J.I., Orringer, M.B., Glover, T.W., Beer, D.G., and Lin, L. 2003a. Amplification and overexpression of the dual-specificity tyrosine-(Y)-phosphorylation regulated kinase 2 (DYRK2) gene in esophageal and lung adenocarcinomas. *Cancer Res* **63**(14): 4136-4143.

Miller, M.A., Nguyen, V.Q., Lee, M.H., Kosinski, M., Schedl, T., Caprioli, R.M., and Greenstein, D. 2001. A sperm cytoskeletal protein that signals oocyte meiotic maturation and ovulation. *Science* **291**(5511): 2144-2147.

Miller, M.A., Ruest, P.J., Kosinski, M., Hanks, S.K., and Greenstein, D. 2003b. An Eph receptor sperm-sensing control mechanism for oocyte meiotic maturation in Caenorhabditis elegans. *Genes Dev* **17**(2): 187-200.

Mootz, D., Ho, D.M., and Hunter, C.P. 2004. The STAR/Maxi-KH domain protein GLD-1 mediates a developmental switch in the translational control of C. elegans PAL-1. *Development* **131**(14): 3263-3272.

Moss, R.L. and McCann, S.M. 1973. Induction of mating behavior in rats by luteinizing hormone-releasing factor. *Science* **181**(95): 177-179.

Munro, E., Nance, J., and Priess, J.R. 2004. Cortical flows powered by asymmetrical contraction transport PAR proteins to establish and maintain anterior-posterior polarity in the early C. elegans embryo. *Dev Cell* **7**(3): 413-424.

Nakahata, S., Katsu, Y., Mita, K., Inoue, K., Nagahama, Y., and Yamashita, M. 2001. Biochemical identification of Xenopus Pumilio as a sequence-specific cyclin B1 mRNA-binding protein that physically interacts with a Nanos homolog, Xcat-2, and a cytoplasmic polyadenylation element-binding protein. *J Biol Chem* **276**(24): 20945-20953.

Nance, J. and Priess, J.R. 2002. Cell polarity and gastrulation in C. elegans. *Development* **129**(2): 387-397.

Nash, P., Tang, X., Orlicky, S., Chen, Q., Gertler, F.B., Mendenhall, M.D., Sicheri, F., Pawson, T., and Tyers, M. 2001. Multisite phosphorylation of a CDK inhibitor sets a threshold for the onset of DNA replication. *Nature* **414**(6863): 514-521.

Nayak, S., Santiago, F.E., Jin, H., Lin, D., Schedl, T., and Kipreos, E.T. 2002. The Caenorhabditis elegans Skp1-related gene family: diverse functions in cell proliferation, morphogenesis, and meiosis. *Curr Biol* **12**(4): 277-287.

Nishi, Y. and Lin, R. 2005. DYRK2 and GSK-3 phosphorylate and promote the timely degradation of OMA-1, a key regulator of the oocyte-to-embryo transition in C. elegans. *Dev Biol* **288**(1): 139-149.

Nusslein-Volhard, C., Frohnhofer, H.G., and Lehmann, R. 1987. Determination of anteroposterior polarity in Drosophila. *Science* **238**(4834): 1675-1681.

O'Connell, K.F., Maxwell, K.N., and White, J.G. 2000. The spd-2 gene is required for polarization of the anteroposterior axis and formation of the sperm asters in the Caenorhabditis elegans zygote. *Dev Biol* **222**(1): 55-70.

Ogura, K., Kishimoto, N., Mitani, S., Gengyo-Ando, K., and Kohara, Y. 2003. Translational control of maternal glp-1 mRNA by POS-1 and its interacting protein SPN-4 in Caenorhabditis elegans. *Development* **130**(11): 2495-2503.

Pagano, J.M., Farley, B.M., McCoig, L.M., and Ryder, S.P. 2007. Molecular basis of RNA recognition by the embryonic polarity determinant MEX-5. *J Biol Chem*.

Pang, K.M., Ishidate, T., Nakamura, K., Shirayama, M., Trzepacz, C., Schubert, C.M., Priess, J.R., and Mello, C.C. 2004. The minibrain kinase homolog, mbk-2, is required for spindle positioning and asymmetric cell division in early C. elegans embryos. *Dev Biol* **265**(1): 127-139.

Peifer, M., Pai, L.M., and Casey, M. 1994. Phosphorylation of the Drosophila adherens junction protein Armadillo: roles for wingless signal and zeste-white 3 kinase. *Dev Biol* **166**(2): 543-556.

Pellettieri, J., Reinke, V., Kim, S.K., and Seydoux, G. 2003. Coordinate activation of maternal protein degradation during the egg-to-embryo transition in C. elegans. *Dev Cell* **5**(3): 451-462.

Pfaff, D.W. 1973. Luteinizing hormone-releasing factor potentiates lordosis behavior in hypophysectomized ovariectomized female rats. *Science* **182**(117): 1148-1149.

Pintard, L., Willis, J.H., Willems, A., Johnson, J.L., Srayko, M., Kurz, T., Glaser, S., Mains, P.E., Tyers, M., Bowerman, B., and Peter, M. 2003. The BTB protein MEL-26 is a substrate-specific adaptor of the CUL-3 ubiquitin-ligase. *Nature* **425**(6955): 311-316.

Plusa, B., Grabarek, J.B., Piotrowska, K., Glover, D.M., and Zernicka-Goetz, M. 2002. Site of the previous meiotic division defines cleavage orientation in the mouse embryo. *Nat Cell Biol* **4**(10): 811-815.

Plusa, B., Hadjantonakis, A.K., Gray, D., Piotrowska-Nitsche, K., Jedrusik, A., Papaioannou, V.E., Glover, D.M., and Zernicka-Goetz, M. 2005. The first cleavage of the mouse zygote predicts the blastocyst axis. *Nature* **434**(7031): 391-395.

Praitis, V., Casey, E., Collar, D., and Austin, J. 2001. Creation of low-copy integrated transgenic lines in *Caenorhabditis elegans*. *Genetics* **157**(3): 1217-1226.

Quintin, S., Mains, P.E., Zinke, A., and Hyman, A.A. 2003. The mbk-2 kinase is required for inactivation of MEI-1/katanin in the one-cell Caenorhabditis elegans embryo. *EMBO reports* **4**(12): 1175-1181.

Raich, W.B., Moorman, C., Lacefield, C.O., Lehrer, J., Bartsch, D., Plasterk, R.H., Kandel, E.R., and Hobert, O. 2003. Characterization of Caenorhabditis elegans homologs of the Down syndrome candidate gene DYRK1A. *Genetics* **163**(2): 571-580.

Reddien, P.W., Bermange, A.L., Murfitt, K.J., Jennings, J.R., and Sanchez Alvarado, A. 2005. Identification of genes needed for regeneration, stem cell function, and tissue homeostasis by systematic gene perturbation in planaria. *Dev Cell* **8**(5): 635-649.

Reese, K.J., Dunn, M.A., Waddle, J.A., and Seydoux, G. 2000. Asymmetric segregation of PIE-1 in C. elegans is mediated by two complementary mechanisms that act through separate PIE-1 protein domains. *Mol Cell* **6**(2): 445-455.

Rizo, J. and Sudhof, T.C. 1998. C2-domains, structure and function of a universal Ca2+-binding domain. *J Biol Chem* **273**(26): 15879-15882.

Rocheleau, C.E., Downs, W.D., Lin, R., Wittmann, C., Bei, Y., Cha, Y.H., Ali, M., Priess, J.R., and Mello, C.C. 1997. Wnt signaling and an APC-related gene specify endoderm in early C. elegans embryos. *Cell* **90**(4): 707-716.

Rogers, E., Bishop, J.D., Waddle, J.A., Schumacher, J.M., and Lin, R. 2002. The aurora kinase AIR-2 functions in the release of chromosome cohesion in Caenorhabditis elegans meiosis. *J Cell Biol* **157**(2): 219-229.

Rogers, S., Wells, R., and Rechsteiner, M. 1986. Amino acid sequences common to rapidly degraded proteins: the PEST hypothesis. *Science* **234**(4774): 364-368.

Roller, R.J., Kinloch, R.A., Hiraoka, B.Y., Li, S.S., and Wassarman, P.M. 1989. Gene expression during mammalian oogenesis and early embryogenesis: quantification of three messenger RNAs abundant in fully grown mouse oocytes. *Development* **106**(2): 251-261.

Rual, J.F., Ceron, J., Koreth, J., Hao, T., Nicot, A.S., Hirozane-Kishikawa, T., Vandenhaute, J., Orkin, S.H., Hill, D.E., van den Heuvel, S., and Vidal, M. 2004. Toward improving Caenorhabditis elegans phenome mapping with an ORFeome-based RNAi library. *Genome research* **14**(10B): 2162-2168.

Runft, L.L., Jaffe, L.A., and Mehlmann, L.M. 2002. Egg activation at fertilization: where it all begins. *Dev Biol* **245**(2): 237-254.

Salles, F.J., Lieberfarb, M.E., Wreden, C., Gergen, J.P., and Strickland, S. 1994. Coordinate initiation of Drosophila development by regulated polyadenylation of maternal messenger RNAs. *Science* **266**(5193): 1996-1999.

Sander, K. and Lehmann, R. 1988. Drosophila nurse cells produce a posterior signal required for embryonic segmentation and polarity. *Nature* **335**(6185): 68-70.

Schlesinger, A., Shelton, C.A., Maloof, J.N., Meneghini, M., and Bowerman, B. 1999. Wnt pathway components orient a mitotic spindle in the early Caenorhabditis elegans embryo without requiring gene transcription in the responding cell. *Genes Dev* **13**(15): 2028-2038.

Schmitt, A. and Nebreda, A.R. 2002. Signalling pathways in oocyte meiotic maturation. *J Cell Sci* **115**(Pt 12): 2457-2459.

Schubert, C.M., Lin, R., de Vries, C.J., Plasterk, R.H., and Priess, J.R. 2000. MEX-5 and MEX-6 function to establish soma/germline asymmetry in early C. elegans embryos. *Mol Cell* **5**(4): 671-682.

Schulman, B.A., Carrano, A.C., Jeffrey, P.D., Bowen, Z., Kinnucan, E.R., Finnin, M.S., Elledge, S.J., Harper, J.W., Pagano, M., and Pavletich, N.P. 2000. Insights into SCF ubiquitin ligases from the structure of the Skp1-Skp2 complex. *Nature* **408**(6810): 381-386.

Schultz, R.M. 2002. The molecular foundations of the maternal to zygotic transition in the preimplantation embryo. *Human reproduction update* **8**(4): 323-331.

Seydoux, G. and Dunn, M.A. 1997. Transcriptionally repressed germ cells lack a subpopulation of phosphorylated RNA polymerase II in early embryos of Caenorhabditis elegans and Drosophila melanogaster. *Development* **124**(11): 2191-2201.

Seydoux, G. and Fire, A. 1994. Soma-germline asymmetry in the distributions of embryonic RNAs in Caenorhabditis elegans. *Development* **120**(10): 2823-2834.

Seydoux, G., Mello, C.C., Pettitt, J., Wood, W.B., Priess, J.R., and Fire, A. 1996. Repression of gene expression in the embryonic germ lineage of C. elegans. *Nature* **382**(6593): 713-716.

Shimada, M., Yokosawa, H., and Kawahara, H. 2006. OMA-1 is a P granules-associated protein that is required for germline specification in Caenorhabditis elegans embryos. *Genes Cells* **11**(4): 383-396.

Shirayama, M., Soto, M.C., Ishidate, T., Kim, S., Nakamura, K., Bei, Y., van den Heuvel, S., and Mello, C.C. 2006. The Conserved Kinases CDK-1, GSK-3, KIN-19, and MBK-2 Promote OMA-1 Destruction to Regulate the Oocyte-to-Embryo Transition in C. elegans. *Curr Biol* **16**(1): 47-55.

Simmer, F., Moorman, C., Van Der Linden, A.M., Kuijk, E., Van Den Berghe, P.V., Kamath, R., Fraser, A.G., Ahringer, J., and Plasterk, R.H. 2003. Genome-Wide RNAi of C. elegans Using the Hypersensitive rrf-3 Strain Reveals Novel Gene Functions. *PLoS Biol* **1**(1): E12.

Simmer, F., Tijsterman, M., Parrish, S., Koushika, S.P., Nonet, M.L., Fire, A., Ahringer, J., and Plasterk, R.H. 2002. Loss of the putative RNA-directed RNA polymerase RRF-3 makes C. elegans hypersensitive to RNAi. *Curr Biol* **12**(15): 1317-1319.

Skowyra, D., Craig, K.L., Tyers, M., Elledge, S.J., and Harper, J.W. 1997. F-box proteins are receptors that recruit phosphorylated substrates to the SCF ubiquitin-ligase complex. *Cell* **91**(2): 209-219.

Skurat, A.V. and Dietrich, A.D. 2004. Phosphorylation of Ser640 in muscle glycogen synthase by DYRK family protein kinases. *J Biol Chem* **279**(4): 2490-2498.

Smibert, C.A., Wilson, J.E., Kerr, K., and Macdonald, P.M. 1996. smaug protein represses translation of unlocalized nanos mRNA in the Drosophila embryo. *Genes Dev* **10**(20): 2600-2609.

Smith, D.J. and Rubin, E.M. 1997. Functional screening and complex traits: human 21q22.2 sequences affecting learning in mice. *Hum Mol Genet* **6**(10): 1729-1733.

Smith, D.J., Stevens, M.E., Sudanagunta, S.P., Bronson, R.T., Makhinson, M., Watabe, A.M., O'Dell, T.J., Fung, J., Weier, H.U., Cheng, J.F., and Rubin, E.M. 1997. Functional screening of 2 Mb of human chromosome 21q22.2 in transgenic mice implicates minibrain in learning defects associated with Down syndrome. *Nat Genet* **16**(1): 28-36.

Sonneville, R. and Gonczy, P. 2004. Zyg-11 and cul-2 regulate progression through meiosis II and polarity establishment in C. elegans. *Development* **131**(15): 3527-3543.

Sonnichsen, B., Koski, L.B., Walsh, A., Marschall, P., Neumann, B., Brehm, M., Alleaume, A.M., Artelt, J., Bettencourt, P., Cassin, E., Hewitson, M., Holz, C., Khan, M., Lazik, S., Martin, C., Nitzsche, B., Ruer, M., Stamford, J., Winzi, M., Heinkel, R., Roder, M., Finell, J., Hantsch, H., Jones, S.J., Jones, M., Piano, F., Gunsalus, K.C., Oegema,

K., Gonczy, P., Coulson, A., Hyman, A.A., and Echeverri, C.J. 2005. Full-genome RNAi profiling of early embryogenesis in Caenorhabditis elegans. *Nature* **434**(7032): 462-469.

Soto, C., Estrada, L., and Castilla, J. 2006. Amyloids, prions and the inherent infectious nature of misfolded protein aggregates. *Trends Biochem Sci* **31**(3): 150-155.

Spieth, J., Brooke, G., Kuersten, S., Lea, K., and Blumenthal, T. 1993. Operons in C. elegans: polycistronic mRNA precursors are processed by trans-splicing of SL2 to downstream coding regions. *Cell* **73**(3): 521-532.

Srayko, M., Buster, D.W., Bazirgan, O.A., McNally, F.J., and Mains, P.E. 2000. MEI-1/MEI-2 katanin-like microtubule severing activity is required for Caenorhabditis elegans meiosis. *Genes Dev* **14**(9): 1072-1084.

Stitzel, M.L., Pellettieri, J., and Seydoux, G. 2006. The C. elegans DYRK Kinase MBK-2 Marks Oocyte Proteins for Degradation in Response to Meiotic Maturation. *Curr Biol* **16**(1): 56-62.

Strome, S. and Wood, W.B. 1982. Immunofluorescence visualization of germ-line-specific cytoplasmic granules in embryos, larvae, and adults of Caenorhabditis elegans. *Proc Natl Acad Sci U S A* **79**(5): 1558-1562.

Strome, S. and Wood, W.B. 1983. Generation of asymmetry and segregation of germ-line granules in early C. elegans embryos. *Cell* **35**(1): 15-25.

Sulston, J.E., Schierenberg, E., White, J.G., and Thomson, J.N. 1983. The embryonic cell lineage of the nematode Caenorhabditis elegans. *Dev Biol* **100**(1): 64-119.

Tabara, H., Hill, R.J., Mello, C.C., Priess, J.R., and Kohara, Y. 1999. pos-1 encodes a cytoplasmic zinc-finger protein essential for germline specification in C. elegans. *Development* **126**(1): 1-11.

Tautz, D. 1988. Regulation of the Drosophila segmentation gene hunchback by two maternal morphogenetic centres. *Nature* **332**(6161): 281-284.

Tejedor, F., Zhu, X.R., Kaltenbach, E., Ackermann, A., Baumann, A., Canal, I., Heisenberg, M., Fischbach, K.F., and Pongs, O. 1995. minibrain: a new protein kinase family involved in postembryonic neurogenesis in Drosophila. *Neuron* **14**(2): 287-301.

Tenenhaus, C., Subramaniam, K., Dunn, M.A., and Seydoux, G. 2001. PIE-1 is a bifunctional protein that regulates maternal and zygotic gene expression in the embryonic germ line of Caenorhabditis elegans. *Genes Dev* **15**(8): 1031-1040.

Tenlen, J.R., Schisa, J.A., Diede, S.J., and Page, B.D. 2006. Reduced dosage of pos-1 suppresses Mex mutants and reveals complex interactions among CCCH zinc-finger proteins during Caenorhabditis elegans embryogenesis. *Genetics* **174**(4): 1933-1945.

Thompson, E.M., Legouy, E., and Renard, J.P. 1998. Mouse embryos do not wait for the MBT: chromatin and RNA polymerase remodeling in genome activation at the onset of development. *Dev Genet* **22**(1): 31-42.

Thorpe, C.J., Schlesinger, A., Carter, J.C., and Bowerman, B. 1997. Wnt signaling polarizes an early C. elegans blastomere to distinguish endoderm from mesoderm. *Cell* **90**(4): 695-705.

Timmons, L. and Fire, A. 1998. Specific interference by ingested dsRNA [letter]. *Nature* **395**(6705): 854.

Vernet, M., Bonnerot, C., Briand, P., and Nicolas, J.F. 1992. Changes in permissiveness for the expression of microinjected DNA during the first cleavages of mouse embryos. *Mech Dev* **36**(3): 129-139.

Vincent, J.P., Oster, G.F., and Gerhart, J.C. 1986. Kinematics of gray crescent formation in Xenopus eggs: the displacement of subcortical cytoplasm relative to the egg surface. *Dev Biol* **113**(2): 484-500.

Walker, A.K. and Blackwell, T.K. 2003. A broad but restricted requirement for TAF-5 (human TAFII100) for embryonic transcription in Caenorhabditis elegans. *J Biol Chem* **278**(8): 6181-6186.

Walker, A.K., Rothman, J.H., Shi, Y., and Blackwell, T.K. 2001. Distinct requirements for C.elegans TAF(II)s in early embryonic transcription. *Embo J* **20**(18): 5269-5279.

Wallenfang, M.R. and Seydoux, G. 2000. Polarization of the anterior-posterior axis of C. elegans is a microtubule-directed process. *Nature* **408**(6808): 89-92.

Wang, X., Paulin, F.E., Campbell, L.E., Gomez, E., O'Brien, K., Morrice, N., and Proud, C.G. 2001. Eukaryotic initiation factor 2B: identification of multiple phosphorylation sites in the epsilon-subunit and their functions in vivo. *Embo J* **20**(16): 4349-4359.

Ward, S. and Carrel, J.S. 1979. Fertilization and sperm competition in the nematode Caenorhabditis elegans. *Dev Biol* **73**(2): 304-321.

Wickens, M., Bernstein, D.S., Kimble, J., and Parker, R. 2002. A PUF family portrait: 3'UTR regulation as a way of life. *Trends Genet* **18**(3): 150-157.

Woodgett, J.R. 2001. Judging a protein by more than its name: GSK-3. *Sci STKE* **2001**(100): RE12.

Xu, L., Wei, Y., Reboul, J., Vaglio, P., Shin, T.H., Vidal, M., Elledge, S.J., and Harper, J.W. 2003. BTB proteins are substrate-specific adaptors in an SCF-like modular ubiquitin ligase containing CUL-3. *Nature* **425**(6955): 316-321.

Yamanaka, A., Yada, M., Imaki, H., Koga, M., Ohshima, Y., and Nakayama, K. 2002. Multiple Skp1-related proteins in Caenorhabditis elegans: diverse patterns of interaction with Cullins and F-box proteins. *Curr Biol* **12**(4): 267-275.

Zernicka-Goetz, M. 2006. The first cell-fate decisions in the mouse embryo: destiny is a matter of both chance and choice. *Curr Opin Genet Dev* **16**(4): 406-412.

Zhong, W., Feng, H., Santiago, F.E., and Kipreos, E.T. 2003. CUL-4 ubiquitin ligase maintains genome stability by restraining DNA-replication licensing. *Nature* **423**(6942): 885-889.

VITAE

Yuichi Nishi was born in Yuasa, Wakayama, Japan, on June 12, 1978, the son of Hiroyoshi Nishi and Kumiko Nishi. After completing his work at Koyo High School, Wakayama-city, Japan in 1997, he entered the University of Tokyo, Japan. He received the degree of Bachelor of Science with a major in zoology from University of Tokyo, in 2001. In August, 2001 he entered the Graduate School of Biomedical Sciences at the University of Texas Southwestern Medical Center at Dallas, and completed his thesis in 2007.